Performance modelling for product development of advanced window systems

David Appelfeld

PhD Thesis

Department of Civil Engineering

2012

DTU Civil Engineering Report R-267 (UK)
May 2012

DTU Civil Engineering
Department of Civil Engineering

Performance Modelling for Product Development of Advanced Window Systems

David Appelfeld

Ph.D. Thesis

Department of Civil Engineering
Technical University of Denmark

2012

Supervisors:

Professor Svend Svendsen, DTU Civil Engineering, Denmark
Associate Professor Toke Rammer Nielsen, DTU Civil Engineering, Denmark

Assesment Committee:

Ph.D. Bengt Hellström, Lund University, Sweden
Ph.D. Karsten Duer, Velux A/S, Denmark
Professor Carsten Rode, DTU Civil Engineering, Denmark

Performance Modelling for Product Development of Advanced Window Systems

Printed by DTU-Tryk
Department of Civil Engineering
Technical University of Denmark
ISBN: 9788778773500
ISSN: 1601-2917
Report: BYG R-267

Preface

This doctoral thesis is submitted as a partial fulfilment of the requirements for the Danish PhD degree. The first part introduces the research topic, and presents and discusses the results and findings. The second part is a collection of articles based on the research, which contain fundamental aspects of the work and present the work in detail from a scientific point of view.

"To get something you never had, you have to do something you've never done." - Unknown

Lyngby, the 31th May 2012

David Appelfeld

Acknowledgements

I want to express my sincere and deep thanks to everyone who has helped me during this research.

First and foremost, I would like to thank my supervisor Professor Svend Svendsen and my co-supervisor Associate Professor Toke Rammer Nielsen for their guidance and discussion over the years as well as for giving me the opportunity to become a PhD.

I would also like to thank all my colleagues in the Section of Building Physics and Services at DTU Civil Engineering for the very friendly and beneficial working environment.

Special thanks go to Eleanor Lee, Andrew McNeil and Jacob Jonsson for all their help, guidance and inspiration during my external stay as a guest researcher at the Lawrence Berkeley National Laboratories.

Finally, I would especially like to thank my parents, girlfriend and friends for supporting me during the work.

Grants

This research was supported partially by grants from the Danish Energy Agency and by the Department of Civil Engineering at the Technical University of Denmark.

Abstract

The research presented in this doctoral thesis shows how the product development (PD) of Complex Fenestration Systems (CFSs) can be facilitated by computer-based analysis to improve the energy efficiency of fenestration systems as well as to improve the indoor environment.
The first chapter defines the hypothesis and objectives of the thesis and then provides an extended introduction and background. The second chapter briefly indicates the PD framework for CFSs. The next two chapters refer to the detailed performance-modelling of their thermal properties (Chapter 3) and optical properties (Chapter 4). The last chapter concludes the thesis and the individual investigations.
It is a complicated matter to evaluate the performance of a prototype system holistically, since simulation programs evaluate standardized products, e.g. aluminium Venetian blinds. State-of-the-art tools and methods which can address the interrelated performance parameters of a CFS are not yet available. Such systems can be evaluated by measurements, but the high cost and the complexity of the measurements are limiting factors. The studies presented in this thesis confirmed that the results from performance measurements of CFSs can be interpreted by simulations, which means simulations can be used for the performance analysis of new systems. An advanced simulation model often needs to be developed and validated against measurements to prove its reliability before the model can be used. The procedures described can be used in the initial stages of PD to foresee the consequences of the innovations involved, and to assist in the development with iterative testing to meet the requirements.
The research showed that, by improving the fenestration system, the overall building energy demand can be reduced by optimizing lighting, heating and cooling. Indoor environment quality can be improved using a careful shading strategy and maximizing the use of daylight. Recent developments in building simulation programs have made it possible to carry out annual, dynamic and climate-based energy evaluation of complex fenestration.
The case study of the development of a slim window frame made of glass fi-

bre reinforced polyester (GFRP) demonstrated that this composite material is suitable for window frames. The combination of the low thermal transmittance and high load capacity of the material resulted in a window with a positive net energy gain net energy gain (NEG). Furthermore, the window uses the glazing cavity to supply outside air to the room, which means that some of the heat loss of the window can be regained by preheating the incoming air, which increases the net energy gain of the window. However, the usage of the window for this purpose is limited by the low heat recovery efficiency, which decreases with increasing airflow. The heat balance of the ventilated window is quite different from the heat balance of a standard window. The theoretical heat balance of the ventilated window was defined in the study.

The research for this thesis investigated the properties of various shading systems, including an analysis of their visual comfort. Simulations of daylight, lighting demand and glare were accomplished using ray-tracing simulations in the software package Radiance. The results from these investigations demonstrate that it is possible to simulate the performance of special shading systems, such as micro-structural shading or light-redirecting systems, but that advanced analysis is needed to evaluate CFS: a simple evaluation, e.g. using the $g - value$ or $U_w - value$, would not provide sufficient information about the new properties. A bi-directional description of the optical properties of the shading system was used to investigate lighting conditions, glare and NEG under various incident angles.

The overall conclusion of the thesis is that it is possible to develop and optimize any CFS with the help of computer performance modelling. The PD methods can clearly identify the objectives of the investigation and set out the appropriate way to achieve the optimal solution.

Resumé

Forskningen der præsenteres i denne ph.d.-afhandling viser, hvordan produktudvikling PD af komplekse vinduessystemer CFSs kan faciliteres af edb-baserede analyser for at forbedre energieffektiviteten af vinduessystemer, samt til at forbedre indeklimaet.
Det første kapitel definerer hypotesen og målet med afhandlingen, som efterfølges af en udvidet introduktion og baggrund. Det tredje kapitel foreslår, i korte træk, et produktudviklingsforløb der er egnet til CFSs. Det fjerde og femte kapitel refererer til detaljeret modellering af termiske egenskaber (kapitel 4) og optiske egenskaber (kapitel 5) af CFSs. Det sidste kapitel konkluderer afhandlingen og de enkelte undersøgelser. Det er kompliceret at udføre en holistisk vurdering af ydeevnen af prototyper, da simuleringsprogrammer evaluerer standardiserede produkter såsom alu-persienner. State-of-the-art værktøjer og metoder, som kan adressere interaktionen mellem forskellige ydelsesparametre, er undersøgt. Det er muligt at vurdere prototyper ved målinger, men den høje omkostning og kompleksitet af målingerne er begrænsende faktorer. Undersøgelserne i denne afhandling bekræftede, at resultaterne fra målingerne af ydeevne kan fortolkes ved simuleringer, og dermed kan simuleringer bruges til at udføre analyser af ydeevne for nye CFSs. En avanceret simuleringsmodel skal ofte udvikles og valideres ved målinger, før modellen kan genbruges. Valideringen af simuleringer mod målingerne viste pålideligheden af simuleringer. De beskrevne procedurer kan anvendes på de indledende stadier af PD til at forudse konsekvenserne af innovative tiltag og sigter mod en iterativ udviklingsproces indtil de opstillede krav er opfyldte. Det blev påvist, at ved at forbedre vinduessystemet, kan det samlede energibehov for bygninger reduceres ved at optimere dagslys, varme og afkøling. Indeklimaets kvalitet kan forbedres ved en omhyggelig solafskærmningsstrategi og ved at maksimere brugen af dagslys. Den seneste udvikling i bygningssimuleringsprogrammer gjorde det muligt at udføre en årlig, dynamisk og klimabaseret energiberegning for CFSs.
Casestudiet om udviklingen af en vinduesramme fremstillet af glasfiberarmeret polyester GFRP viste, at dette kompositmateriale er egnet til vinduesram-

mer. Et vindue med positivt energitilskud NEG og en slank vinduesramme blev udviklet ved en kombination af en lav termisk transmission og høj materialestyrke. Endvidere blev et ventileret vindue, hvor udeluft tilføres efter at have passeret det ene glashulrum, undersøgt. Ved dette koncept kan en del af varmetabet af vinduet genvindes til forvarmning af luft som tilføres og dermed øge nettoenergigevinster af vinduet. Imidlertid er brugen af vinduet til et sådant formål begrånset af varmegenvindingseffektivitet i ventilationssystemet, som falder med forøgelsen af luftstrømmen. Varmebalancen for det ventilerede vindue adskiller sig betydeligt fra varmebalancen for et standardvindue. Den teoretiske varmebalance for det ventilerede vindue blev defineret i undersøgelsen.
I denne afhandling blev egenskaber for flere solafskærmningssystemer undersøgt, herunder en analyse af den visuelle komfort. Simuleringerne af dagslys, lysbehov og blænding blev udført ved ray tracing simuleringer i softwaren Radiance. Resultaterne fra disse undersøgelser viste, at udførelsen af unikke solafskærmningssystemer kan simuleres, såsom mikro-strukturelle solafskærmninger eller lysdirigerende systemer. Det blev vist, at en avanceret analyse er nødvendig for at vurdere en CFS, en simpel evaluering som f.eks. g-$værdi$ eller $U_w - værdi$, ikke vil give tilstrækkelig viden om de nye egenskaber. Bidirektionel beskrivelse af de optiske egenskaber af solafskærmningssystemet blev anvendt til undersøgelse af lysforhold og blænding samt NEG under forskellige indfaldsvinkler.
Den overordnede konklusion er, at det er muligt at udvikle og optimere ethvert CFS ved hjælp af edb-baseret modellering. PD metoderne kan klart identificere målene for undersøgelsen og fastsætte en passende måde at opnåden optimale løsning.

Contents

List of Figures

List of Tables

Acronyms

ASHRAE	American Society of Heating, Refrigeration and Air-Conditioning Engineers
BBM	Black-Box-Model
BSDF	bi-directional scattering function
CFD	Computational Fluid Dynamics
CFS	Complex Fenestration System
DA	daylight autonomy
DC	daylight coefficient
DF	daylight factor
DGP	Daylight Glare Probability
DOE	Department of Energy
EPBD	Energy Performance of Building Directive
GFRP	glass fibre reinforced polyester
GHB	Guarded Hot Box
HVAC	Heating, Ventilation, Air Conditioning
IA	incidence angle
IEA	International Energy Agency
IESNA	Illuminating Engineering Society of North America
ISI	Institute for Scientific Information

ISO	International Organization for Standardization
LBNL	Lawrence Berkeley National Laboratory
LPD	lighting power density
MSPSS	micro-structural perforated shading screen
NEG	net energy gain
NIR	near-infrared
PD	product development
SHGC	solar heat gain coefficient
TPM	three-phase method
TRY	test reference year
UDI	useful daylight illuminance
WPI	working plane illuminance

Nomenclature

Symbol	Units	Description
A_f	m^2	Projected frame area
A_g	m^2	Projected visible glazing area
A_w	m^2	Projected window area
$U-value$	W/m^2K	Thermal transmittance
$U_f-value$	W/m^2K	Thermal transmittance of a window frame
$U_g-value$	W/m^2K	Thermal transmittance of a glazing material
$U_w-value$	W/m^2K	Thermal transmittance of a single window
l_Ψ	m	Visible perimeter of glazing
Ψ	W/mK	Linear thermal transmittance due to combination of thermal effect of the glazing, spacer and frame
$g-value$	$-$	Total solar transmittance
τ_{sol}	$-$	Solar transmittance
τ_{vis}	$-$	Light transmittance
τ_{sw}	$-$	Total solar energy transmittance of a window
τ_g	$-$	Solar energy transmittance of a glazing
τ_f	$-$	Solar energy transmittance of a frame
	$-$	Solar transmittance of a frame
NEG	$kWh/(m^2year)$	Net energy gain
I	kWh/m^2	Coefficient for solar gains
D	kWh	Coefficient for heat loss
E	$kWh/(m^2year)$	Total primary energy demand of buildings
$U_{w,trans,ext}$	W/m^2K	Thermal transmittance of a ventilated window
$U_{w,vent}$	W/m^2K	Ventilation heat loss of window
$U_{w,trans}$	W/m^2K	Total thermal transmittance of a window in a ventilated window
$Q_{w,trans}$	W	Energy flux from indoor environment to window
$Q_{w,trans,ext}$	W	Energy flux from window to outdoor environment
$Q_{air,vent}$	W	Energy flux to heat up ventilated air to room temperature

$Q_{w,vent}$	W	Advective energy flux (energy transported by ventilated air)
A_w	m^2	Window area
h_{ci}	W/m^2K	Indoor convective heat transfer coefficient
h_{ce}	W/m^2K	Outdoor convective heat transfer coefficient
h_{ri}	W/m^2K	Indoor radiative heat transfer coefficient
h_{re}	W/m^2K	Outdoor radiative heat transfer coefficient
c_p	(J/kgK)	Specific heat capacity
ϕ	m^3/s	Volume flow
ρ	kg/m^3	Density
q_{sp}	W/m^2	Heat flow rate density of sample
ϕ_{in}	W	Corrected metering box heat input
ϕ_{sur}	W	Surround panel heat flow rate
ϕ_{edge}	W	Edge zone heat flow rate
T_{si}	$^\circ C$	Indoor surface temperature of a window
T_{sie}	$^\circ C$	Outdoor surface temperature of a window
$T_{gap,in}$	$^\circ C$	Air temperature in a window inlet valve
$T_{gap,out}$	$^\circ C$	Air temperature in a window outlet valve
T_{ni}	$^\circ C$	Interior environmental temperature
T_{ne}	$^\circ C$	Exterior environmental temperature
T_{vent}	K	Mean ventilation air temperature
W	m	Width
H	m	Height
Δ	$-$	Uncertainty

The structure of the thesis

About the thesis

This doctoral thesis consists of two parts. **Part I - Introduction and summary**, describes and discusses the background, methods, results, and discussion and conclusion of the thesis. Part I is supported by and refers to **Part II - Appended papers** which contains research publications in the form of the four scientific articles published or submitted to Institute for Scientific Information (ISI) journals. The research is presented in the four main ISI papers. Their connection is illustrated in Figure 1. There are three main aspects: product development, thermal performance modelling, and optical performance modelling. Product development is represented in every article. The focus in Papers I and II is on the thermal performance modelling of fenestrations, and Papers III and IV are oriented to the optical performance modelling of fenestrations, but both aspects are mentioned in every article.

Thesis outline - Part I

The motivation for the research in this thesis is presented in Chapter 1, followed by an introduction and background, including energy requirements, performance modelling methodology and terminology. Chapter 2 describes the product development methods for developing CFSs. Chapter 3 focuses on discussing the thermal performance modelling of CFSsand presents results from the investigations. Chapter 4 discusses optical performance modelling of CFSs and presents results of the investigations. The conclusions are given in Chapter 5.

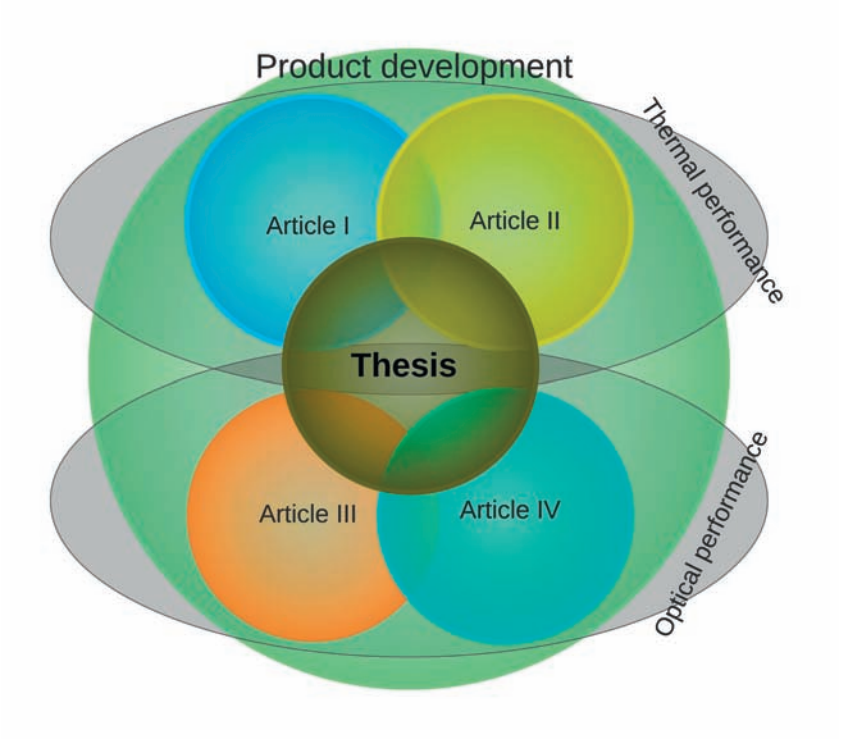

***Figure 1**: Visualization of the whole project structure.*

List of Publications

The ISI articles are listed below, including the abstracts:

Paper I
D. Appelfeld, C.S. Hansen & S. Svendsen, *"Development of a slim window frame made of glass fibre reinforced polyester"*, Published in: Energy & Buildings

Abstract
This paper presents the development of an energy efficient window frame made of a GFRP material. Three frame proposals were considered. The energy and structural performances of the frames were calculated and compared with wooden and aluminium reference frames. In order to estimate performances, detailed thermal calculations were performed in four successive steps including solar energy and light transmittance in addition to heat loss and supplemented with a simplified structural calculation of frame load capacity and deflection. Based on these calculations, we carried out an analysis of the potential energy savings of the frame. The calculations for a reference office building showed that the heating demand was considerably lower with a window made of GFRP than with the reference frames. It was found that GFRP is suitable for window frames, and windows made of this material are highly competitive in their contribution to the energy savings. A rational product development method was followed, and the process clearly identified the objectives of the investigation and set out the appropriate way to attain them. Using simple rational development methods, a well-defined and effective window was achieved smoothly and quickly, as is illustrated in the case study.

Paper II
D. Appelfeld & S. Svendsen, *"Experimental analysis of energy performance of a ventilated window for heat recovery under controlled conditions"*, Published in: Energy & Buildings

Abstract
A ventilated window in cold climates can be considered as a passive heat recovery system. This study carried out tests to determine the thermal transmittance of ventilated windows by using the Guarded Hot Box. By testing under defined boundary conditions, the investigation described the heat balance of the ventilated window and clarified the methodology for thermal performance evaluation. Comparison between windows with and without ventilation using

the window-room-ventilation heat balance revealed that a ventilated window can potentially contribute to energy savings. In addition, it was found that a significant part of preheating occurred through the window frames, which positively influenced the heat recovery of the window but increased the heat loss. Results also showed that increasing air flow decreased the recovery efficiency until the point when the additional thermal transmittance introduced by the ventilation was higher than the effect of heat recovery. Accordingly, the use of the ventilated windows might be most suitable for window unit with low ventilation rates. The results correlated with theoretical calculations in standards and software. However, the concept of a window thermal transmittance (U_w) value is not applicable for energy performance evaluation of ventilated window and requires deeper analysis.

Paper III

D. Appelfeld, A. McNeil & S. Svendsen, *"An hourly-based performance comparison of an integrated micro-structural perforated shading screen with standard shading systems"*, Published in: Energy & Buildings

Abstract

This article evaluates the performance of an integrated micro-structural perforated shading screen (MSPSS). Such a system maintains a visual connection with the outdoors while imitating the shading functionality of a venetian blind. Building energy consumption is strongly influenced by the solar gains and heat transfer through the transparent parts of the fenestration systems. MSPSS is angular-dependent shading device that provides an effective strategy in the control of daylight, solar gains and overheating through windows. The study focuses on using direct experimental methods to determine bi-directional transmittance properties of shading systems that are not included as standard shading options in readily available building performance simulation tools. The impact on the indoor environment, particularly temperature and daylight were investigated and compared to three other static complex fenestration systems. The bi-directional description of the systems was used throughout the article. The simulations were validated against outdoor measurements of solar and light transmittance.

Paper IV

D. Appelfeld, S. Svendsen, *"Performance of a daylight-redirecting glass-shading system"*, Published in: Energy & Buildings

Abstract

This paper evaluates the daylighting performance of a prototype external dy-

namic shading and daylight redirecting system, and the main focus is on the performance simulation. The demonstration project was carried out on a building with an open-plan office. Part of the original façade was replaced with the prototype façade. This layout allowed the use of the same orientation and surroundings for both facçades. The working plane illuminance was measured over several months and the measurements were accompanied with annual daylight simulations. The prototype system improved the daylighting conditions compared to the original system. The visual comfort was evaluated by glare analysis and the redirected daylight did not cause an additional discomfort glare. The higher utilization of daylight can save 20% of the lighting energy. The thermal insulation of the fenestration was maintained, with slightly increased solar gains, but without producing an excessive overheating.

Part I

Introduction and summary

Chapter 1

Introduction and background

In recent decades, there has been an increased national and international focus on reducing the energy demand of buildings [1, 2].Buildings currently account for 40% of the energy use in most countries. So buildings hold great potential for cost-effective energy savings [3]. The International Energy Agency (IEA) has identified the building sector as one of the most cost-effective sectors for reducing energy consumption, with estimated potential energy savings of 1509 million tonnes of oil equivalent (Mtoe) by 2050 [4]. Lighting represents almost 20% of global electricity consumption. This consumption is similar to the amount of electricity generated by nuclear power [5]. Electrical lighting often accounts for between 20-40% of energy used in commercial buildings [6].
Interest is growing among architects and consultants in intelligent building components which can achieve energy effectiveness in buildings, complying with the strict energy codes and national emission reduction goals [7, 8].
Contemporary commercial and institutional buildings have high internally-generated loads from people, lights, equipment and their well-insulated envelopes, which cause low heating and high cooling loads [9] compared to residential buildings, which have relatively low internal loads vs. their envelope loads. Most energy used in buildings is attributed to heating, cooling and electrical lighting. Windows, façades and shading systems affect all three, and are among the most crucial elements in the building envelope, which also affects the indoor environment. Detailed evaluation of the interaction between façade performance, energy demand and the indoor environment needs to be carried out. By optimizing window elements, the energy consumed for heating, cooling and electric lighting can be reduced. Optimization strategies take account of heating by increasing solar gains, cooling by providing solar protection and lighting by utilizing daylight [10]. Traditional windows cannot do all this. The traditional window needs to be combined

with a shading system in what is known as a Complex Fenestration System (CFS). Since a significant portion of energy in buildings is devoted to lighting and ventilation, there is a large energy saving potential in the use of advanced solar shading systems.
Today, a window is considered as energy-efficient if it has a low thermal transmittance, $U_w - value$. However, that is not sufficient to describe a window's energy performance, because the evaluation should address the interaction between window performance, energy demands and the indoor environment. Another currently used evaluation parameter is normal-incidence light transmittance, which is not an accurate indicator for angular-dependent systems because they need a bi-directional description [11]. An angular-dependent system is any fenestration system which is not simply a continuous layer, such as pane of glass or coating.
The factors to be taken into account are thermal transmittance, solar energy transmittance, visual transmittance, durability, shape, cost, effect on a building's energy consumption, including the supply of fresh air, artificial light savings by use of daylight, and the visual and thermal comfort of occupants. These performance parameters can be split into two categories, **thermal** and **optical** performance. The challenge is to evaluate these parameters in the interconnected context, since some of the functions conflict, e.g. increasing solar gains in winter while providing shading in summer [9]. The simulation programs currently available cannot easily evaluate unique CFSs using standardized methods, since they are mostly created to evaluate specific solutions. All these prerequisites and parameters indicate the need for comprehensive performance analysis of CFS solutions. Such detailed evaluation can reveal the potentials of unique fenestration solutions. Moreover, detailed evaluation can speed up the introduction of innovative solutions to the market by spreading awareness and better understanding of the complex properties involved.

1.1 Hypothesis and objectives

The central hypothesis of the thesis is that by using comprehensive modelling of the thermal and optical performance of a CFS it is possible to develop a CFS which will serve several functions, fulfil new energy regulations, ensure comfortable thermal and visual indoor environment, and form the basis for the design of low-energy buildings in the future.

The aim of the research was to investigate and establish product development methods for the development of new advanced energy-effective window systems. These systems will work as complex lighting systems with improved energy performance with respect to heat loss, solar gain, solar shading, visual transmittance and ventilation. Such a complex lighting system is considered in relation to both newly built low-energy buildings and the refurbishment of existing buildings.

The main problem discussed in this thesis is the accessibility and accuracy of tools and methods to carry out an adequate performance evaluation of newly developed fenestration technologies, e.g. windows, façades, shadings, and their combinations. The focus is on performance prediction using simulations with respect to energy use and indoor climate. The objectives for the development of CFSs are visualized in Figure 1.1, including their multifunctionality.
The complexity and inaccuracy of current evaluation methods limits the effective implementation of new solutions in the construction industry. The limitations of the currently available simulation tools and testing methods can be overcome by performing state-of-the-art simulations. The performance of various CFSs was tested so that the simulations could be validated against measurements.
The main motivation for this research was to establish procedures for generating information that can be used during the product development of CFSs or during the initial phase of a building's design. Performance simulations are used in the early stages of building design to predict the impact of the given CFS on the overall performance of the building and ensure that the requirements of both legislation and client can be met. Furthermore, the predictions are needed to optimize building performance. The most difficult part is to describe the CFS's properties in sufficient detail to see the impact of the changes and innovation. The current practice simplifies the solar and

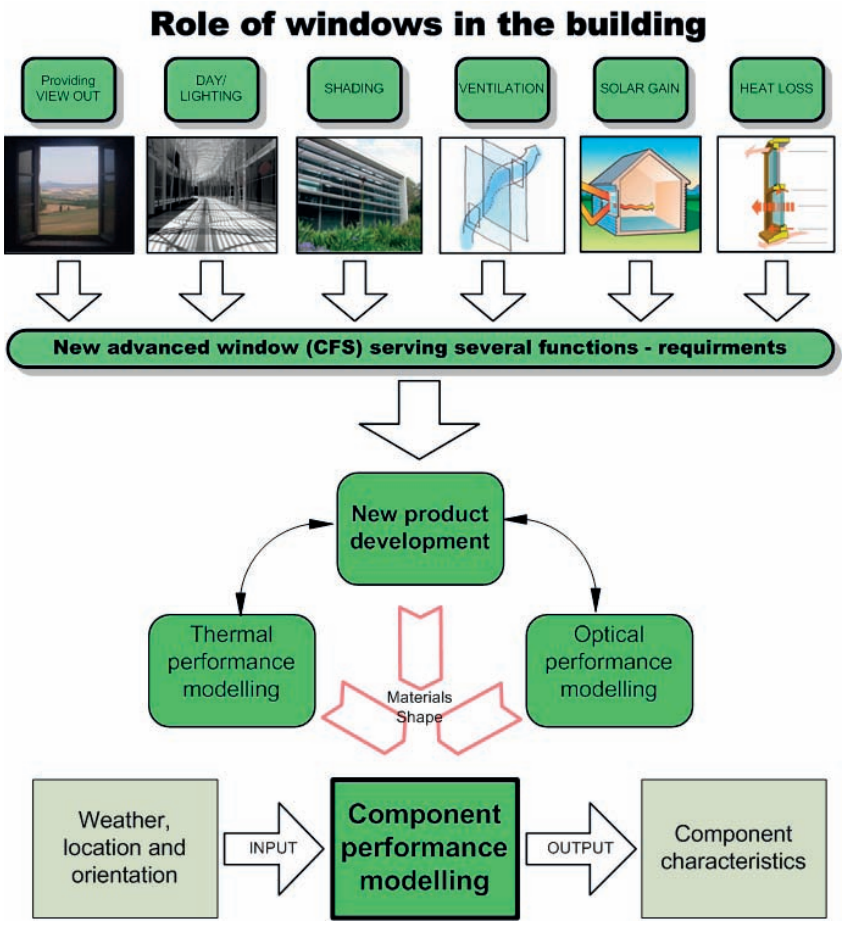

***Figure 1.1**: Schematic description of the objetive of the performance development of a CFS.*

thermal properties and makes debatable assumptions. The material properties and system's geometry are often replaced with similar existing solutions. In many cases, this removes the innovative element of the solution.

1.1.1 Limitations

The development and testing process presented in this thesis is an attempt to deal with the performance evaluation of CFSs from a scientific perspective. The aim is not a perfect CFS, because there is no generically correct solution for all situations and each has different requirements. What the thesis is suggesting is a process for analytically achieving the optimal solution.

1.2 Background

Windows are typically responsible for a large fraction of the heat loss in buildings because windows, and especially window frames, have higher thermal transmittance than other parts of the building envelope. However, windows can contribute to heating by allowing solar gains [12]. Another major feature of windows is providing daylight. Daylight is the preferred source of lighting for human beings and has a positive effect on both the environment and productivity [13]. Furthermore, using daylight reduces the energy used for artificial light [14].
Windows are also mediators of ventilation and air exchange in both old and new buildings. The thermal transmittance of façades has been reduced in recent decades by introducing glazing with coating, sealed glazing, and limiting heat loss with heat breaks in the frames. Window frames have been improved by using new materials and new designs which has led to highly insulated and high performance windows [15, 16]. Nevertheless, although the natural air exchange of the façade through air leaks and air infiltration has been significantly reduced, windows are still large contributors of heat loss. To achieve standards for the total energy consumption of buildings, we have to include heating, cooling, ventilation, hot water and lighting [17]. So additional ventilation, possibly using a heat exchanger, should be considered for energy consumption and to enhance the quality of the indoor environment [18, 19, 20].
The increased thermal resistance of building envelopes can lower heating loads, but also increase the risk of overheating by capturing excessive solar gains, especially in office buildings. Moreover, glazed areas in new office buildings are getting larger, which increases solar gains during the cold periods of year and increases the working plane illuminance working plane

illuminance (WPI). However, during the warmer seasons, these large glazed areas can generate overheating and glare, making solar shading necessary. Removing overheating using mechanical cooling and ventilation is expensive and can negate the savings from solar gains in winter. Cooling loads are becoming increasingly important [21, 22]. So solar shading is an effective strategy to reduce overheating and diffuse direct sunlight to reduce energy consumption. There are many different shading systems, and it is difficult to precisely describe the performance of a non-standard solution, especially in the overall context of a building.

Transparent parts of building envelopes serve several functions [21]:

1. They provide light transmittance, and daylight utilization.
2. They give thermal insulation to ensure a healthy and comfortable indoor environment.
3. They should provide sufficient solar energy transmittance during cold months, to reduce heating demand.
4. They should prevent indoor space from overheating during warm months by shading excessive solar gains.
5. 5. They provide a view of the outside which is desirable and should be unobstructed and maintained.

1.3 Energy, environment, indoor climate

The purpose of CFSs is to help reduce the building's overall annual energy consumption and eliminate heat loss through the envelope when the space is heated. The transparent part of a CFS is a source of renewable energy in the form of solar energy. Furthermore, CFSs provide a direct connection to the outdoors, providing a view of the outside and a supply of fresh air through windows that can be opened. In this way, they contribute to a comfortable and healthy indoor climate.
The immediate goal of the CFS is to provide occupants with a cost-effective and easy way to operate and maintain indoor spaces without a negative impact on health and comfort.

The sustainability of the CFS is ensured by focusing on three main factors:

- **Energy** - A CFS provides a positive contribution to the energy balance of buildings. It provides thermal insulation and enables solar gains.

- **Environment** - Every building interacts with the surrounding environment. So the performance of a CFS depends on the surrounding conditions and the solution has focus on utilizing its location.

- **Indoor climate** - The thermal and visual comfort of occupants requires a healthy and comfortable indoor climate supplied with daylight and fresh air.

All these aspects interact with each other. The diagram in Figure 1.2 illustrates the interaction. Windows and transparent elements of a façade in general should positively contribute to human health and well-being, because the indoor environment can be affected by them. Moreover, the transparent areas work as a source of renewable energy.
When we are talking about CFSs, building energy consumption is heating, lighting and cooling, and they interact with each other; see Figure 1.3. The heating is influenced by the solar gains through a fenestration. When the façade is extensively transparent, it can provide large solar gains, which increase the risk of overheating and therefore influence cooling loads. Energy is needed to increase the ventilation air flow or for cooling to reduce the overheating. With optimal use of solar shading, this energy can be reduced because the overheating can be avoided. When enough daylight is provided to reach the required level of WPI, artificial light can be turned off. This also reduces cooling loads because lighting produces heat. On the other hand, the low solar energy transmittance of the façade will increase the heating loads during the heating season because the solar gains will be smaller. Since a significant portion of energy in buildings is devoted to lighting and ventilation, daylight and cooling have considerable energy-saving potential [23].

1.4 Product development of CFS

The development of a fenestration system is a complex process because a holistic solution is often required. The transparent parts of a building envelope always serve several purposes, as mentioned in Section 1.2 on page 8. Furthermore, fenestration affects building energy: firstly with the heat exchange to outdoors, thus *thermally*, and secondly by allowing light to penetrate indoors, thus *optically*. Both factors explicitly affect the indoor environment. The design and development process of a CFS is no trivial task because it involves a web of interdependent variables [10]. So this thesis presents a sequence of steps. The first step is to identify the purpose and

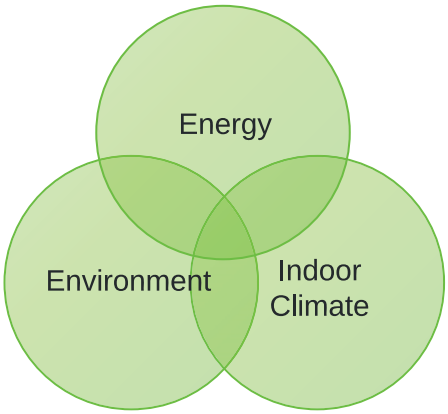

***Figure 1.2**: Interaction between the three sustainable aspects of windows/CFS*

need for fenestration and quantification and qualification of these requirements is suggested. The whole process is discussed in Section 2 on page 29 and in the papers in Part II.

1.5 Performance simulations of CFS

There is usually a lack of information and knowledge in the early stages of design to understand the complexity of the interrelated performance indicators for an actual building. The building industry needs a comprehensive reference which describes both the fenestration design and the performance of such systems in a building [10].
In many cases, the results from performance simulations can be hard to understand in the holistic context. This thesis suggests a framework for the design of high performance CFSs which might facilitate the usability of performance simulations. The CFS serves several functions which makes it difficult to decide the best solution in the overall context. For example, the system might be good from one perspective, allowing lots of daylight and solar gains, but from another perspective might run the risk of overheating. The performance modelling suggested is designed to reduce the energy consumption of buildings and to improve the quality of the indoor environment. Fenestration systems which incorporate innovative technology are often not included in commonly used building performance simulation programs, e.g.

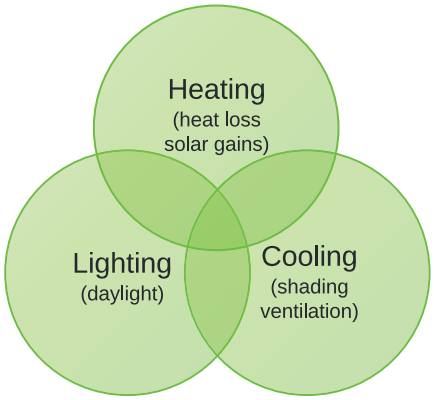

***Figure 1.3**: Interaction between heating, cooling and lighting*

ESP-r [24], TRNSYS [25], EnergyPlus [26]. So it may be difficult to predict their performance and further improve new and existing solutions. Moreover, designers and building owners cannot fully indicate the advantages of these innovative solutions [27]. Conservative assumptions of performance are often made when evaluating the CFS's impact on a building. The inaccuracy of current performance prediction limits the introduction of innovative and advanced technology on the market.
Current building simulation programs mainly focus on performance simulations of buildings with little detail about the performance of CFS. They usually allow only standardized and commonly used shading systems, and the use of new materials, shapes and concepts is limited. The latest version of ESP-r integrates a module in the program which allows the input of information about state-of-the-art CFS solutions [28]. This allows any CFS to be used without modelling all the details in the program.
With regard to CFS product development, it is important to move the focus from the building to the CFS, but always retaining the connection, because the building's energy consumption is influenced by the CFS. There are several reasons to focus on the façade in performance simulations:

- Newly developed façades are often too complex for modelling in the building simulation programs. This often slows down the development of innovative and unique solutions. Moreover, market penetration would limp along because designers would not be able to employ the

new features.

- Accuracy plays a major role, because designers need to know the performance of the real product. In some cases, the product's improvement cannot be discovered because the inaccuracy of the simulation equals or exceeds the performance improvement. This is especially the case when the performance depends on the new and unique features of the system.

- To further develop new and high performance CFS solutions, it has to be possible to carry out comparison and benchmarking against existing solutions.

1.5.1 Thermal performance modelling

Calculating the thermal properties of CFS elements is important for estimating the heat loss through the fenestration. The energy performance can be evaluated at several levels, e.g. starting with the heat loss coefficient of a window frame and ending with a study of window's effect on the building's overall energy consumption. It is advisable to carry out multiple calculations, starting with simple evaluations and continuing to a more comprehensive assessment to find out the overall performance.

The thermal transmittance of a window

A window's thermal transmittance, its $U_w - value$, is the basic indicator of the thermal properties of all windows and façades. The standard $U_w - value$ calculation is described in ISO 10077-2 [29]. There are several programs on the market specifically designed for these calculations, e.g. Therm [30], WinIso [31] or Heat2 [32]. These programs can solve the conductive and convective heat transfer equations and they use radiation models to calculate heat loss in accordance with ISO 15099 [33]. The standard calculation of a window's thermal transmittance is based on the thermal transmittance of the glazing $U_g - value$ and the frame $U_f - value$, and on the linear transmittance of the glazing edge Ψ [29, 34]. The $U_w - value$ of the whole window is obtained by Eq. 1.1. The $U_f - value$ is calculated in the absence of glazing, which is replaced with a highly insulated panel to eliminate the effect of the thermal bridge at the glazing edge and the spacer. ISO 10077-2 requires the calculation of the linear thermal transmittance of a glazing edge, in other words, the spacer. The edge effect is different for every combination of frame, spacer and glazing, and it is necessary to calculate it for each individual

solution. For the calculation of Ψ, the spacer is replaced with a simplified shape with an equivalent thermal conductivity [35].

$$U_w = \frac{U_g \times A_g + U_f \times A_f + \Psi \times l_\Psi}{A_w} \tag{1.1}$$

The thermal transmittance of a ventilated window

In this research, an experimental study of a ventilated window with heat recovery was carried out; see Paper II and Chapter 3.2 for detailed information. The principle of the thermal transmittance of a window, $U_w - value$, is not directly applicable for a ventilated window. The ventilated window can serve two additional purposes to a regular window: they provide a supply of fresh air and they preheat this air by recovering the heat loss of the window. The schematic picture of a ventilated window is shown in Figure 1.4. The thermal properties of the ventilated window depend on various parameters, including the unit itself, its boundary conditions, the direction of heat flux, temperature differences, and the airflow.
The difference from the standard understanding of a window's thermal transmittance, $U_w - value$, is that the heat loss through the window is increased by introducing the air flow, but is partly reclaimed by the air flow. Since the ventilation changes the heat balance of the window/building and generates an additional heat loss, a different evaluation process is needed for the heat balance definition. Various studies have provided models for specific examples and ideas for improving the performance of ventilated windows, but the experimental results are rarely available [36, 37, 38]. The energy balance of the ventilated window has been documented in several mainly theoretical and numerical investigations [20, 39, 36, 40, 41].

Net energy gain of window

As the next step, the net energy gain net energy gain (NEG) method was used to calculate the effect of the window in the context of heat losses and solar gains [12, 42]. There are various ways of assessing the energy performance of a window, but it is clearly insufficient to evaluate the window in terms of thermal transmittance only. To achieve a positive NEG, a large glazing, slim frames and glazing with high transmittance are desirable, because these improve both the thermal transmittance and the solar gains [16, 15]. The NEG method is based on the window's solar gains minus the window's heat loss during a standard period, which is defined as the heating season depending on the outdoor air temperature. This takes into account the tilt and relative

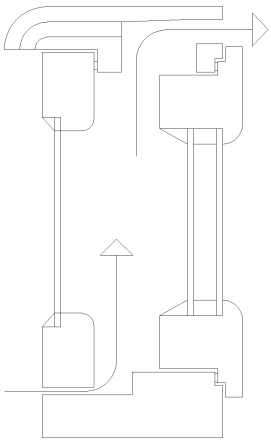

***Figure 1.4**: SSchematic picture of the ventilated window used, with air flow marked.*

orientation of the window in the reference building [12]. Sometimes, a window with a very low $U_w - value.$ has a lower NEG than a window with a higher $U_w - value.$
For example, a window with $U_w - value.$ of 1.27 W/m^2K ($U_f - value$ 1.33 W/m^2K) can have higher NEG than a window with $U_w - value$ 0.79 W/m^2K ($U_f - value$ 0.75 W/m^2K) [43, 15]. This results from the greater area of glazing in the case of the window with the higher $U_w - value.$, which means that the heat loss can be compensated by the extra solar gains. The NEG formula is described by Eq. 1.2.

$$NEG = \tau_{sw} \times I - U_w \times D \tag{1.2}$$

where D is the coefficient for heat loss and I is the coefficient for solar gains. Both coefficients depend on the location and window orientation. For Denmark, I is 196.4 kWh/m^2 and D is 90.36 kKh [12]. This approach to an energy performance evaluation allows an easy and quick comparison of various windows.
The total solar energy transmittance of a window τ_{sw} is needed for the calculation of NEG and is combined from the solar energy transmittance of the glazing and frame; see 1.3 [33].

$$\tau_{sw} = \frac{\sum \tau_g \times A_g + \sum \tau_f \times A_f}{A_w} \tag{1.3}$$

Analysis of window impact on building energy use

The last step in the thermal energy performance assessment was a comprehensive evaluation of the effect of the window on the energy consumption of the building. The energy impact on an office building, a residential building, and a single-cell office is evaluated in different parts of this thesis and the details are described in the appended papers.
Again, several different software programs were used for these analyses:

- **iDbuild** is a building simulation tool for the evaluation of energy performance and indoor environment based on hourly weather data. The program is able to illustrate how performance parameters, individually and in combination, affect energy performance, thermal indoor environment, air quality, and daylight conditions [44].
- **Be06**[1] calculations were carried out in accordance with the procedure in the EU Directive on the energy performance of buildings and Danish Building Regulations [2, 1, 17]. The Be06 software calculates the energy supply needed for any type of building for room heating, ventilation, cooling, hot water and artificial lighting, and compares it with the energy framework set by the Building Regulations [45].
- **ESP-r** an integrated energy modelling tool for simulating the thermal, visual and acoustic performance of buildings and their energy use associated with environmental control systems. The system is equipped to model heat, air, moisture and electrical power flows in a user-determined resolution [46, 24]. ESP-r was used because its Black-Box-Model (BBM) enables it to model the optical properties of CFSs without having to model the details of the façade [28].

It has been found that bi-directional information about fenestrations provides a more accurate estimation of heating and cooling loads [47]. For this purpose the BBM with a resolution of 5°of azimuth and altitude is ideal. The standard method of evaluation, in which only the normal-incidence value of transmittance is used, overestimates heating demand by up to 23% and underestimates cooling demand by as much as 99% compared to using bi-directional information according to a study by Kuhn [48, 49].

[1]Program Be06 has been replaced by the more recent version of the program, Be10. However, Be06 was the current version of the program when the research for Paper I was carried out.

1.5.2 Optical performance modelling

This section gives some background on optical performance modelling, including the simulation techniques and methods used in this research. Papers III and IV focus on the optical performance and characterization of various newly developed and unique shading systems. Paper I touches on the topic too, mainly in connection with the investigation of the NEG and solar transmittance of the window developed.
Almost every fenestration system provides some level of optical connection between interior and exterior. The connection is described by the transmittance of the CFS, which depends on the incidence angle and the solar radiation. The amount of solar energy transmitted through a window at a given time depends on its location, orientation and system geometry. The program Radiance was used to investigate daylighting and visual comfort. Radiance is an accurate backward ray-tracing Unix-based program[50]. Radiance has been validated in similar research [51, 52]. Window6 was used for the generation the bi-directional scattering function (BSDF) matrices describing the transmittance of windows and CFSs [30]. The program iDbuild was mainly used for the calculation of energy performance, thermal indoor environment, but also for daylighting conditions in an office [44]. The program WIS was used to calculate the directional transmittance of the glazing or CFS [53]. The programs Columen [54], Spectrum [55] or Caluwin [56] were used to calculate the visible and solar transmittance of various glazing materials.

Daylight

Visual comfort and daylight are central points for providing buildings with a healthy indoor environment [57]. Increased use of daylight and careful design of the lit environment have the potential for both health benefits and increased safety and productivity [58]. Design with daylight in mind can provide comfortable indoor daylight conditions without excessive solar gains [59]. Careful design and a well-defined fenestration solution can provide enough daylight without requiring a larger Heat, Ventilation, Air Conditioning Heating, Ventilation, Air Conditioning (HVAC) system than a windowless room. Such design combines shading, glazing and façade orientation with respect for the site and local climate. This can be achieved using an active or passive daylighting design that includes glare control or light redirection. Both components of daylight (direct and diffuse daylight) are important, because they determine not only indoor daylight conditions, but also cooling

loads, which are heavily impacted by direct sunlight [21].

Daylight simulations

The performance of any fenestration system varies during a year and is dependent on the sun position and sky distribution. Annual simulations provide useful information about a CFS and do not suffer from the drawback of standard static daylight simulations, which focus only on extreme conditions, e.g. on 21^{st} of December. Annual simulations are also more realistic because they use weather data measured over several years. The test reference year test reference year (TRY) weather file for Copenhagen, Denmark [60] was used in this research. Hourly weather data were used for the simulations because the resolution is sufficient and provides realistic results [61]. The daylight simulations were computer-based calculations mainly based on the sky conditions and information about a building, including its interior description. In the literature, annual daylight simulations are also referred to as dynamic daylighting simulations. They are conducted in steps using the three-phase method [62, 63], which is explained in the paragraph headed Three Phase Method below.

1 Create a sky model with irradiance/illuminance data.

2 Use time steps within working hours.

3 Make a Radiance simulation for each time step and each sensor position or rendering, i.e. view, daylighting and transmission matrix combination.

4 Assess how many times the required working illuminance is satisfied (or partly satisfied).

5 Count how much artificial light is needed to satisfy the minimum WPI.

Daylight evaluation matrices

There are several standards and design recommendations for working plane illuminance (WPI). This section defines the thresholds used for various daylight evaluation matrices. Annual evaluation is best for performance modelling because the evaluation of a single scenario would not reflect the real daylighting performance of a CFS. Moreover, information about useful daylight conditions in an indoor environment is more valuable than only knowing the conditions during extreme conditions. The commonly used daylight factor (DF) does not use any of the above-mentioned requirements and it does

not quantify the redistribution of direct light to provide diffuse illuminance. Furthermore, DF underestimates the daylight levels within a room for south-orientated rooms and overestimates the illuminance values for north-facing rooms [64]. Instead of DF, this thesis uses useful daylight illuminance (UDI) and daylight autonomy daylight autonomy (DA) [65, 66, 52, 67, 57].
DA is the percentage of hours satisfying the minimum design WPI out of the total number of working hours in a year [68]. The commonly used design WPI is between 300 - 500 lux.
The **UDI** matrix quantifies when daylight is perceived as useful for occupants. It is calculated as the percentage of the occupied working hours when the WPI is between the lower and upper threshold.
Several different WPI levels were used in the research for this thesis. They are based on a review of the following literature [66, 52, 69, 67, 70, 57, 71]:

- **100 lux** - Is considered as insufficient for performing tasks under daylighting conditions and it is the lower limit for UDI.
- **300 lux** - Is often considered as sufficient for performing working tasks.
- **500 lux** - Is described as the minimum WPI for office work and it is used as the threshold for DA analysis.
- **4500 lux** - 30% of people find horizontal illuminance above this level too high and uncomfortable [71]. The upper limit is not clearly defined in literature, so 4500 lux is used as the upper limit for UDI.

The midrange between 100 lux and 4500 lux is considered as usable for most occupants. Some subjects may consider some values in this range as uncomfortable, but these values should not be considered as useless, since every subject perceive illuminance levels differently[57, 71].

Three phase method

The three-phase method (TPM) is based on the daylight coefficient (DC) principle by which annual daylight simulations can be performed effectively with a relatively small amount of computational resources [72]. The DC approach subdivides the sky into divisions, and then the contribution from each division/direction is calculated independently. For more information, see the section below headed Bi-directional characteristics of acCFS on page 21. The TPM can generate both renderings and illuminance values. The renderings are mainly used for the analysis of a visual comfort, e.g. glare, and the illuminance readings are used for daylight distribution analysis. The TPM

is used to calculate the annual illuminance on a working plane throughout the thesis. The method makes separate calculations for the effect of the sky, outdoors, indoors and the fenestration, resulting in a vector with illuminance values $\boldsymbol{i}$ [63].

$$i = V \times T \times D \times s \tag{1.4}$$

Four matrices are generated and multiplied together in accordance with Eq. 1.4 [73, 63]. The Radiance program **rtcontrib** was used to generate the transmission results in the matrix form. The transmission of fenestration system matrix, **T** matrix, describes the bi-directional transmission through a fenestration. In the research for this thesis, the bi-directional scattering function (BSDF) matrix was either generated by the Radiance tool genBSDF [27] or by Window6 [30] or it was measured using a goniophotometer [74, 75]. The exterior daylighting matrix, **D** matrix, describes the light transmission between the sky and the fenestration and is divided into 145 subdivisions [76]. The interior view matrix, **V** matrix, describes the lighting scene indoors and defines either points for illuminance readings or views for renderings. The sky vector **s** describes the sky distribution by assigning luminance values to each patch representing sky directions. The sky was divided into 2305 patches in accordance with Reinhart's subdivision for detailed results [77].
The TPM approach reuses already generated matrices because some of them do not change over a year; e.g. when static shading is investigated then only one T-matrix is needed, because neither the exterior nor the interior changes over a year. In many situations, the sky is the only changing variable because the luminance of the sky is a time-dependent variable which continuously changes. Moreover, changing only one of the matrices makes it possible to investigate various aspects effectively: different orientations by changing the daylighting matrix; location by changing the sky vector; and different CFS by changing the BSDF matrix [63].

Glare

Optimally, a CFS should provide both visual comfort and sufficient daylight penetration. In many cases, these two features are in conflict, because introducing higher illuminance levels from daylight can implicitly cause glare problems. Glare analysis is needed because the view to the outside may include looking into direct sunlight [78]. Moreover, glare can create discomfort and reduce productivity. However, the perception of glare is often reduced, even under high glare index values, when working under daylighting conditions [79]. The perception of glare depends on view direction and position, sometimes referred to as the visual zone [71, 80]. So every analysis has to

define a view and preferably several different views. Daylight Glare Probability (DGP) was selected as the glare index, because it is based on an extensive human evaluation study [81, 82]. Furthermore, when glare is evaluated, the analysis should be made during working hours, which are often set between 8:00 and 18:00. An enhanced simplified Daylight Glare Probability (DGP) calculation method is appropriate for annual DGP analysis, because it makes it possible to include direct sunlight in the analysis [81]. Glare readings were made from rendered images in Radiance, because it is not possible to evaluate the discomfort glare just from horizontal illuminance [57].

Electrical light savings from using daylight

Apart from people favouring daylight as a light source for visual tasks, there is also a desire to save electricity for artificial lighting. The use of daylight depends on the daylight-linked lighting control strategy, so the percentage of working hours in which daylighting conditions are satisfied has to be found if these savings are to be evaluated. The potential artificial light energy savings are equal to the lighting energy which can be replaced by daylight. The substitution is linear and thus idealized. The baseline is a situation in which no daylight is used. The WPI for office work required by the European standard CEN-EN 15251 is 500 lux and the Illuminating Engineering Society of North America (IESNA) requires 300 lux [70, 83, 57]. However, no minimum light power density lighting power density (LPD) has been set to reach the required WPI. Standard EN 15193 prescribes an LPD of 15 W/m^2 as the basic and 25 W/m^2 as the comprehensive requirement [84].
Since daylight illuminance decreases with the depth of space, more artificial light is needed at the back of a room. It is therefore appropriate to split the space into a few reasonably sized zones which can be evaluated individually. If the minimum required WPI can be met by daylight at the back of each zone, this means that the whole zone is lit sufficiently.
In the research for this thesis, three different daylight-linked lighting control strategies were used:

1 **On/off-control:** This controls the electric lighting within a zone. Lighting is switched off when the WPI from daylight is sufficient.

2 **Bi-level switching control:** Half of the lamps in a zone are switched off when daylight fulfils at least half of the required WPI and are switched off when the WPI criteria are fully met.

3 **Continuous control:** The electrical lighting is linearly dimmed by an amount equal to the available daylight until a minimum supplied

output of 20%, and then switched off when the criteria are met.

Bi-directional characteristics of CFSs

Light transmittance-related analysis, such as daylight, visual comfort, or artificial light energy-saving analysis, is by definition angular-dependent. In the context of CFS, this dependency is strongly related to outdoor illuminance conditions, time, and indoor space distribution [74]. To obtain information about visual transmittance, T_{vis}, and solar transmittance, T_{sol}, that is as accurate and detailed as possible, the bi-directional scattering function (BSDF) helps by providing necessary data on the directional optical properties. Using a BSDF matrix in combination with knowledge of local conditions, a fenestration design can be adjusted to maximize its performance. The BSDF matrix consists of eight matrices with information about front and back, visible and NIR light, and the reflectance and transmittance of a CFS. Using a BSDF matrix, it is possible to picture the resultant light distribution for a given incidence direction [85]. Access to this information can facilitate CFS development and optimization. An example depicting the visible transmittance of clear glazing using BSDF is shown in Figure 1.5. The BSDF coordinates are translated into perpendicular XY coordinates with altitude and azimuth between 90°and -90°. From Figure 1.5, it is easy to see how the transmittance varies with the incidence angle.

Furthermore, using the TPM and BSDF, it is possible to carry out inexpensive parametric studies varying geometry or materials. The latest development of the program Radiance can generate BSDF matrices that describe transmittance depending on an incidence angle (IA). The program **genBSDF** was used to generate most of the BSDF matrices in this thesis [27]. This program generates blocks of values which describe 145 Klems' incidence angles for each of 145 oppositely placed outgoing directions [76, 86] based on Tregenza coordinates [87]. The 145 subdivisions describing 145 incidence angle is defined in Task 21 of the International Energy Agency [88, 89]. The illustration of incoming and outgoing Klems' directions is in Figure 1.6. The models tested in this research were created in accordance with the physical geometry and material properties, and the results were validated against the measurements. All the analyses were carried out in a series of sequential steps with an increasing level of information to ensure compactness of analysis.

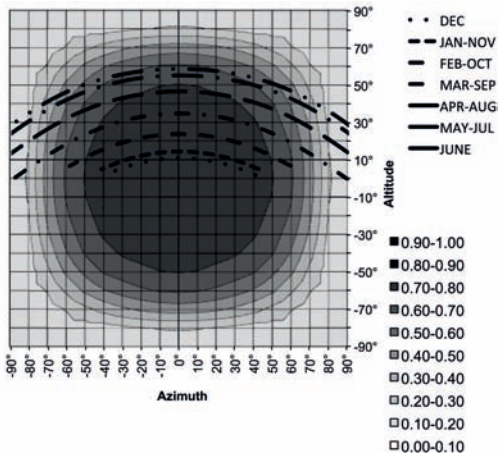

***Figure 1.5**: Example of BSDF for the visible transmittance of clear glazing with the solar path of Copenhagen*

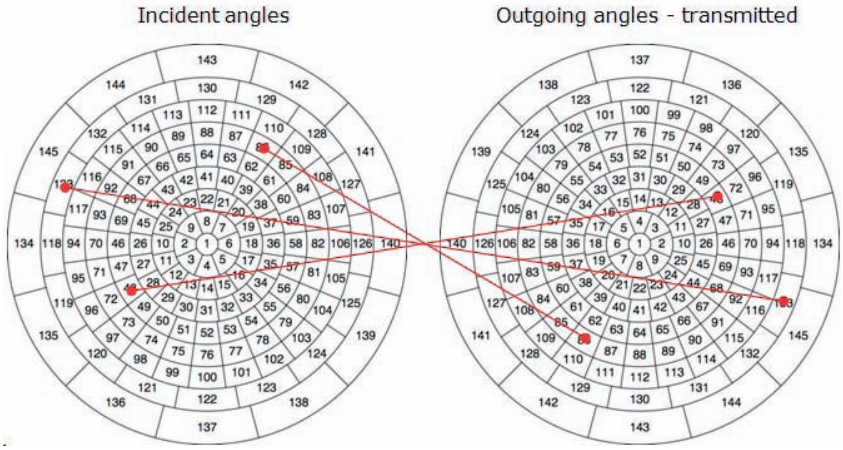

***Figure 1.6**: Angular projection of the distribution of Klems' angles over the hemisphere*

1.6 Solar shading

The transparent parts of a fenestration can be considered as light and energy sources. Allowing daylight and solar radiation to penetrate an indoor space can create visual discomfort and overheating due to unobstructed and excessive radiation from the sun and sky. High solar transparency can cause space-overheating, especially in new office buildings because their heating loads are low. This also applies for buildings in moderate climates, e.g. Denmark, because cooling loads are significant contributors to the total energy consumption of buildings [90]. Modern buildings are thermally well-insulated, so shading against solar gains becomes important, especially for façades facing south, southeast or southwest.
These drawbacks can easily negate savings from the solar gains achieved during the winter and savings in energy for artificial lighting. Using mechanical cooling and ventilation to remove overheating is expensive, so southern orientated façades should be equipped with solar shading to maintain both thermal and visual comfort. The importance of cooling loads is increasing because commercial buildings often have low heating gains and high cooling loads. Residential buildings have low internal loads relative to their envelope loads [9]. On the other hand, while there will be big differences in the performance of windows without shading in different orientations, there will be very little difference in the performance of properly shaded windows whatever the orientation. Solar shading is an effective strategy for reducing overheating, diffusing direct sunlight, and therefore reducing energy consumption [10]. In this research, the shading systems investigated were designed to reduce visual discomfort from bright sky and direct view of the sun, as well as maintain daylight conditions. In most cases, CFSs have several functions and detailed simulations of the systems are therefore needed. Papers III and IV deal with multifunctional solar shadings.

1.7 Energy requirements and consumption

In Denmark, the building code follows the Energy Performance of Building Directive (EPBD), which specifies requirements on the total primary energy demand of buildings. The total energy demand includes heating, cooling, domestic hot water, ventilation and (for offices, commercial and public buildings only) lighting. The calculation formula for offices, commercial and public buildings is Eq. 1.5a and for residential buildings and hotels is Eq. 1.5b, where $\boldsymbol{A}$ is a heated floor area [1]. $\boldsymbol{E}$ is the maximum specific annual primary energy use in $kWh/(m^2 year)$. Energy produced by renewable energy

***Table 1.1**: The energy gain requirements for windows*

	$kWh/(m^2year)$		
	Until Jan 2015	After Jan 2015	After Jan 2020
Vertical windows	-33	-17	0
Roof windows	-10	0	10

sources, such as a solar heating and solar electricity, is subtracted from the total.

$$E_{frame,offices} = 71.3 + \frac{1650}{A} \qquad [kWh/(m^2year)] \tag{1.5a}$$

$$E_{frame,dwellings} = 52.5 + \frac{1650}{A} \qquad [kWh/(m^2year)] \tag{1.5b}$$

Apart from the energy framework, which defines the minimal requirements, two classes for low-energy buildings are defined in BR10 [1]. A Class 2015 low-energy building is defined for offices in accordance with Eq. 1.6a and for residential buildings and hotels in Eq. 1.6b. The low-energy Class 2020 for offices is defined as in Eq. 1.6c and for residential buildings as in Eq. 1.6d.

$$E_{frame2015,offices} = 41 + \frac{1000}{A} \qquad [kWh/(m^2year)] \tag{1.6a}$$

$$E_{frame2015,dwellings} = 30 + \frac{1000}{A} \qquad [kWh/(m^2year)] \tag{1.6b}$$

$$E_{frame2020,offices} = 25 \qquad [kWh/(m^2year)] \tag{1.6c}$$

$$E_{frame2020,dwellings} = 20 \qquad [kWh/(m^2year)] \tag{1.6d}$$

The Danish building code also defines the energy gain, E_{ref}, for the standard window size of 1.23 m $\times$ 1.48 m. The energy gains for windows in the heating season until January 2015, after January 2015, and after January 2020 are defined in Table 1.1. These design requirements have to be kept in mind for the construction of any new building and for large renovations. The WPI required for visual comfort is defined in CEN-EN 15251 [70]. The limits of the LPD are defined in European standard EN 15193 [84], with 15 W/m^2 as the basic requirement and 25 W/m^2 as the comprehensive requirement with regard to visual comfort.

1.8 Measurements

Most of the research results from the simulations were supplemented with measurements because it is important to combine measurements with simulations, especially in cases when the reference case for a comparison is not available. Measurements were necessary for the validation of the numerical models used in this work. The simulated models validated by measurements can be used for performance assessment, which means the cost of measurements can be reduced or eliminated [48].
Guarded Hot Box (GHB) measurements were used in this research to measure the thermal transmittance of windows. Furthermore, to ensure the reliability of simulated illuminance and irradiance, photometric measurements were carried out using lux and irradiance meters.

1.8.1 Guarded Hot Box

The thermal transmittance of the ventilated window was measured using adjusted GHB measurements of the "dark $U_w - value$". The adjustments were necessary to provide an air flow through the glazing cavity to enable the measurement of the properties of such a window. A window of a standard size of 1.23 m × 1.48 m was placed between a cold and warm chamber in a measuring box with the constant temperature difference of 20K. Steady-state conditions were maintained by an electrical heater in the measuring box. The input power defined the total heat flow through the specimen. The GHB was calibrated according to standards EN ISO 12567-1 and EN ISO 8990 [91, 92].

1.9 Test office

In this research, four different test rooms or/and buildings were used for simulations.
In Paper I, a Class 2020 low-energy office building with 60 offices and a large glazed staircase space was examined. The office building was simulated to investigate its energy use and the effect on the indoor environment of temperature and daylight. Furthermore, a residential building was simulated in accordance with the mandatory calculation procedure prescribed in the EU Directive on the energy performance of buildings [2, 1, 17].
In Paper II, a simplified mid-size room of 4 m × 5 m × 3 m, with an external wall of 15 m^2 and a total volume of 60 m^3 was used to assess the ventilated window in the building before and after renovation. The simple renovation consisted of adding 10 cm of insulation to the 70 cm brick wall.

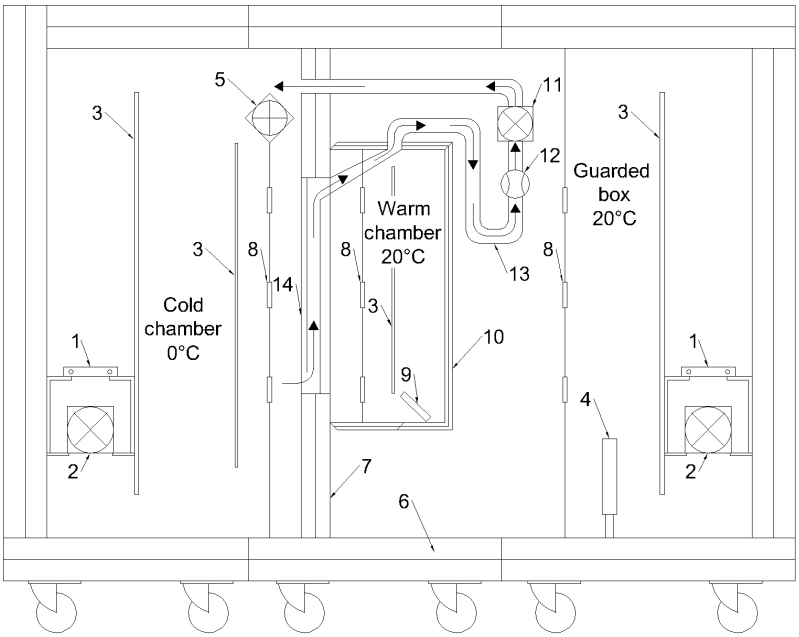

Figure 1.7*: Set-up of the GHB with air flow, and micro manometer. 1) cooling element; 2) fan; 3) baffle; 4) guarded box electrical heater; 5) cold side wind simulator; 6) sandwich element with polyurethane core; 7) surround panel wall of polystyrene foam (XPS) - 170 mm; 8) air temperature sensors; 9) electrical heater in metering box; 10) metering box wall of polystyrene; 11) fan with variable transformer; 12) micro manometer; 13) flexible sucking duct; 14) measured sample of size 1230 mm × 1480 mm (w × h).*

Furthermore, the windows were changed from the original with a $U_w - value$ of 2.5 W/m^2K to 1 W/m^2K for traditional window and between 1.1 W/m^2K and 1.3 W/m^2K for the window with integrated ventilation.
The research for Paper III used a standard test office. The room model was based on the test office in IEA Task 27 in order to have standardized model [93]. The model simulated was a single office for three occupants with dimensions of 3.5 m wide, 5.4 m deep, and 2.7 m high, and with a large window. Paper IV describes a demonstration building equipped with a prototype external dynamic integrated shading and light-redirecting system. The whole building has dimensions of 66 m × 28 m with the longer façade oriented 11°west of south. The space investigated in the building was approximately 9.5 m wide and 14 m deep with a ceiling height of 3.45 m. The building and façade layout allowed for a reference space with the same orientation and similar layout as the space investigated.

Chapter 2

Product development of complex fenestration systems

This chapter focuses on how to evaluate Complex Fenestration Systems (CFSs) during the development of new products. The aim of this chapter is not to present one particular way of doing evaluation, but rather to form a perspective on how to define an evaluation process for any specific solution. The methodology focuses on how to evaluate the performance of a CFS in an accurate, detailed and understandable way. The framework presented describes a product development methodology centred on thermal and optical modelling. The interaction between the three elements of the methodology is illustrated in Figure 2.1. The objective and output of the thesis would lie in the intersection of the three circles in the figure.

Generally, a comparison of simulations with measurements can be considered as the only way to achieve reasonable and accurate validation of simulations. During this research, results from simulations were validated by measurements of unique CFSs. The appended papers describe the test methods used in each investigation, so the reader is referred to the appended papers for detailed information, but the principle results are presented in the thesis.

Indoor climate conditions, i.e. visual and thermal comfort, could be assessed by questionnaires. However, the physical measurement approach was chosen because it does not depend on the participation of large numbers of people, which could prolong the time needed for the evaluation.

This chapter focuses primarily on product development methodology. The next chapter focuses on the second key area of **thermal performance** evaluation, and Chapter 4 focuses on the third key area of textbfoptical/visual performance evaluation.

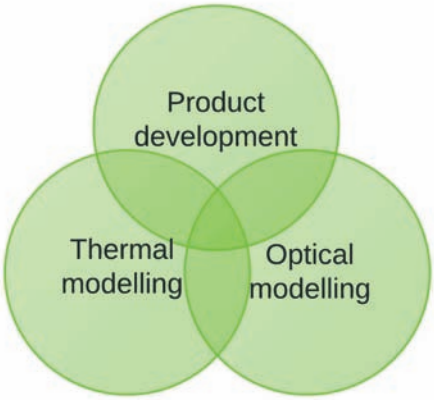

***Figure 2.1**: Schematic description of areas of methodology within the thesis.*

2.1 Product development method

In the development of CFSs, there is a need for tools and methods to clearly and quickly understand the complexity of interrelated performance criteria. Such tools could help generate knowledge in the early stages of building design about significance of the fenestration in the context of an actual building. This chapter suggests a reference procedure for the design of fenestration systems. The framework is complex despite the fact that it would be useful to have a simply defined succession of steps leading to the desired solution assessment.

The complexity comes from the large number of interdependent criteria for the evaluation. Performance analysis should be carried out at several levels, with an increasing level of detail, in order to increase the understanding of the overall performance. Starting with a single parameter assessment, e.g. the thermal transmittance of the window, its $U_w - value$, and continuing towards an overall evaluation. In this way, a more holistic evaluation can be achieved.

The rational product development method suggested by Nigel Cross [94] is appropriate for the building industry [15]. The main and general principle of rational product development is shown in Figure 2.2. The process starts with the identification of opportunities and potentials in a project. The objective and problem specification defining the overall problem comes next. Based on requirements for solving the problem, sub-problems can be defined. Several

design alternatives are generated as sub-solutions, and they are evaluated by quantitative performance calculations. The performance calculations vary from project to project, but some examples are described in the Section 2.2 below. This evaluation approach enables the selection of the final and the most appropriate solution.

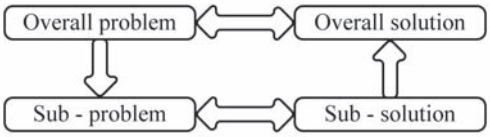

***Figure 2.2**: Skeleton of the rational product development method.*

The objectives of product development product development (PD) can be clarified based on the opportunities identified. The problem objectives can be defined at several levels and their relationships and the connections between the levels can be explored. For example, a well-performing CFS can serve several purposes as illustrated in the objective tree in Figure 2.3. This figure shows how the objectives are clarified from the top level to the bottom level by asking the question "HOW?", and the individual sub-objectives are fulfilled from the lower level to the top by asking the question "WHY?".

2.2 Evaluation parameters

Solar gains and heat losses through windows have a large impact on building cooling and heating loads. By providing natural light, windows can reduce

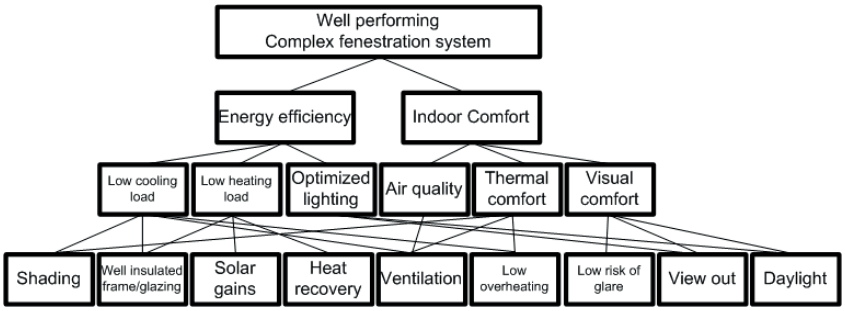

***Figure 2.3**: Example of hierarchical diagram of relationships between design objectives.*

lighting electricity demand. The proper selection of windows and shadings can reduce heating and cooling loads. The direct load reduction has secondary impacts, reducing operational cost and allowing equipment to be downsized [10].
A fenestration system can be evaluated using several different but interconnected parameters. This introduces considerable variation and complexity into the performance assessment. It is not possible to assess a façade using just simple indicators. Windows do not work simply as a construction blocking the heat losses or opening to the outside, so a combination of parameters and criteria has to be used in the performance evaluation. The overall design criteria for windows and CFSs in modern buildings can typically be:

- Energy use - heating, cooling and electrical lighting.
- Thermal comfort - overheating, ventilation.
- Visual comfort - daylight, glare and view.

All these criteria depend on each other and could be addressed in the context of the following parameters:

- Façade orientation.
- Building location and external obstructions.
- Time and day of the year.
- Window size and position on façade.
- Shading geometry and position.
- Shading control strategy.
- Human factors - view direction, contrast, temperature.
- Material properties (glazing, shading, frames, etc.).

A building location specifies climate conditions, including sun position and sky distribution, which is further dependent on the actual time and date, because these conditions are time dependent. Another criterion is the light transmittance T_{vis} and solar transmittance T_{sol} of the CFS, which is also related to the façade orientation and the building location [48]. These parameters can be used to derive the solar heat gain coefficient solar heat gain coefficient (SHGC), which is also referred to as the total solar energy transmittance, the g-value. This is a factor by which the solar gains can be roughly estimated. The thermal transmittance of a window is one of the main energy performance characteristics defining the heat loss. There are also criteria, such as the venting or air leakage of a window, which are considered when

the window is used for venting and the supply of fresh air.
This research focused on determining the interconnection of all the parameters, which can be defined by a performance matrix which includes various criteria. A detailed description of the evaluation performance matrix is in the Section 2.3 below.
There are many other relevant parameters to include in the performance evaluation, but thermal and optical comfort are the most important for the performance analysis of a CFS with regard to energy consumption and the indoor environment.

Main design evaluation parameters:

- **Total energy use**
  - Heating
  - Cooling
  - Electric lighting
  - Solar gains
- **Daylight**
- **View out**
- **Shading**
- **Visual comfort (e.g. glare)**
- **Thermal comfort (e.g. over heating)**

2.3 Framework

Figure 2.4 illustrates an example of a case with four CFSs solutions and six variables. This is a generic example used only illustrate the principle. Each axis represents one parameter, but each of the parameters can consist of several sub-parameters, e.g. energy can consist of energy for cooling and for heating of a building. In other cases, it might be only a NEG [12]. The ranking scale is not fixed because the parameters have different units or can be evaluated differently. The most important thing is to be consistent with each parameter for every solution, because only comparable results can be compared. Furthermore, this evaluation method is ideal for a relative and quantitative evaluation because every solution has to be ranked among other solutions.

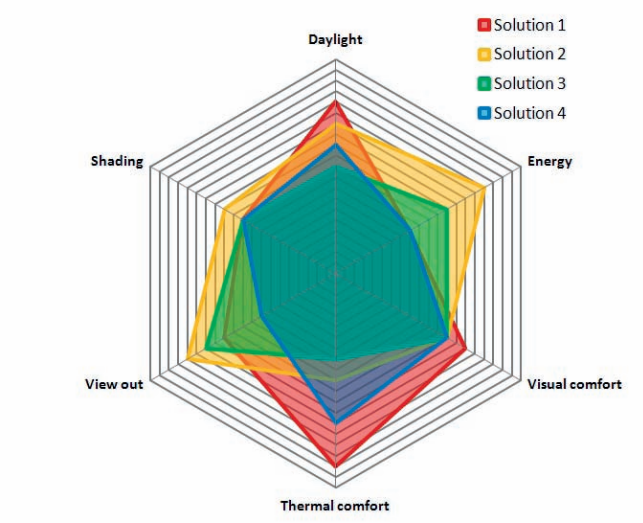

***Figure 2.4**: Example of an evaluation of various performance criteria using a radar chart.*

Chapter 3

Optimization of thermal properties of fenestration components

The results from measurements and simulations of two different types of windows are presented and discussed in this chapter.
Firstly, we look at the investigation of a window with a frame made of glass fibre reinforced polyester (GFRP). This study uses the rational product development method to structure and organize the development of the window frames. Three proposed frame designs are compared with each other and with two reference commercial frames. In addition, increasing the solar and light transmittance of the façade by reducing the frame thickness is discussed. The detailed investigation is presented in Paper I.
Secondly, we look at the experimental investigation of the ventilated window and discuss the theoretical definition of the heat balance of a ventilated window. The detailed results are in Paper II.
Both studies focus on the thermal performance of windows, but the connection with the question of optical performance presented in Chapter 4 is also discussed because there is a logical link between optical and thermal performance. The structure of both investigations is based on the methodology presented in Section 2.1. This means that various parameters are evaluated and compared to a reference in order to quantify the results.
The main hypotheses of this chapter are:

1a Using an appropriate product development method it is possible to develop an energy-efficient window with a positive effect on the indoor environment.

1b Window frames made of a composite material can significantly improve

the overall window performance.

2 A window with an integrated ventilation system can regain some of the heat loss from the window and thereby increase the window's net energy gain.

3.1 Slim window frame made of glass fibre-reinforced polyester

This investigation is twofold. Firstly, it aims to use the rational product development method to facilitate a development of an energy-efficient window. Secondly, several designs of a window frame made of GFRP are suggested. The suggested frames are holistically evaluated by the simulations. The GFRP is used because the window industry is seeking new technologies and materials to further improve the energy performance of windows. The thermal evaluation of the frames is split into 4 steps as described in 1.5.1. These are:

1 Thermal transmittance of the frame: $(U_f - value)$.

2 Thermal transmittance of the window: $(U_w - value)$.

3 Net energy gain of whole window.

4 Building energy demand.

Moreover, the load capacity and deformation of the frames were assessed against a wind load.
To focus on the evaluation of the performance of the frames, the other variables, such as the glazing, were maintained constant and unchanged throughout the investigation.

3.1.1 Identification of objectives

According to the rational product development method, problem specification is needed to define the evaluation process. It was given that the calculations would have to focus on the detailed thermal performance evaluation of the frame and that solar energy gains would have to be taken into account. The requirement was to use triple glazing and GFRP as the frame material. The objectives and their relationships were identified and Figure 3.1 shows the hierarchical tree diagram. This clarification of objectives serves several purposes and is defined by user specifications and requirements, as

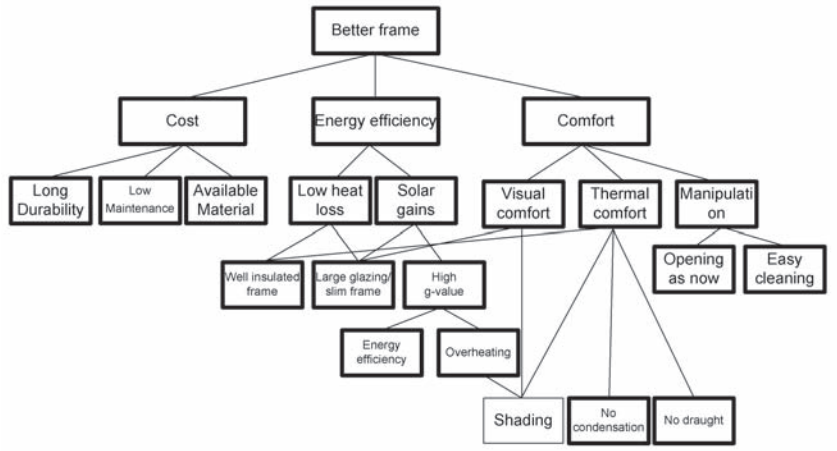

Figure 3.1*: Hierarchical diagram of relationships between objectives for the improved window frame.*

well as by the limitations of production and technology. The specifications identified are listed in Table 3.1. Based on the specifications, three frames made of GFRP were suggested and these are shown in Figure 3.2, which also shows the two reference cases. The parameters that determined the evaluation procedure were the frame width, thermal resistance of the frame, solar gains of the window as a whole, its operability, easy maintenance and gasket tightness. The frames investigated were as follows:

(a) **Reference Frame 1** is the traditional wooden window used in Danish houses with a single side-hung casement opening outwards.

(b) **Reference Frame 2** is an aluminium window, which is typically used in office buildings but also in residential buildings.

(c) **Alternative 1** is a sliding projecting window with top-hung casement opening outwards. The window's outer surface can be turned to the interior for easy cleaning.

(d) **Alternatives 2a** is a tilt and turn window which opens inwards. The window is equipped with a standard tilt and turn hinge.

(e) **Alternatives 2b** is a tilt and turn window which opens inwards. The window is equipped with a special hinge that can be hidden in the

***Table 3.1**: Thermal and energy properties of the frame alternatives evaluated.*

Specification-Window frame from GFRP		
Number	R or W*	Requirements
1	R	Use standard double or triple glazing
2	R	Glue glazing into the frame using silicon or epoxy resin
3	W	Frame visible thickness of max. 50mm
4	R	Sides of the frame connected by mechanical connections in the corners
5	W	Use same profiles for both triple and double glazed window
6	R	Wooden appearance from inside
7	W	The finishing of the frame has to be available in several colours
8	R	Manipulation by one hand
9	R	Easy operation and easy to clean
10	R	Slim hinges for placement into the frame
11	R	Hinges screwed directly into the wall
12	R	Water and air tight gasket between sash and frame - 2mm
13	R	Maximum deformation 1/300 of a window side length or max 8mm
14	R	Minimum strength of frame 300MPa
15	R	Net energy gain above -20kWh/m^2 per year for double glazed window
16	R	Net energy gain above 0kWh/m^2 per year for triple glazed window
17	R	Insulation in the wall has to be covered water-tight by the frame
18	R	Minimum thickness of profile wall 1.5mm

**R, requirements; W, wishes.*

casement frame, which reduces the thickness of the frame by 12mm compared to Alternative 2a.

The last step in the PD method and decision process is to evaluate the proposed alternatives. This can be repeated several times to optimize the frame design.

3.1.2 Results and discussion

This section discusses the results of the calculations. The energy and thermal performance evaluation is split into four consequence assessment steps and is followed by the load capacity analysis. Table 3.2 lists the basic results and characteristics for each frame. This table is followed by more comprehensive results, presented in Table 3.3.
GFRP has several distinctive properties compared to typical materials used for window frames, such as aluminium, PVC or wood. GFRP is eight times stronger than PVC and three and half times stronger than wood. The thermal conductivity of GFRP is several times lower than that of aluminium and is similar to that of wood and PVC. For all the details, see Paper I.

Thermal properties

The discussion is divided into four steps as follows:

STEP 1 Starting with the thermal transmittance of the frame, its $U_f - value$, the best-performing frame is Reference 1 with a $U_f - value$ of 1.22 W/m^2K. The low value is achieved due to the low thermal conductivity of wood. The $U_f - value$ of alternative frames 2a and 2b is a significantly higher than for alternative 1 due to the large air cavity between the window and the sash frame, which is connected to the exterior. Unfortunately the cavity is necessary for smooth window opening. The $U_f - value$ is not a complete description of window energy performance because it evaluates only one element of the window without any connection to its overall performance. With a low $U_f - value$, the risk of condensation in the frame is higher. The temperature was calculated at critical places, and the condensation resistance factor was sufficiently high to prevent condensation in all the alternatives.
STEP 2 The overall thermal transmittance of a window, its $U_w - value$, was calculated for a window size of 1.23 m × 1.48 m. The main factor in overall $U_w - value$ is the ratio of frame area to glazed area in the window. Traditional frames account for around 20% to 30% of the window area, while the

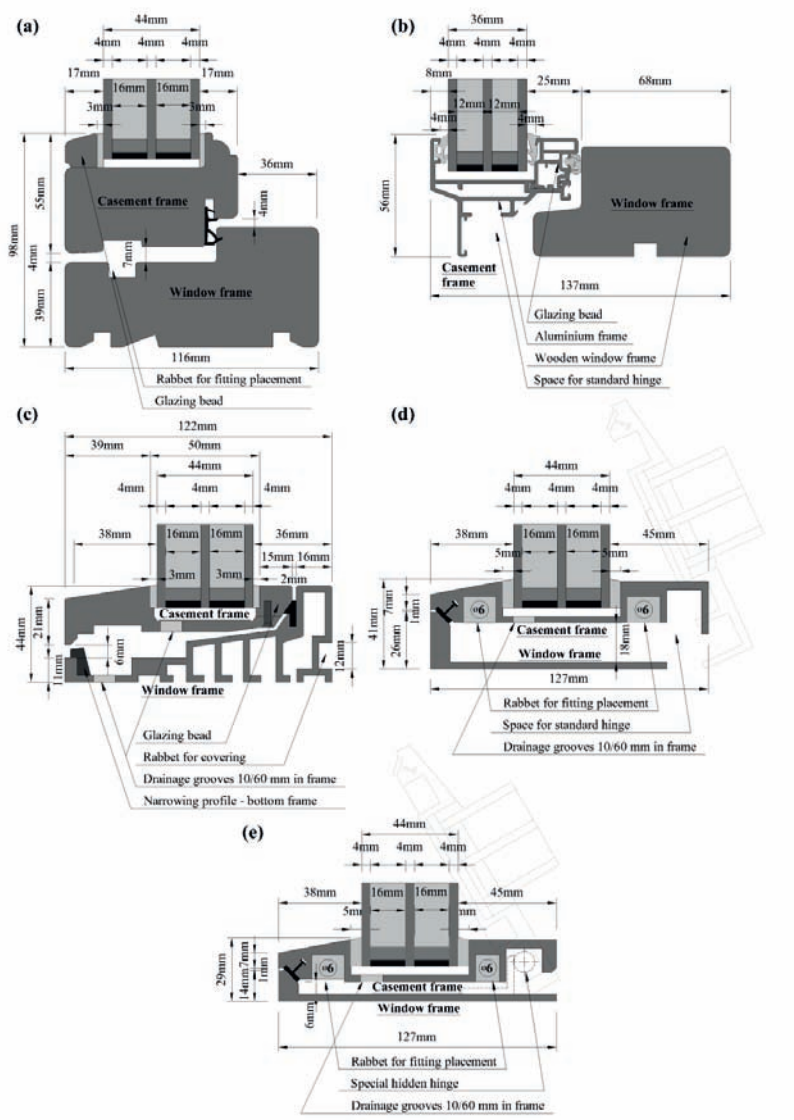

Figure 3.2: *(a) Reference 1-wooden frame, (b) Reference 2-aluminium frame, (c) Alternative 1, (d) Alternative 2a, (e) Alternative 2b.*

***Table 3.2**: Window and frame properties of the alternatives evaluated.*

Window characteristics	Reference 1	Reference 2	Alternative 1
Thickness of frame $[mm]$	98	56	44
Linear transmittance-Ψ $[W/mK]$	0.034	0.053	0.032
g-value glazing/window [−]	0.51/0.37	0.51/0.43	0.51/0.45
Light transmittance of glazing/window [−]	0.7/0.51	0.7/0.59	0.7/0.61
Frame area of window* [%]	27	16.1	12.7

Window characteristics	Alternative 2a	Alternative 2b
Width of frame $[mm]$	41	29
Linear transmittance-Ψ $[W/mK]$	0.031	0.032
g-Value glazing/window [−]	0.51/0.45	0.51/0.47
Light transmittance of glazing/window [−]	0.7/0.62	0.7/0.64
Frame area of window* [%]	11.8	8.4

* *The standard window size of 1.23 m × 1.48 m is used.*

proposed frames account for around 10%. The detailed numbers on frame coverage are shown in Table 3.2. The $U_w - value$ for all the windows is between 0.85 W/m^2K and 0.79 W/m^2K, except for Reference 2, which has a $U_w - value$ of 1.24 W/m^2K W/m2K. The decrease in the $U_w - value$ of the windows with the proposed frames is due to the reduced thickness of the frames, which means that frame is replaced by glazing with a lower $U_g - value$. An additional effect of the larger glazed area is that solar gains increase linearly with the size of the transparent area. This is evaluated using the NEG method in the next step.

STEP 3 The proposed windows all have positive NEG, which means that they become a net source of heat rather than a net sink of heat. In contrast, the reference windows both have greater heat loss than solar gain. The larger glazed area created by the slimmer frames also increases visible light transmittance, which can improve indoor daylight conditions. The best performance is comes from the slimmest frame, alternative 2b, which provides the highest NEG, 19.3 $kWh/(m^2year)$. This is an improvement of 23.2 $kWh/(m^2year)$ compared to Reference 1 and of 47.7 $kWh/(m^2year)$ compared to Reference 2. Alternatives 1 and 2a also provide a high NEG

performance of 15.7 $kWh/(m^2year)$ and 11.2 $kWh/(m^2year)$, respectively.
STEP 4 The last and the most comprehensive evaluation is the simulation of the energy performance of the whole building using iDbuild and Be06. The two cases are studied in depth. The first case is the total energy consumption of an office building (Case 1). The second case is the total energy consumption of a residential building (Case 2). The total energy consumption includes heating, cooling, ventilation, hot water and lighting.
Case 1 The aluminium window frame is widely used in office buildings and is used in the study as the reference frame. The best performing frames are Alternatives 1 and 2b which reduced the total energy consumption in the reference building from 34.5 $kWh/(m^2year)$ to 28 $kWh/(m^2year)$. This improvement in overall performance is due to the slim frame made of GFRP, which increases the transparent part of window and reduces the total heat loss of the window. Furthermore, the larger glazing area provides more visible light transmittance and therefore increases the daylight factor (DF) in the middle of the room from 5.4% (Reference 1) to 6.3% (Alternative 2b).
Case 2 The wooden window frame is widely used in residential buildings and is used in the study as the reference frame. Again, Alternative 2b ranks best among all the proposed frames. By using this frame, the heating energy demand can be reduced by 3.5 $kWh/(m^2year)$ compared to the wooden frame, Reference 1, and by 9.8 $kWh/(m^2year)$ compared to the aluminium frame, Reference 2. The total energy reduction of Alternative 2b and Alternative 1 is 0.8 $kWh/(m^2year)$ compared to the frame Reference 1.
The conclusion from the thermal and energy investigation of the various window frames is that Alternative 2b has the best performance of all the proposed frames in respect of overall energy performance. Moreover, the DF in the office building was increased.

Structural performance

There were three separate criteria for the evaluation of the feasibility and structural performance of the windows.

1. A maximum deformation limit with regard to air tightness of the seal, where a serviceability state wind pressure was used.

2. A maximum deformation limit with regard to a failure of the glass. An ultimate limit state wind load was applied to the windows.

3. A load capacity check was made to ensure that the bending stresses in the frames due to movement would not exceed the strength of the material.

***Table 3.3**: Thermal and energy properties of evaluated frame alternatives.*

	Window characteristics	Reference 1	Reference 2	Alternative 1
1	$U_f - value$ (W/m^2K)	1.22	3.19	1.43
2	$U_w - value$ (W/m^2K)	0.85	1.24	0.79
3	NEG (kWh/m^2)	-3.9	-28.4	15.7
4	Building energy demand/heating			
	Case 1 (kWh/m^2)	29.5/11	34.5/15	28/9
	Case 2 (kWh/m^2)	67.7/61.1	74.9/67.4	66.9/58.1

	Window characteristics	Alternative 2a	Alternative 2b
1	$U_f - value$ (W/m^2K)	2.00	1.9
2	$U_w - value$ (W/m^2K)	0.85	0.8
3	NEG (kWh/m^2)	11.2	19.3
4	Building energy demand/heating		
	Case 1 (kWh/m^2)	29/10	28/9
	Case 2 (kWh/m^2)	67.8/58.9	66.9/57.6

For a given side length, it is possible to calculate the largest possible second side length using the above three requirements. Figure 3.3 illustrates the results, with the lines in the figure indicating the boundaries for a maximum window size. As can be seen, the proposed alternatives allow for a larger window size, which means that the design and the material properties of GFRP allow larger windows in buildings without risk of wind failure.

3.1.3 Conclusion

From the results of the study, it can be concluded that the best energy performance window can be achieved by using a slim frame with low thermal transmittance combined with a large glazed area. This provides higher solar gains, while load capacity is maintained, so GFRP can be considered as competitor to other window frame materials. Savings of 6.5 $kWh/(m^2year)$ were obtained in the office building with this frame, compared to the window with a traditional aluminium frame. Through all the individual steps of the evaluation, it has been shown that the performance of windows has to be evaluated in the context of several parameters in order to get the overall performance. The development process was facilitated by using the rational product development method.

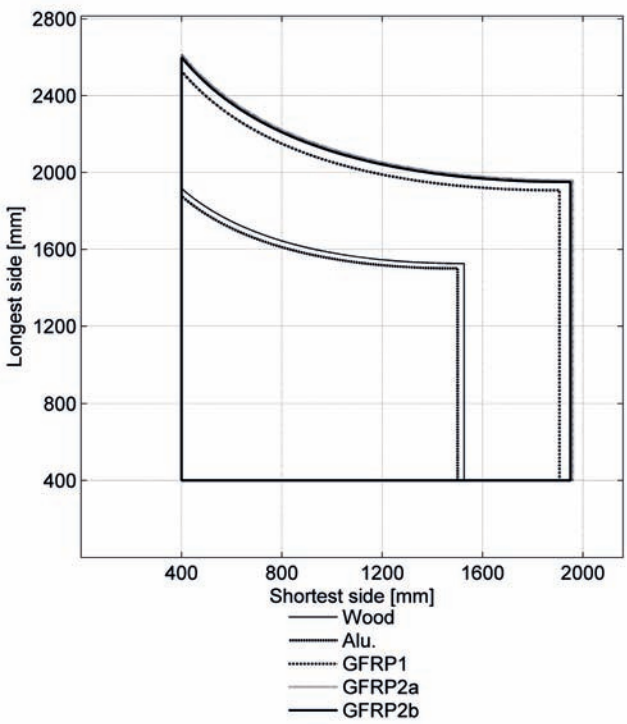

***Figure 3.3**: Envelope of possible window sizes for different frame types.*

3.1.4 Future work

This research used models with simplified radiation modelling of the frame cavities and it would be useful to further investigate the thermal behavioural of frame cavities using more detailed models, e.g. with Computational Fluid Dynamics (CFD) modelling. Moreover, enlarging the glazed areas by using slim frames introduces more solar gains, which may increase the risk of overheating. So it would be useful to carry out further investigation and optimize the window size in order to maximize the benefit from higher solar gains.

3.2 Energy performance of a ventilated window

This section presents the experimental study of a window with integrated ventilation. Firstly, it is necessary to define the heat balance of the ventilated window because an air flow thorough an air cavity changes the heat balance compared to the standard principle of the $U_w - value$. Secondly, the measurements and results are described. Thirdly, the section concludes with the calculations of potential savings, illustrated in a case study comparing three different scenarios. The first case is a building before renovation with old windows; the second case is the same building after renovation with new standard windows; and the third case is the same building after renovation with the ventilated window instead.
Ventilated windows would be most often used for renovations, when it is either difficult or expensive to use balanced mechanical ventilation with a heat exchanger. Renovated buildings are more air tight and air infiltration is significantly reduced compared to the situation before the renovation. Since fresh air has to be supplied, exhaust ventilation is often used and the ventilated air has to be warmed up to the room temperature, therefore the ventilation heat loss is significant [20, 95, 19].
The results from this investigation should have general application. The effect of the ventilation itself was separated and boundary conditions were kept the same. The experimental work focused on quantifying the regained heat loss of the window.

3.2.1 Heat balance

To be able to define the impact of a ventilated window on energy consumption, the transmittance heat losses of the window and ventilation heat loss have to be distinguished. The effect of solar radiation was removed by measuring the "dark U-value", which is driven by temperature difference only and in this case was 20 K [39]. The basis of the theory for calculations and the definition of heat balance are based on the standard ISO 15099 [33], which is integrated in the program WIS [96, 97]. Furthermore, a study by Lau Markussen RaffnsÃ¸e was used to help define the heat balance [98].
As mentioned before, the thermal transmittance of a window, its $U_w - value$, cannot be used for the calculation of the heat transmittance of a ventilated window, so $U_{w,trans}$ was used instead. $U_{w,trans}$ consists of the heat loss from the window, $U_{w,trans,ext}$, and the heat loss from the ventilation, $U_{w,vent}$. The latter is equal to the energy needed to preheat the supplied air. $U_{w,trans}$

is generally given in Eq. 3.1e and is defined so that it can be calculated for a window with or without ventilation air flow. The heat balance of the window/room is based on the combination of the heat balance between the interior and the window, between the window and the exterior, and for ventilation. The energy flux from the interior to the window $Q_{w,trans}$, between the exterior and the window $Q_{w,trans,ext}$, and the energy carried by ventilated air $Q_{w,vent}$ are all defined in Eqs. 3.1b - 3.1d. By combining these equations, the total energy flux $Q_{w,trans}$ and the total heat transmittance of the window can be defined as in Eq. 3.1e, where $Q_{w,trans}$ is based on the energy fluxes, the area of the sample, and the environmental temperature difference. This concept is applicable for windows with or without ventilation.

$$Q_{w,trans} = Q_{w,trans,ext} + Q_{w,vent} \tag{3.1a}$$
$$Q_{w,trans} = (h_{ci} + h_{ri}) \times A_w \times (T_{ni} - T_{si}) \tag{3.1b}$$
$$Q_{w,trans,ext} = (h_{ce} + h_{re}) \times A_w \times (T_{se} - T_{ne}) \tag{3.1c}$$
$$Q_{w,vent} = \rho \times c_p \times \varphi \times (T_{gap,out} - T_{gap,in}) \tag{3.1d}$$
$$U_{w,trans} = \frac{Q_{w,trans,ext} + Q_{w,vent}}{A_w \times (T_{ni} - T_{ne})} \tag{3.1e}$$

where, h is either convective *(c)* or radiative *(r)* heat transfer for the outdoor *(e)* or indoor *(i)* surface. T_{ni} and T_{ne} are the temperatures of the interior and exterior environments, and T_{si} and T_{se} are the temperatures of the interior and exterior surfaces. $T_{gap,in}$ is the temperature of the air entering the glazing cavity, and the temperature of preheated air at the exhaust is $T_{gap.out}$.

3.2.2 Measurements

The aim of the measurements is to determine the heat recovery efficiency of the ventilated window under various airflows. The temperatures of the glazing surfaces and in the ventilated cavity were monitored, while the cold chamber in GHB had a steady temperature of 0°C and the warm chamber was between 19°C and 19.5°C. Figure 3.4 shows that the temperatures of the glazing surfaces and the ventilated cavity decreased as the airflow increased. The increase was mainly caused by raising the surface heat transfer coefficient. The translation of the airflow volume to air speed is 1.3 l/s to 0.015 m/s and 8 l/s to 0.091 m/s.
The mean air temperature in the ventilated cavity decreased more steeply than the surface temperatures of the glazing. This is due to the increase in the volume of ventilated air in the cavity, and the surface heat flux through

the glazing could not increase the air temperature equally. Thus, the mean air temperature was approximating the mean temperature of the cavity surface closer to the exterior. By increasing the temperature difference over the glazing as shown in 3.4, it was demonstrated that the airflow rate affects the increase of the heat flux through the glazing..
The heat flux through the sample was obtained by monitoring the input of the electrical heater in the measuring box. The total heat flux was between 35.8 W and 77.8 W, which corresponds to the window with no airflow and the window with an airflow of 8 l/s, respectively.

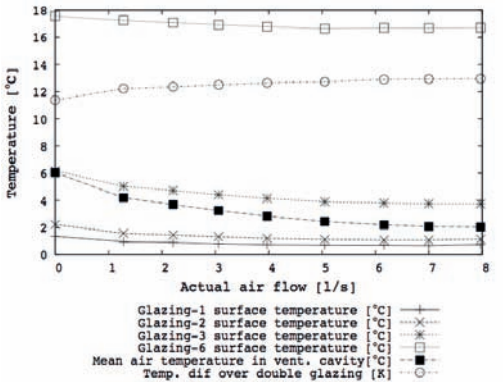

Figure 3.4*: Surface temperatures of glass at positions 1, 2, 3 and 6 and the air temperature in the ventilated cavity between the glass panes.*

3.2.3 Results and discussion

Heat recovery

With ventilated air, some of the heat loss is recovered. The heat exchange happens through the glazing surfaces as well as within the ventilated valves in the frames. The temperatures in the inlet and outlet valves were monitored and they are shown in Figure 3.5. The ventilated air was preheated in the inlet valve by approximately 3°C under an airflow of 1.3 *l/s* and by 1°C with an airflow of 8 *l/s*. The temperature of the air at the outlet was increased by 8°C for an airflow of 1.3 *l/s* and 3.3°C for an airflow of 8 *l/s*. The temperature of the preheated air in the outlet was used to define the regained energy from the heat loss. Figure 3.6 shows that the regained heat energy varied between 12.9 W (7 W/m^2) and 34.2 W (18.2 W/m^2) for airflows between 1.3 *l/s* and 8 *l/s*, respectively.

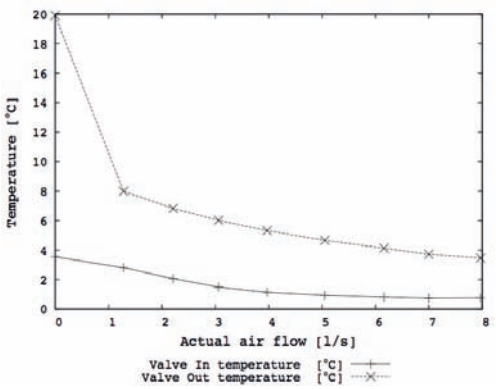

***Figure 3.5**: Air temperatures in the inlet and outlet valves.*

The temperature difference in the frames increased, which consequently caused a higher surface heat exchange coefficient. However, the thermal transmittance of the frames also increased to 1.8 W/m^2K for the bottom frame, 2.3 W/m^2K for the top frame and 1.7 W/m^2K for the side frames. The higher airflow increased the heat loss of the frames, which was partly regained but also partly transmitted to the exterior. Figure 3.7 shows the combination of the regained energy and the window's extra heat loss. The energy of the ventilated air was calculated from Eq. 3.1d and depends on the outlet temperature. The extra heat loss of the window was calculated as the difference between the heat loss of the window without and with ventilation. This combination of heat losses shows that the energy recovery efficiency of the ventilated window lost its effect at an airflow of around 6 *l/s*; see Figure 3.7. This relationship shows that it is not worthwhile increasing an airflow rate because it increases the extra heat loss through the window which cannot be regained. This indicates that the lower airflow rates are more efficient for heat recovery.

Case study

The case study and its evaluation were based on heating up the required amount of ventilated air to a room temperature of 20°C from an outdoor temperature of 0°C. The air preheating inside the ventilated window was compared to a standard window combined with exhaust ventilation. Different airflows through the window were defined by the number of windows used, each of a standard size of 1.48 m × 1.23 m. This meant that the scenario with one window represented an airflow of 8 *l/s*, with two windows

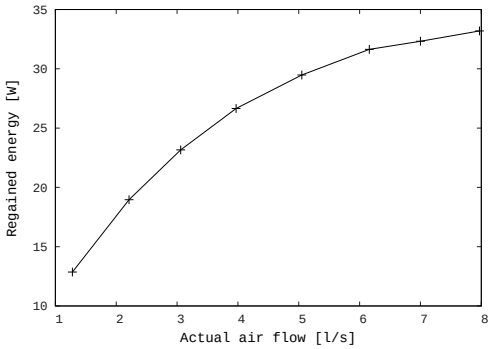

***Figure 3.6**: Amount of heat recovered by the ventilated window.*

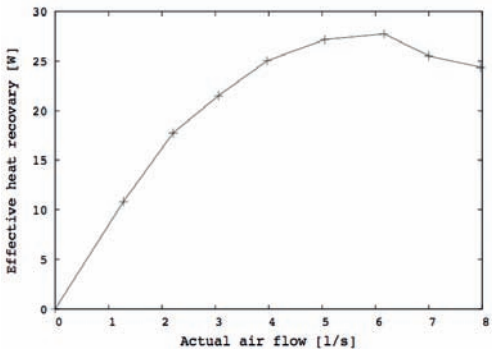

***Figure 3.7**: Effective heat recovery of the window.*

an airflow of 4 l/s, and with three windows and airflow of 2.5 l/s. All other parameters were kept the same to investigate the preheating effect alone.
In total, nine cases were calculated, based on three airflows and three scenarios as follows:

1 The first scenario depicted the energy for heating a room in the building before the renovation.

2 The second scenario evaluated the room after renovation with standard new windows installed.

3 The third scenario was the same as the second scenario but with ventilated windows installed.

The performance of windows was evaluated by $U_{w,trans}$. By comparing the heat loss by ventilation to the total energy heat loss, it was found that, after the building renovation, the ventilation heat loss is around 1/2 of the total heat loss, compared to 1/4 before. In more detail, the change was from 26.6% to 50.2%, from 24.8% to 47.6% and from 23.3% to 45.3% respectively for the rooms with one, two and three windows installed. This illustrates how ventilation heat loss becomes a more significant part of the total energy demand for heating after the building renovation.
When the ventilated air is preheated in the ventilated window, the air entering the room changed the temperature from 20 K to 16.5 K, 14.7 K and 13.5 K respectively for the rooms with one, two and three windows. This reduced the total energy demand of the room by 8.8%, 10.9% and 9.8% respectively for the rooms with one, two and three windows. The energy savings were calculated using a ventilated air exchange of 0.5 h^{-1}. It was assumed that the air infiltration in the residential building was 0.5 h^{-1} before renovation and 0.07 h^{-1} after renovation when the building was air tightened and the windows replaced. The savings just for the ventilation were 17.5%, 26.5% and 32.5% respectively for the rooms with one, two and three windows. From the total energy decrease, it was found that the greatest benefits occur in the room with two windows installed, which indicates that optimization of the wall-window ratio is necessary as well as that the heat recovery of the window decreases with higher airflows. Furthermore, lower airflow rates are preferable, because in most cases several windows could be used for space ventilation and higher airflow velocity from the window outlet could be uncomfortable and cause draught. The detailed results are presented in Table 3.4, including the potential heating energy savings in each room.

***Table 3.4**: Heat energy savings comparison for the room with and without the ventilated window.*

Scenario 1	Before renovation		
	1 win	2 win	3 win
Heat loss by ventilation [W]	201.7	201.7	201.7
Heat loss by infiltration [W]	201.7	201.7	201.7
Heat loss by external wall [W]	263.6	227.2	190.8
Heat loss by window [W]	91.0	182.0	273.1
Total heat loss [W]	757.9	812.6	867.2
Ventilation vs. total [%]	26.6	24.8	23.3
Energy decrease by VW [%]	-	-	-
Scenario 2	After renovation		
	1 win	2 win	3 win
Heat loss by ventilation [W]	201.7	201.7	201.7
Heat loss by infiltration [W]	28.2	28.2	28.2
Heat loss by external wall [W]	131.8	113.6	95.4
Heat loss by window [W]	40.0	80.1	120.1
Total heat loss [W]	401.7	423.6	445.4
Ventilation vs. total [%]	50.2	47.6	45.3
Energy decrease by VW [%]	-	-	-
Scenario 3	After renovation + ventilated window		
	1 win	2 win	3 win
Heat loss by ventilation [W]	166.4	148.2	136.1
Heat loss by infiltration [W]	28.2	28.2	28.2
Heat loss by external wall [W]	131.8	113.6	95.4
Heat loss by window [W]	40.0	87.4	142.0
Total heat loss [W]	366.5	377.4	401.7
Ventilation vs. total [%]	45.4	39.3	33.9
Energy decrease by VW [%]	8.8	10.9	9.8

3.2.4 Conclusion

The experiment showed that the ventilated air can be partly preheated in the ventilated window by recovering some of the heat loss of the window. The heat exchange takes place in the glazing and in ventilation valves in the frame. However, the heat exchange in the frame also introduces a greater heat loss through the frame and consequently caused an increase of the total thermal transmittance of the window. The efficiency of the heat recovery is strongly dependent on the airflow rate, decreasing with higher airflows, so ventilated windows are more appropriate for buildings where a low ventilation rate is required. In the case investigated, the savings in total energy demand were more than 10%. Moreover, the heat balance for the window-room-ventilation system was defined and can be used for comparison of traditional windows with ventilated windows.

3.2.5 Future work

Windows are always placed in exterior building envelopes and exposed to solar radiation. Further investigation should therefore aim at having realistic outdoor conditions, including solar radiation. The solar energy absorbed in the glazing can also be used for preheating the ventilated air. The large glazing cavity used for the ventilation is an ideal place to put solar shading, which can absorb solar energy and significantly affect the heat balance of the ventilated window. This could be particularly useful during the summer when the ventilated air can be vented from outdoors thru ventilated cavity back outdoors and remove excessive solar gains absorbed in the glazing and shading material. More detailed studies on absorbed solar energy and its removal by the air flow in the ventilated window should be carried out.

Chapter 4

Utilizing of the optical properties of integrated shading systems

This chapter presents and discusses the results from measurements and simulations of two different and unique shading systems. Firstly, an investigation of an integrated micro-structural perforated shading screen (MSPSS) is presented, and the system is compared to three conventional shading systems; see Paper III. Secondly, the performance of a daylight-redirecting glass shading system is discussed and presented; see Paper IV. The discussion focuses primarily on optical properties, but since thermal performance is inseparable from optical performance, the investigation also relates to the discussion in Chapter 3. The structure of both cases is based on the methodology presented in Chapter 2. This means that various parameters are evaluated and compared to a reference. The parameters include daylight, glare and visual comfort, lighting energy, energy performance and thermal comfort, etc. The main hypotheses of this chapter are:

1 A micro structural screen layer can be used as a shading system to shade and reduce cooling loads without blocking the view to the outside. Furthermore the performance of such a system can be evaluated by simulation tools.

2 A carefully designed daylight-redirecting glass shading system can improve daylight conditions at the back of a room while maintaining visual comfort and a view to the outside.

4.1 Performance modelling of a micro-structural perforated shading screen

The system is made of an insulated double glazed unit with a low-E coating on the interior glass pane on the surface inside the glazing cavity (glazing surface 3) and with a micro-structural perforated shading screen (MSPSS) on the opposite surface (glazing surface 2). The MSPSS is consists of a stainless steel sheet with elliptical holes smaller than 1 mm. The holes are cut in a downward direction (when viewed from the inside) to reduce transmission from outdoor sources above the horizon - the sun and sky. An increased transmission for negative altitude compared to the normal incidence, when looking from inside, allows a better view to the outside. The view through the MSPSS and the unobstructed view are shown in Figure 4.1. The MSPSS combines solar and glare protection and provides a direct view out. Some of the features are in conflict with each other, and the system is angular-dependent and asymmetrical. These features, and the fact that this system is not included in any building performance simulation program, are the reasons why this system was selected as a test example.

***Figure 4.1**: View through MSPSS (left) and unobstructed view (right)*

To enable validation of the simulations, measurements under outdoor conditions were carried out. The measurement procedure is presented in Section 4.1.1. The MSPSS was also compared with three other fenestration systems: a clear double glazed window without shading, a clear double glazed window with horizontal Venetian blinds, and a clear double glazed window with a semi-transparent roller shade. To provide comparable results, all conditions

other than the shading system were kept the same, e.g. the same glazing, and all the shading systems were placed in a glazing.
The reference case with clear glazing was studied in order to be able to separate the effect of the shading systems from the effect of the glazing. A commonly used Venetian blind system was used because it has similar features to those of the MSPSS, e.g. it provides shading and permits a view out. A roller shade was used as a reference because it blocks solar gains and glare more efficiently than a semi-opened system, but blocks the view to the outside.

4.1.1 Measurements and simulations

The outdoor measurements were carried out on sunny days in June and July. The movable measuring rig is shown in Figure 4.2, including the test sample. The rig allowed the sample to be adjusted in accordance with the sun position, so several different incidence angles (IAs) could be measured in a relatively short time. However, the size of the sample did not allow the measurement of IAs greater than 60°.

***Figure 4.2**: Movable measurement test rig with a sample mounted.*

The illuminance and irradiance sensors were placed behind and on the side of the sample. The ratio of these two measurements gives the relative light transmittance of the sample. The use of relative measurements meant that

the surroundings of the measurement location could be ignored and that no obstacle could introduce a large error in the results. By recording the time, sun position, total horizontal hemispherical diffuse illuminance and direct normal illuminance, it was possible to reproduce sky conditions in the simulations.
The program Radiance was used for the transmittance calculations and the daylight and glare analysis for all the CFSs investigated. The results from Radiance were then used to calculate the electrical lighting savings from using daylight. BSDF matrices generated by the program genBSDF were combined with thermal transmittance calculations in the program Window6 to investigate NEG. The matrices were also used in ESP-r to calculate the total energy demand of the test office.

4.1.2 Results and discussion

This section presents the results of the simulations of all four tested CFSs and compares the measurements of the MSPSS with the simulations. The evaluating criteria of the MSPSS were energy use, and visual and thermal comfort. They were addressed in the context of façade orientation, building location, time of day and year, shading strategy, and human factors (view, comfort and temperature). Since the performance of a shading system depends on the sky distribution, a year-round performance evaluation was carried out, using bi-directional information on the light transmittance (T_{vis}) and solar transmittance (T_{sol}) of the CFSs.

Validation of simulations

Figure 4.3 shows the comparison of the Radiance simulations with the measurements. The comparisons of T_{vis} and T_{sol} correlated, which indicates that simulations can be used for such evaluation and that the results are reliable. The curve variation is between 0% and 4%, except for visible transmittance at an IA of 60°where the discrepancy is 18%. However, this error is relative, and it is small when the absolute values are taken into account. Moreover, the position during the measurements could be slightly off because the IA was at its maximum. The validation of the simulations of the BSDF of the CFSs is important because it is a complex description and a relatively new approach. The measurements were not done in all directions, but it was sufficient to vary the IA in one direction.

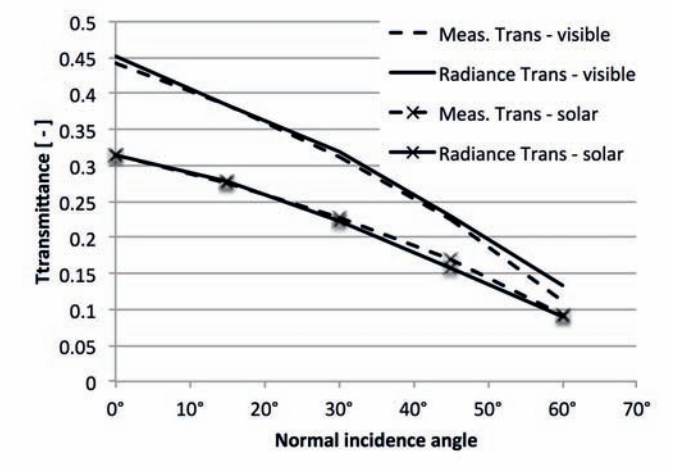

***Figure 4.3**: Validation of the Radiance simulation by measurements - comparison of the results.*

Bi-directional transmittance

Figure 4.4 gives a visualization of the visible transmittance, T_{vis}, for all the CFSs tested. The graphs are independent of location and orientation, so they are applicable for any situation. That is why the annual sun path for Copenhagen has been added to the graphs. This adds a level of understanding for a location with a south-oriented façade. By combining information about bi-directional transmittance and location, it is possible to see how the performance of an angular-dependent CFS will change during a year. For instance, during the winter, when the sun altitude is low, more solar gains can be obtained because the transmittance is higher, while more effective solar shading is provided in the summer. The maximum transmittance of the MSPSS and the Venetian blind was between 0.5 and 0.6, while for clear glazing it was up to 0.8. The glazing with the roller shade had a high shading coefficient and the transmittance was as low as 0.2.

Daylight performance

The transparency of a fenestration affects WPI and savings in electrical lighting energy from using daylight. The roller shade limits daylight penetration and thus significantly reduces the lighting energy savings. Incidence-angle-

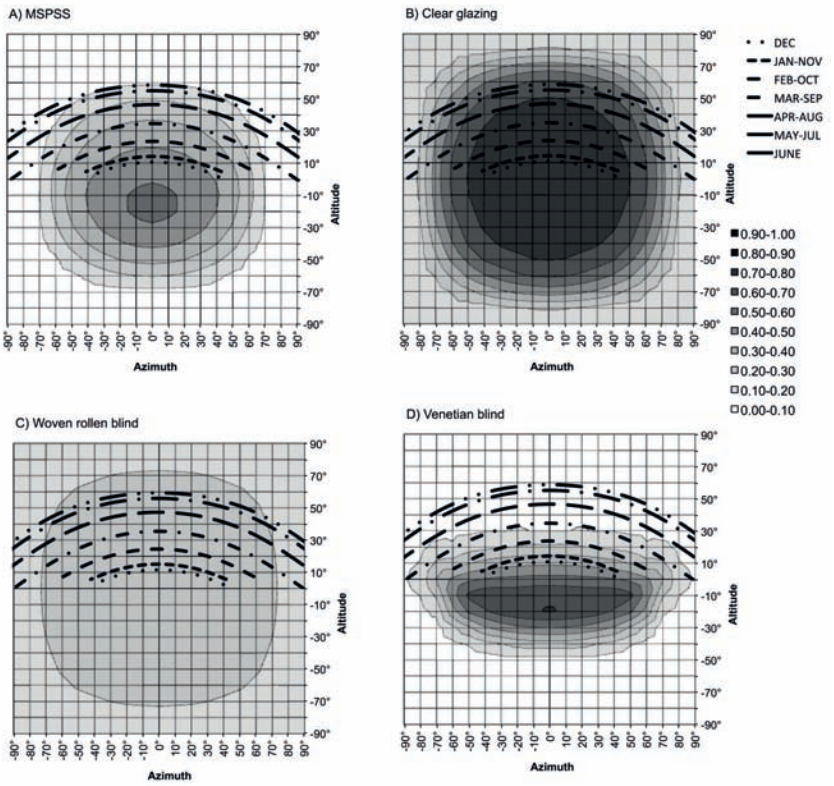

***Figure 4.4**: Visible transmittance of CFSs with solar path of Copenhagen.*

dependent shading systems like the MSPSS and the Venetian blind have higher transmittance at negative degrees of altitude than at normal incidence. The systems are designed to block light radiation from the sky and increase the view to the outside. The highest transmittance is at about -15°of altitude, looking from inside.
daylight autonomy (DA) was used for the evaluation of daylight in the single office space. Figure 4.5 shows DA for all four CFSs and indicates the percentage of time during which a certain level of illuminance is reached. For example, the CFS with MSPSS provided at least 216 lux in the distance of 0.5 m from the façade for 80% of working hours. The solutions with shading performed similarly, with a slightly better performance for the MSPSS. The high WPI at the front of the room with clear glazing cannot be used because

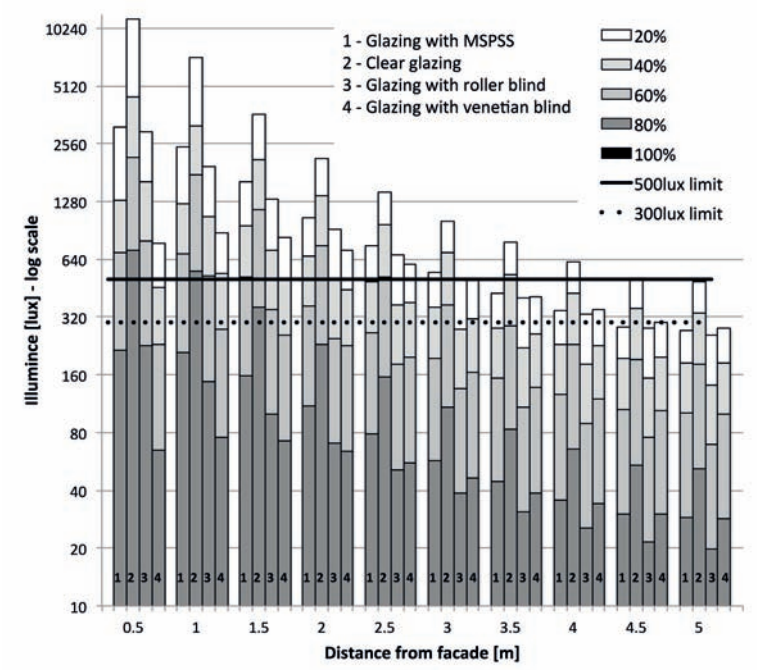

***Figure 4.5**: Daylight autonomy*

the high illuminance can cause uncomfortable glare and overheating because it reached 10 klux. So the other CFSs provide equivalent or better performance. At the back of the room, the minimum WPI was not achieved with any of the solutions.

Energy performance

As expected, the solar transmittance follows the same pattern as the visible transmittance. The standard calculation of NEG has been adjusted for IA, but it is simplified. Figure 4.6 illustrates the effect of IA on NEG. The figure shows NEG separately for each façade in different orientations as well as the total NEG. Since NEG is primarily based on solar gains and increased by shading efficiency, the MSPSS performed the worst with regard to NEG. However, shading will be used mainly for south-facing façades, and potentially for east/west façades, to reduce the risk of overheating during the

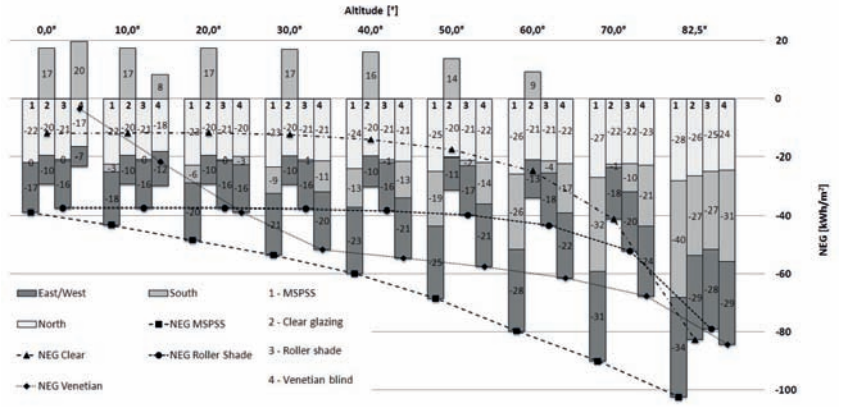

***Figure 4.6**: NEG for four different CFSs, split for different orientations and dependent on IA.*

summer. So the MSPSS performed well with regard to solar shading. The angular-dependent systems give most shade under a high altitude sun, while the roller shade and clear glazing have a relatively constant NEG.
The NEG method does not include cooling loads, so more comprehensive analysis is required. The program ESP-r can handle BSDF matrices for any CFS. Table 4.1 contains the results for heating and cooling loads calculated in ESP-r. The calculations were carried out for three different locations with different geographical latitudes, so each location has a different solar radiation.
All the shading solutions (roller shade, MSPSS, Venetian blind) provided similar shading protection and reduced cooling loads by 20-30% compared to the window without shading (clear glazing). However, the roller shade reduces a visibility and therefore its usage is limited, because most users prefer to have a view to the outside.

Glare analysis

The visual connection with the outside and to bright sky and direct sunlight can cause discomfort glare. So, in addition to shading from solar radiation, it is desirable that a Complex Fenestration System (CFS) should provide glare protection. The DGP index was investigated in a single-cell office with 3 different view positions; see Figure 4.7. Different views are necessary for the analysis because glare depends on both the light intensity and view direction. Figure 4.8 shows carpet plots of the annual glare assessment using the DGP

***Table 4.1**: Energy loads for heating and cooling for all CFSs and locations investigated.*

Location	Energy performance ($kWh/m^2/year$)							
	MSPSS		Clear		Roller shade		Venetian blind	
	HL	CL	HL	CL	HL	CL	HL	CL
Copenhagen	8.5	22.5	6.6	30.4	9.0	22.8	9.3	20.3
Prague	12.3	24.4	10.5	30.4	12.7	24.3	13.2	23.2
Rome	0.0	63.5	0.0	78.1	0.0	63.9	0.1	59.4

Note: HL-heating loads; CL-cooling loads.

index for every hour and for the four different CFSs. The sky distribution was generated based on the weather data file for Copenhagen, so the sky changed every hour. Each view in Figure 4.7 had different conditions, as follows:

- **View 1** was parallel along the window pointing to the east, so the highest DGP values occurred before noon.
- **View 2** faced south-west and the highest DGP values were in the afternoon.
- **View 3** was oriented south, towards the window, and the highest DGP value was at noon.

The clear glazing provides no glare protection, because direct sunlight is not blocked, so the risk of discomfort glare is highest. The glare is present all year round for the clear glazing. In contrast, the shading systems block some glare at various periods of the year. The roller shade blocks the view completely and blocks all glare for Views 1 and 3. However, glare occurred with View 2, because the view position was close to and facing the window and the roller shade was partly transparent. View 2 experienced the most glare for all the CFSs. The Venetian blind performed slightly better than the MSPSS, because the transmittance under high IAs is lower, as can be seen in Figure 4.4. The investigation showed that for visual comfort it is necessary to block direct sunlight, and that glare can occur even with a completely closed roller shade.
The BSDF matrices provided useful information for all analyses; the normal-incidence values were otherwise similar for all the CFSs investigated.

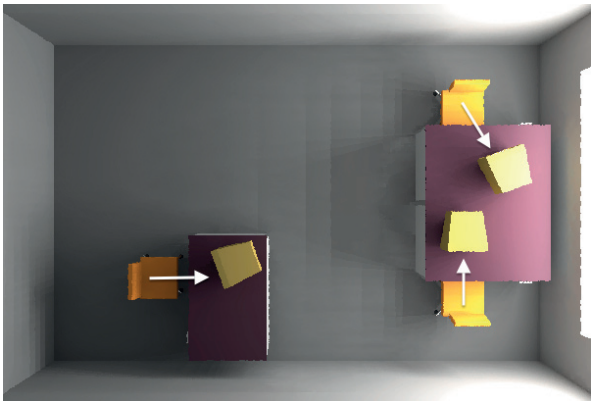

***Figure 4.7**: A plan view of the office with view directions.*

Lighting energy savings

As mentioned in the introduction, the utilization of daylight can provide large energy savings by reducing the use of artificial lighting. This investigation primarily evaluated shading properties, but disproportional shading of visible light is undesirable. Section 1.5.2 described the on/off and bi-level lighting control strategy used to supplement WPI. The front lighting zone, closest to the façade, has the highest WPI from daylight and provides more savings compared to the back zone. In Zone 1, closest to the façade, the savings were up to 80% compared to the situation with the light on all the time. In Zone 1, it did not matter if the lighting control system was on/off or bi-level because the WPI was higher than the threshold most of the time. This is in contrast to the back of the room where a significant part of the savings was achieved by using the bi-level control. In general, illuminance levels were lower at the back of the room. There is a minimal difference between the shading solutions in the front zone, and the greatest savings in the back zone would be achieved with clear glazing. The clear glazing provided savings of up to 55% while the other CFSs achieved around 30% savings with bi-level control. However, the savings by using clear glazing are not significantly higher. It is also worth mentioning that most of the savings are during the winter, which is desirable because there is a shortage of daylight during this period of the year. More detailed information is presented in the Paper III.

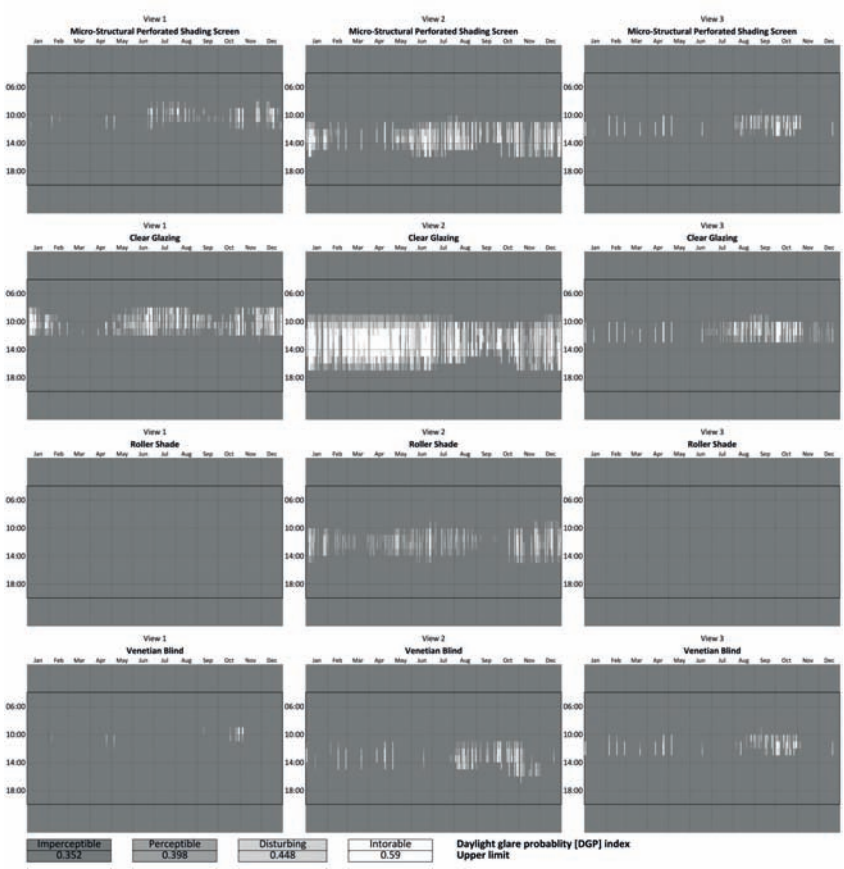

Figure 4.8*: Annual plots of the DGP for three views and all CFS in the location of Copenhagen.*

4.1.3 Conclusion

Various interrelated parameters for four Complex Fenestration System (CFS) were compared. The main focus was on the evaluation of an integrated micro-structural perforated shading screen (MSPSS). It was found that angular dependent shading systems can be beneficial all year round. They provide daylight and solar gains while decreasing the risk of overheating during the summer when the sun's altitude is high. Visual comfort was evaluated using the Daylight Glare Probability (DGP) index, and it was demonstrated that visual comfort depends on blocking direct light as well as optimal positioning of view directions.

4.1.4 Future work

The performance of angular-dependent CFSs depends on the incidence angle which is related to the time of year and location. The performance of such systems could be investigated for different locations and then the geometry could be optimized for a specific location.

4.2 Demonstration of redirecting glass shading system

The shading and daylight-redirecting system is an exterior shading system made of highly reflective solar control glass. The experimental study was based on simulations and measurements which were carried out at the demonstration building. The space investigated was a deep open-office which lacks natural light at the back of the room. Figure 4.9 shows the layout of the building, the test and reference areas (highlighted), the lighting control zones, building orientation, and the position and direction of views for glare analysis. The evaluation of this shading system was based on several parameters because the system is multi-functional. The main functions are:

- Daylight transmittance and redirection, and daylight utilization.
- Sufficient solar energy transmittance during cold months.
- Preventing indoor space from overheating during warmer months by shading excessive solar radiation.
- Maintaining an unobstructed view to the outside.

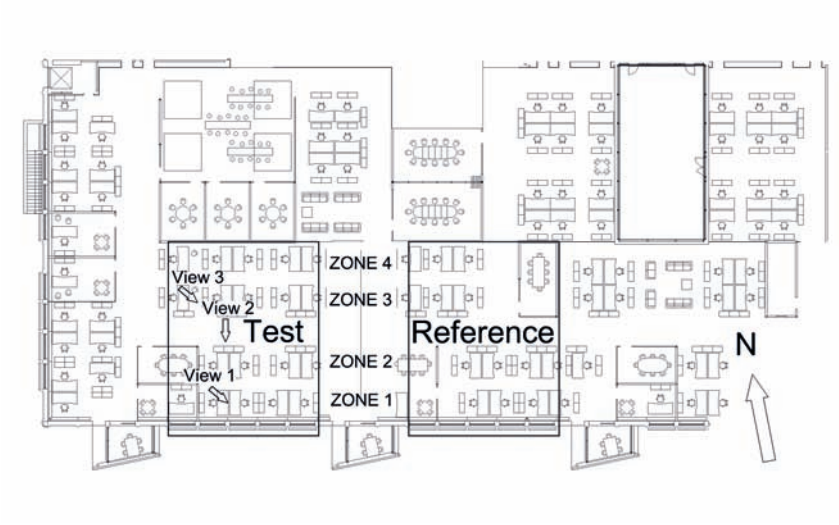

Figure 4.9*: The layout of the building with open-space offices and marked view directions and lighting zone positions.*

The main aim of this system is to increase the daylight illuminance in the indoor space and reduce lighting demand by increasing daylight utilization. Daylight utilization also depends on a daylight-linked lighting control strategy. The quality of a daylight-lit space depends on several factors, e.g. luminance distribution and direction, and glare [65]. This CFS is based on daylight redirection, so glare analysis and visual comfort are critical. Moreover, the CFS's thermal performance was analysed because the system can increase the solar energy gains of the building envelope.

4.2.1 Shading systems and shading strategy

This CFS is designed to increase the WPI at the back of a room by redirecting daylight to the ceiling using reflective surfaces. The design is based on previous studies by Laustsen and Iversen [99, 100]. A high visible transparency and view through the glass allows a view to the outside. The shading effect is achieved by the highly reflective solar control glass, which reflects unwanted solar radiation back to the exterior when the system is in shading mode.
Figure 4.10 shows the operation scheme for the system. The rotation of the four upper redirecting lamellas is towards the façade (counter-clockwise) when the shading is closing. This is different from the reference (original) shading system. The lower four lamellas are independently moved and can stay in the closed or open position. The control strategy has two determiners. Firstly to redirect daylight during overcast or intermediate sky (redirecting position), and secondly to shade during sunny days (closed position). The best performing redirecting position is 30°rotated toward the façade, a design that avoids reflecting directly into the occupants' faces. The angle of 30°was based on the profile angle of the sun for the location of the building, so the shading system can use this position all year round, except for May and June when the position is 25°. The system has three possible positions:

- Redirecting position - 30°(25°), oonly for the four upper lamellas in the system tested.
- Opened position - 0°, in both tested and reference system.
- Closed position - 90°, in both tested and reference system.

4.2.2 Results and discussion

All the features of the shading system are reflected in the analysis, which evaluates the multi functionality of the system from different perspectives as

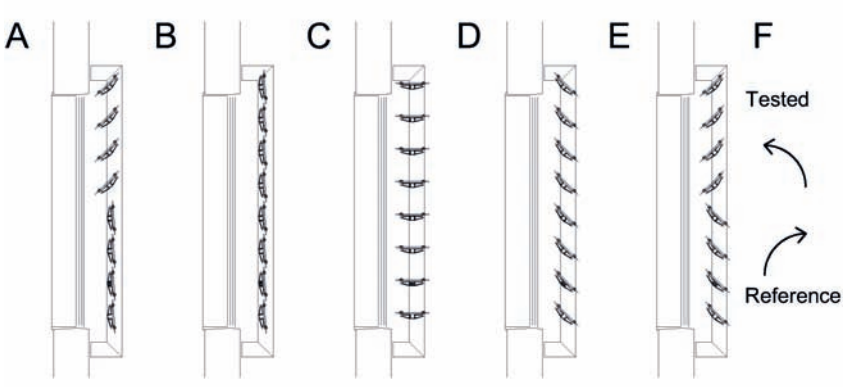

***Figure 4.10**: Illustration of the positions and rotations of the shading system.*
A) Tested system in redirecting position with lower 4 lamellas closed.
B) Whole shading system in the closed position.
C) Whole shading system in the open position.
D) Reference shading system in the rotation of 45°.
E) Tested shading system in redirecting position with lower for lamellas in the rotation of 45°.
F) Rotation direction of tested and reference system from the open position to the closed position.

suggested in Section 2.1. Again, the simulations were initially validated by measurements because the system is not included in any standard building performance simulation tool. The analyses carried out were daylight analysis, evaluation of glare, and energy performance analysis.

Validation of simulations

The simulations were first validated against the measurements made at the demonstration building. The measurement and simulation sensors had a free view of the window. The sensors for illuminance were placed at a distance of 3.6 m from the window, which is approximately the distance at which daylight conditions could be improved. The comparison is shown in Figure 4.11. There are several discrepancies between the measured and the simulated results. The furniture in the open-space office was movable and could have been moved during the measurements, and there was no control of the interior manual shading devices. These problems were kept in mind assessing the

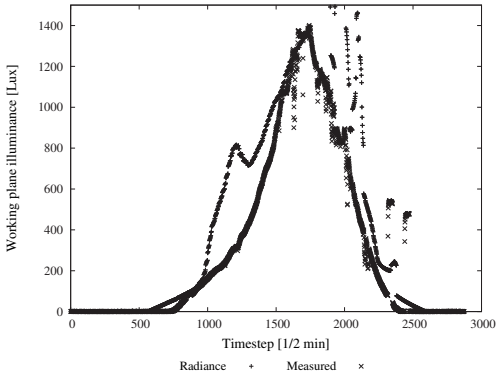

***Figure 4.11**: Validation of the Radiance model by measurements.*

discrepancies. Moreover, on a day without occupancy, it was ensured that artificial lighting was switched off. The curves in 4.11 partially correlate. During the time period between 16:30 and 21:00 (time steps 2000 and 2500), it was common for both curves that the data are scattered, which is probably due to reflection from surrounding surfaces. The peak in the morning in the simulations is not shared with the measured data, and this is probably due to the unknown position of the internal shading or by (moved) furniture blocking direct sunlight coming from one side of the sensor.

Daylight performance

The main feature, redirecting daylight to the ceiling where it is reflected further into the room, is demonstrated in Figure 4.12. The figure shows that the illuminance on the ceiling 3.4 m from the façade increased by approximately 500 lux, which increases the utilization of daylight further into the room. With the increase in illuminance proved, the next step in the evaluation was to assess the daylighting conditions. The annual WPI was investigated using Radiance calculations and the three-phase method (TPM).
Annual daylight autonomy (DA) was evaluated. Figure 4.13 shows DA for the new redirecting system with dynamic control. The original system is presented in Figure 4.14. The depth of room at which there was an illuminance of at least 500 lux for at least 50% of the time was extended from 3.2 m to 4.5 m into the room. The improvement in daylight conditions is visible throughout the depth of the space investigated. Furthermore, the room depth with at least 300 lux for 20% of the time was extended from 7.8 m to 10.2 m from the façade and covers most of the working area in the

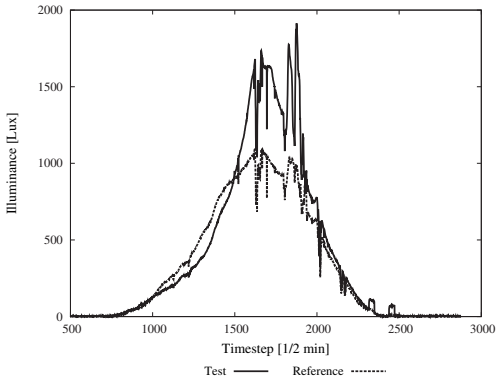

***Figure 4.12**: Comparison of illuminance measured under the ceiling for test and reference areas.*

office. So it can be stated that the tested system has higher illuminance more often and covers a larger area. The next annual daylight evaluation ma-

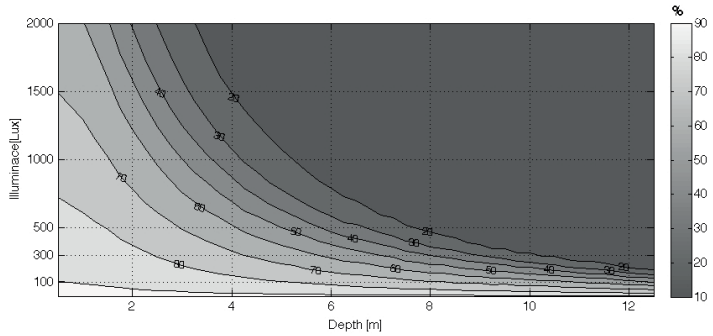

***Figure 4.13**: Daylight autonomy of the tested shading system with dynamically controlled position.*

trix used was useful daylight illuminance (UDI), which indicates the useful range of the illuminance and evaluates whether the illuminance is too high or too low. Once more, the investigation was throughout the space and the results were split according to the different rotation positions of the system. The UDI value increased especially at the back of the room where the tested system provided 20% more UDI above 100 lux. All over the room, UDI was improved. Near the façade, approximately 1 m from the faÃ§ade, the upper

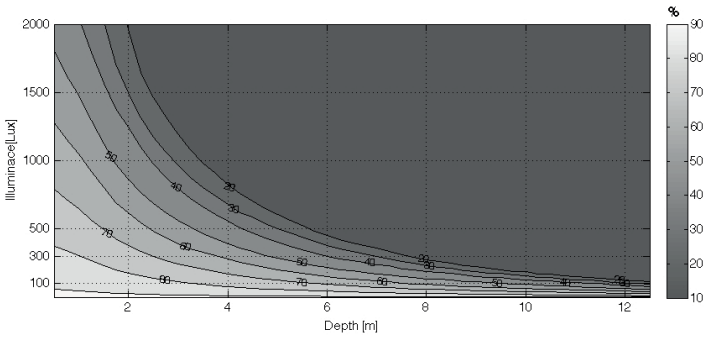

***Figure 4.14**: Daylight autonomy of the reference shading system in the closed position.*

limit of UDI was exceeded more frequently. However, most working places are outside this zone, so it would not cause many visual discomfort problems.

Energy performance

The system's thermal transmittance was calculated using BSDF matrices generated in Window 6, including visible and solar transmittance information. It was found that the $U_w - value$ of both systems in all positions was around 0.9 W/m^2K, so there is no difference in the thermal insulation. The system in the redirecting position provides 17% more visible transmittance but only an 11% increase in solar energy transmittance. This means that the daylight utilization can be higher while solar gains do not increase proportionally.

Glare analysis

The main feature of the system is to redirect daylight to the ceiling, which could have the side effect of increasing discomfort glare. This was limited by optimizing the redirecting position of the system, but in a situation of changing sky conditions (intermediate sky) or low altitude of the sun, some glare can occur. The glare was simulated with the dynamically positioning system reacting to outdoor horizontal illuminance on the roof. The system automatically closed when the threshold of 25 klux was exceeded. As expected, the tested system had approximately 5% higher values of the DGP index. The increase mainly happened in positions close to the façade. However, the change was noticeable in only 1% of cases and the glare caused discomfort.

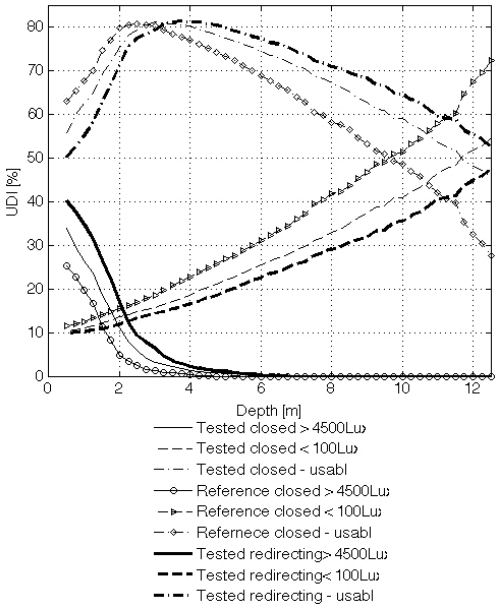

Figure 4.15*: Annual useful daylight illuminance matrix for different scenarios.*

This indicates that the system did not increase glare significantly by redirecting daylight to the ceiling. Carpet plots with the DGP index are shown in Figure 4.16.

Lighting energy savings

The last parameter evaluated in this study was electrical lighting energy savings from maximizing daylight. The on/off, bi-level switching, and continuous dimming control strategies were used for artificial lighting. In all cases, the new system provided higher WPI from daylight. For the various light controlling systems, the difference in lighting Zone 1, that closest to the windows, was between 9-15%. The difference between the savings from the various control strategies increased towards the back of the room, and the savings with the continuous dimming system were up to 23% more than a situation in which the light was on all the time. For more details on lighting energy savings, see Paper IV.

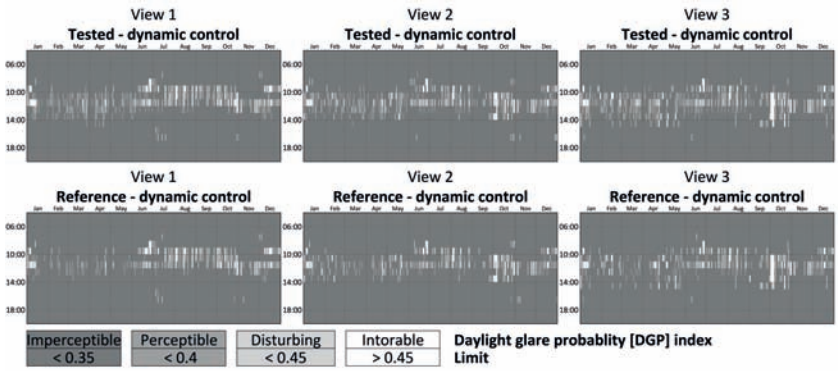

***Figure 4.16**: Annual DGP plots of glare index for the tested and the reference shading systems under dynamic control.*

4.2.3 Conclusion

From this study it can be concluded that daylight improvement in the indoor space was achieved with the daylight-redirecting shading system compared to the reference system. Glare analysis indicated that the redirecting system would not cause additional glare because the positioning of the lamellas was optimized to reflect daylight to the ceiling. The energy demand for artificial lighting was reduced by utilizing daylight. Depending on the daylight-linked lighting control strategy, the savings were up to 20% compared to the reference system and up to 80% in the lighting zone closest to the windows when compared to using artificial light only.

4.2.4 Future work

Since the simulations and measurements correlated only partially, more extensive measurements monitoring all the interior and exterior conditions should be carried out. This would help us to understand the redistribution of daylight in the indoor space and would reduce the high number of changing variables which are difficult to simulate.
The system directly interacts with the indoor working environment by redirecting daylight, which can affect the visual comfort of occupants by changing light intensity or contrast. So it would be beneficial to carry out a study including individual observations of occupants.

Chapter 5

Conclusion

This chapter presents the main conclusions of the research work. The overall conclusion is supplemented by four sub-conclusions which conclude each individual investigation.

Experimental and simulation-based investigations showed that it is possible to evaluate the performance of unique and innovative Complex Fenestration Systems (CFSs). Product development methods can help to optimize CFSs as well as facilitate the development process by identifying objectives and defining the testing procedures. CFSs usually combine several functions, so it is important to evaluate all the interconnected parameters to obtain a reliable and overall overview about their performance.
Optimal usage of a CFS makes it possible to improve visual comfort by utilizing daylight, increasing the transparency of windows, and controlling glare. Careful design of CFSs can reduce the energy demand of buildings. Such design should include reducing heat losses by using highly insulated fenestration components, controlling cooling loads by using integrated shading systems, and saving energy for lighting by making better use of daylight. Finally, it was demonstrated that it is possible to evaluate unique shading systems, which are not usually included in building performance simulation tools, by comprehensive thermal and optical performance modelling.

5.1 Slim window frame made of glass fibre reinforced polyester

This research focused on investigating the potential of using new innovative materials and designs of window frames to reduce the energy demand of buildings. In addition, the use of the product development method to facilitate such development was tested.
Several designs of window frame were suggested, and the designs were based on the design objectives identified with the help of the rational product development method. The rational product development method was also used to structure the testing procedure and evaluation process. The best energy performance was achieved by the slimmest frame, which combined a low Uf-value for the frame with the largest glazed area. This provided higher solar gains, while the load capacity was maintained with glass fibre reinforced polyester (GFRP) as the frame material. Savings of 6.5 $kWh/m^2/year$ were achieved in the office building with this frame, compared to an office using a traditional aluminium frame. Moreover, the investigation showed that the frame could also be used for a renovation, because the same window opening size was used and the energy savings were still obtained.
It can be concluded that the GFRP is a suitable material for window frames, that it can reduce the energy demand of buildings, and that it is a serious competitor to other window frame materials. Furthermore, the rational product development method helped to smooth the transition from the problem definition to the solution with a structured process, and showed that it is a feasible method for stimulating innovation in the window industry.

5.2 Energy performance of a ventilated window

The second investigation dealt with the idea of using the window as a heat recovery system. The thermal performance of a ventilated window was compared to the thermal performance of a traditional window combined with an exhaust ventilation. In experimental testing in a Guarded Hot Box, several airflows through the window were tested, ranging from 1.3 l/s to 8 l/s. The experiment showed that the ventilated air can be partly preheated and some of the heat loss recovered. The heat exchange takes place inside the glazing and in ventilation valves in the frame. However, the heat exchange in the frame also introduced a higher heat loss through the frame and consequently caused an increase in the total window thermal transmittance. The

heat recovery efficiency of the ventilated window strongly depends on the airflow, and the critical airflow is around 6 l/s, when the efficiency starts to decrease. Airflows higher than that further increased the heat transmittance of the window which reduced the heat recovery efficiency of the window. For the case investigated, the total energy demand savings were more than 10%. Efficiency drops with higher airflow rates, so ventilated windows are more suitable for buildings where a small ventilation rate is required. In addition to the experimental work, the research formed and unified a methodology for the assessment of the energy performance of ventilated windows. The heat balance for the window-room ventilation system was defined and can be used for comparing traditional windows with ventilated windows.

5.3 Modelling of micro structural perforated shading screen

Four Complex Fenestration Systems (CFSs) were compared and their performance was evaluated for several interrelated parameters to provide an overall picture of the performance. The main focus was on the evaluation of an integrated micro-structural perforated shading screen (MSPSS). This case was also used for the validation of the simulations. The results from the measurements and calculations showed good correlation.
It was found that angular-dependent shading systems are beneficial all-year-round in providing daylight, reducing heating load using solar gains while decreasing the risk of overheating during summer when the sun's angle of altitude is high. Visual comfort was evaluated using the Daylight Glare Probability (DGP) index, and it was demonstrated that visual comfort depends on blocking direct light as well as optimal positioning of view directions. Furthermore, using bi-directional information about the angularly selective CFS made it possible to simulate and accurately depict the shading system. The results were provided in the context of the incidence angle and location. The MSPSS performed well compared to the other fenestration systems tested, mainly due to its angular shading properties and unobstructed view to the outside.

5.4 Redirecting daylight glass shading system

This research study investigated a multifunctional dynamic integrated shading and daylight-redirecting system. The performance evaluation methodology was linked to the previous investigation because both evaluated a shad-

ing system and visual comfort. The simulation results were compared with measurements and the results correlated with some discrepancies. Improved daylighting was achieved with the redirecting shading system compared to the original system. Glare analysis indicated that the daylight-redirecting system would not cause additional glare.
It can be concluded that visual comfort was maintained and the daylight conditions in the office were improved. By introducing higher daylight penetration into the back of the office, the need for artificial lighting was decreased. Depending on the daylight-linked lighting control strategy, the savings were up to 20% compared to the reference system and up to 80% in the lighting zone closest to the windows when compared to using artificial lighting only. The thermal insulation of the faccade was the same for all the systems tested. Solar energy transmittance increased, but the increase was small and was not expected to increase the cooling demand significantly.

Bibliography

[1] BR10. Danish Building Regulations, 2010.

[2] Directive. 2010/31/EU of the european parliament and of the council. Technical report, 2010.

[3] IEA. Energy Performance Certification of Buildings. Technical report, 2010.

[4] IEA. Energy technology perspectives. Technical Report 1, 2010.

[5] IEA. 25 Energy Efficiency Policy. Technical report, 2011.

[6] Pyonchan Ihm, Abderrezek Nemri, and Moncef Krarti. Estimation of lighting energy savings from daylighting. *Building and Environment*, 44(3):509–514, March 2009.

[7] Carlos Ernesto Ochoa and Isaac Guedi Capeluto. Advice tool for early design stages of intelligent facades based on energy and visual comfort approach. *Energy and Buildings*, 41(5):480–488, May 2009.

[8] Eleanor Lee, Stephen E. Selkowitz, Vladimir Bazjanac, and Christian Kohler. High-Performance Commercial Building Façades. *LBNL*, 2002.

[9] Marco Sala. The intelligent envelope: the current state of the art. *Renewable energy*, 5(5-8):1039–1046, 1994.

[10] J. Carmody, Stephen E. Selkowitz, Eleanor Lee, Dariush Arasteh, and T. Willmert. *Window systems for high-performance buildings*. WW Norton, 2004.

[11] R Sullivan, L Beltran, Eleanor Lee, Michael Rubin, and Stephen E. Selkowitz. Energy and daylight performance of angular selective glazings. In *Proceedings of the ASHRAE/DOE/BTECC Conference*, number December, pages 7–11, 1998.

[12] Toke Rammer Nielsen, Karsten Duer, and Svend Svendsen. Energy performance of glazings and windows. *Solar Energy*, 69(1):137–143, July 2001.

[13] S. Hubalek, M. Brink, and C. Schierz. Office workers' daily exposure to light and its influence on sleep quality and mood. *Lighting Research and Technology*, 42(1):33–50, January 2010.

[14] Moncef Krarti, Paul M. Erickson, and Timothy C. Hillman. A simplified method to estimate energy savings of artificial lighting use from daylighting. *Building and Environment*, 40(6):747–754, June 2005.

[15] David Appelfeld, Christian Skodborg Hansen, and Svend Svendsen. Development of a slim window frame made of glass fibre reinforced polyester. *Energy and Buildings*, 42(10):1918–1925, October 2010.

[16] Arild Gustavsen, B. P. Jelle, and Dariush Arasteh. State-of-the-art highly insulating window frames-Research and market review. 2007.

[17] DS/EN 15603. Energy performance of buildings - Overall energy use and definition of energy ratings. 2008.

[18] David Appelfeld and Svend Svendsen. Experimental analysis of energy performance f a ventilated window for heat recovery under controlled conditions. *Energy and Buildings*, 43(11):3200–3207, November 2011.

[19] P.H. Baker and M.E. McEvoy. An investigation into the use of a supply air window as a heat reclaim device. *Building Services Engineering Research and Technology*, 20(3):105–112, January 1999.

[20] JR Gosselin. A dual airflow window for indoor air quality improvement and energy conservation in buildings. *HVAC&Research*, 14(3):359–372, 2008.

[21] David Appelfeld, Andrew McNeil, and Svend Svendsen. An hourly based performance comparison of an integrated micro-structural perforated shading screen with standard shading systems. *Energy and Buildings*, 2012.

[22] David Appelfeld and Svend Svendsen. Performance of a daylight redirecting glass shading system demonstration in an office building. In *Building simulation 2011*, page 8, Sydney, Australia, 2011.

[23] Eleanor Lee. Advanced High-Performance Commercial Building Facades Research. In *LBNL*, 2009.

[24] J. Clarke. Energy Simulation in Buiding Design, 2001.

[25] TRNSYS. The Transient Energy System Simulation Tool, 2011.

[26] EnergyPlus. EnergyPlus Energy Simulation Software, 2011.

[27] Andrew McNeil, Jacob Jonsson, David Appelfeld, Greg Ward, and Eleanor Lee. A validation of a ray-tracing tool used to generate bi-directional scattering distribution functions for complex fenestration systems. *Solar Energy*, submitted, 2012.

[28] F. Frontini, Tilmann E Kuhn, S. Herkel, Paul Strachan, and G. Kokogiannakis. IMPLEMENTATION AND APPLICATION OF A NEW BI-DIRECTIONAL SOLAR MODELLING METHOD FOR COMPLEX FACADES WITHIN THE ESP-R BUILDING SIMULATION PROGRAM - Annex. In *Building simulation 2009*, page 75, 2009.

[29] EN ISO. EN ISO 10077-2 Thermal performance of windows, doors and shutters - Calculation of thermal transmittance - Part 2: Numerical method for frames, 2003.

[30] Robin Mitchell, Christian Kohler, Ling Zhu, and Dariush Arasteh. THERM 6.3 / WINDOW 6.3 NFRC Simulation Manual. *LBNL*, (January), 2011.

[31] Sommer Informatik GmbH. WinIso2D Professional, 2011.

[32] Www.buildingphysics.com. HEAT2, A PC-program for heat transfer in two dimensions Update manual, 2011.

[33] EN ISO. ISO 15099_Thermal performance of windows, doors and shading devices - Detailed calculations, 2003.

[34] Natural resources Canada. *Consumer' s Guide To Buying Energy-Efficient Windows and Doors*.

[35] Svend Svendsen, Jacob Birck Laustsen, and Jesper Kragh. Linear thermal transmittance of the assembly of the glazing and the frame in windows. In *Proceedings of the 7th Symposium on Building Physics in the Nordic Countries*, pages 995–1002, Raykjavik, Iceland, 2005.

[36] D Saelens, S Roels, and H Hens. Strategies to improve the energy performance of multiple-skin facades. *Building and Environment*, 43(4):638–650, April 2008.

[37] Heinrich Manz, A Schaelin, and H Simmler. Airflow patterns and thermal behavior of mechanically ventilated glass double façades. *Building and Environment*, 39(9):1023–1033, September 2004.

[38] M.J. Holmes. Optimisation of the thermal performance of mechanically and naturally ventilated glazed facades. *Renewable Energy*, 5:1091–1098, 1994.

[39] Jun Tanimoto and Ken-ichi Kimura. Simulation study on an air flow window system with an integrated roll screen. *Energy and buildings*, 26(3):317–325, 1997.

[40] D Saelens, S Roels, and H Hens. The inlet temperature as a boundary condition for multiple-skin facade modelling. *Energy and Buildings*, 36(8):825–835, August 2004.

[41] EN ISO. EN ISO 673, Glass in building - Determination of thermal transmittance (U value) - Calculation method, 1997.

[42] Arild Gustavsen, Dariush Arasteh, B. P. Jelle, C. Curcija, and Christian Kohler. Developing Low-conductance Window Frames: Capabilities and Limitations of Current Window Heat Transfer Design Tools – State-of-the-Art Review. *Journal of Building Physics*, 32(2):131–153, October 2008.

[43] Jacob Birck Laustsen and Svend Svendsen. Improved windows for cold climates. In *7th Symposium on Building Physics in the Nordic Countries*, pages 987–994, 2005.

[44] Toke Rammer Nielsen, A.C. Hviid, and S. Petersen. iDbuild, BuildingCalc and LightCalc User Guide - Version 3.2.2, 2008.

[45] Aalborg University Research, Danish Building Institute. The Calculation Programme Be06, 2005.

[46] ESPR. ESP-r energy modelling tool, 2012.

[47] Tilmann E Kuhn. Evaluation of overheating protection with sunshading systems. *Solar Energy*, 69:59–74, 2001.

[48] Tilmann E Kuhn, Sebastian Herkel, Francesco Frontini, Paul Strachan, and Georgios Kokogiannakis. Solar control: A general method for modelling of solar gains through complex facades in building simulation programs. *Energy and Buildings*, 43(1):19–27, January 2011.

[49] Tilmann E Kuhn. Solar control : A general evaluation method for facades with venetian blinds or other solar control systems. *Energy and Buildings*, 38:648–660, 2006.

[50] Greg Ward and R.A. Shakespeare. *Rendering with Radiance: The Art and Science of Lighting Visualization*. Morgan Kaufmann, California, USA, 1998.

[51] John Mardaljevic. Validation of a lighting simulation program under real sky conditions. *Lighting Research and Technology*, 27(4):181–188, 1995.

[52] Christoph F. Reinhart and Jan Wienold. The daylighting dashboard - A simulation-based design analysis for daylit spaces. *Building and Environment*, 46(2):386–396, February 2011.

[53] H.A.L. van Dijk and H. Oversloot. WIS, the European tool to calculate thermal and solar properties of windows and window components. In *Proceedings of Building Simulation*, volume 3, pages 259–266, 2003.

[54] Saint Gobain Glass. Columen II, http://exprover.saint-gobain-glass.com/b2c/default.asp?nav1=act&id=13922, 2012.

[55] Pilkington. Pilkington Spectrum, http://spectrum.pilkington.com /Main.aspx?country=GB, 2012.

[56] Swisspacer. Caluwin, http://www.swisspacer.com/en/ service/caluwin.html, 2012.

[57] John Mardaljevic, Lisa Heschong, and Eleanor Lee. Daylight metrics and energy savings. *Lighting Research and Technology*, 41(3):261–283, September 2009.

[58] A Webb. Considerations for lighting in the built environment: Non-visual effects of light. *Energy and Buildings*, 38(7):721–727, July 2006.

[59] R Compagnon. Solar and daylight availability in the urban fabric. *Energy and Buildings*, 36:321–328, 2004.

[60] United States Department of Energy. Weather data - Copenhagen.

[61] Anne Iversen, Svend Svendsen, and Toke Rammer Nielsen. The effect of different weather data sets and their resolution in climate-based daylight modelling. *Lighting Research and Technology*, pages 1477153512440545–, March 2012.

[62] Axel Jacobs. Understanding rtcontrib. Technical report, London, UK, 2010.

[63] Greg Ward. Simulating the Daylight Performance of Complex Fenestration Systems Using Bidirectional Scattering Distribution Functions within Radiance. *Journal of the Illuminating Engineering Society*, (January), 2011.

[64] John Mardaljevic. Simulation of annual daylighting profiles for internal illuminance. *Lighting Research and Technology*, 32(3):111–118, January 2000.

[65] F. Cantin and M.-C. Dubois. Daylighting metrics based on illuminance, distribution, glare and directivity. *Lighting Research and Technology*, 43(3):291–307, February 2011.

[66] A Nabil and John Mardaljevic. Useful daylight illuminance: a new paradigm for assessing daylight in buildings. *Lighting Research and Technology*, 37(1):41–59, January 2005.

[67] Andrew McNeil and Eleanor Lee. Annual Assessment of an Optically-Complex Daylighting System Using Bidirectional Scattering Distribution Functions with Radiance. *LBNL*, pages 1–29, 2010.

[68] Christoph F. Reinhart. Validation of dynamic RADIANCE-based daylight simulations for a test office with external blinds. *Energy and Buildings*, 33:683–697, 2001.

[69] John Mardaljevic. *Daylight simulation: validation, sky models and daylight coeffcients*. Phd thesis, De Montfort University, UK, 2000.

[70] CEN EN 15251. Indoor environment input for design and assessment of energy performance of buildings addressing indoor air quality, thermal environment, lightning and acoustics, 2007.

[71] Jan Wienold. *Daylight Glare in Offices*. Phd thesis, 2009.

[72] P.R. Tregenza and I.M. Waters. Daylight coefficients. *Lighting Research and Technology*, 15(2):65–71, January 1983.

[73] Andrew McNeil. The Three-Phase Daylight Coefficient Method for Simulating Complex Fenestration with Radiance. Technical report, 2011.

[74] Marilyne Andersen and Jan de Boer. Goniophotometry and assessment of bidirectional photometric properties of complex fenestration systems. *Energy and Buildings*, 38(7):836–848, July 2006.

[75] Marilyne Andersen. *Innovative bidirectional video-goniophotometer for advanced fenestration systems*. PhD thesis, 2004.

[76] J.H. Klems. A new method for predicting the solar heat gain of complex fenestration systems - I Overview and Derivation of the Matrix Layer Calculation. *LBNL*, 1994.

[77] Greg Ward. Complex Fenestration and Annual Simulation. In *8th International Radiance workshop*, Boston, USA, 2009.

[78] N Tuaycharoen and P.R. Tregenza. View and discomfort glare from windows. *Lighting Research and Technology*, 39(2):185–200, June 2007.

[79] L Roche, E Dewey, and P Littlefair. Occupant reactions to daylight in offices. *Lighting Research and Technology*, 32(3):119–126, January 2000.

[80] J. Jakubiec and Christoph F. Reinhart. The 'adaptive zone' - A concept for assessing discomfort glare throughout daylit spaces. *Lighting Research and Technology*, October 2011.

[81] Jan Wienold. Dynamic daylight glare evaluation. In *Building simulation 2009*, pages 944–951. Citeseer, 2009.

[82] Jan Wienold and Jens Christoffersen. Evaluation methods and development of a new glare prediction model for daylight environments with the use of CCD cameras. *Energy and Buildings*, 38(7):743–757, July 2006.

[83] IESNA. *Lighting Handbook, Illuminating Engineering, 9th edition,*.

[84] DS/EN 15193. Energy performance of buildings - Energy requirements for lighting, 2007.

[85] CIE 38 (TC-2.3). Commission Internationale de l'Eclairage. Radiometric and photometric characteristics of materials and their measurement, 1977.

[86] J.H. Klems. A new method for predicting the solar heat gain of complex fenestration systems - II Detailed description of the matrix layer calculation.pdf. *LBNL*, 1994.

[87] P.R. Tregenza. Subdivision of the sky hemisphere for luminance measurements. *Lighting Research and Technology*, 19(1):13–14, January 1987.

[88] International Energy Agency. Daylight in Buildings - A source book on daylighting systems and components. IEA SHC Task 21/ECBCS Annex 29.

[89] Marilyne Andersen, Michael Rubin, and Jean-louis Scartezzini. Comparison between ray-tracing simulations and bi-directional transmission measurements on prismatic glazing. *Solar Energy*, 74(2):157–173, 2003.

[90] Stefan Lechtenböhmer and Andreas Schüring. The potential for large-scale savings from insulating residential buildings in the EU. *Energy Efficiency*, 4(2):257–270, September 2010.

[91] EN ISO. prEN ISO 12567-1_Thermal performance of windows and doors - Determination of thermal transmittance by the hot-box method - Part 1: Complete windows and doors, 2009.

[92] EN ISO. EN ISO 8990 - Thermal insulation - Determination of steady-state thermal transmission properties - Calibrated and guarded hot box, 1997.

[93] IEA TASK 27. Performance of Solar Facade Components. Technical report, 2005.

[94] Nigel Cross. *Engineering Design Methods: Strategies for Product Design*, volume 58. Wiley, 2008.

[95] Jingshu Wei, Jianing Zhao, and Qingyan Chen. Optimal design for a dual-airflow window for different climate regions in China. *Energy and Buildings*, 42(11):2200–2205, November 2010.

[96] WinDat. Window Information System software (WIS), WinDatThematic Network, 2006.

[97] H A L Van Dijk and Richard Versluis. Definitions of U- and g-value in case of double skin facades or vented windows. Technical report, 2004.

[98] Lau Markussen Raffnsoe. *Master Thesis Thermal Performance of Air Flow Windows*. PhD thesis, 2007.

[99] Jacob Birck Laustsen, Ines D.P. Santos, Svend Svendsen, Steen Traberg-Borup, and Kjeld Johnsen. Solar Shading System Based on Daylight Directing Glass Lamellas. In *Building Physics 2008 - 8th Nordic Symposium*, pages 111–119, 2008.

[100] Anne Iversen and Jacob Birck Laustsen. Udvikling af nye typer solafskærmnings- systemer baseret pådagslysdirigerende solafskærmende glaslameller. Technical report, 2009.

Part II

Appended Papers

Paper I

"Development of a slim window frame made of glass fibre reinforced polyester"

D. Appelfeld, C.S. Hansen & S. Svendsen

Published in: *Energy & Buildings, 2010*

Energy and Buildings 42 (2010) 1918–1925

Contents lists available at ScienceDirect

Energy and Buildings

journal homepage: www.elsevier.com/locate/enbuild

Development of a slim window frame made of glass fibre reinforced polyester

David Appelfeld*, Christian S. Hansen, Svend Svendsen

Department of Civil Engineering, Technical University of Denmark, Brovej, Building 118, DK-2800 Kgs. Lyngby, Denmark

ARTICLE INFO

Article history:
Received 30 March 2010
Received in revised form 13 May 2010
Accepted 26 May 2010

Keywords:
Product development
Energy performance
Efficient window
Composite material

ABSTRACT

This paper presents the development of an energy efficient window frame made of a glass fibre reinforced polyester (GFRP) material. Three frame proposals were considered. The energy and structural performances of the frames were calculated and compared with wooden and aluminium reference frames. In order to estimate performances, detailed thermal calculations were performed in four successive steps including solar energy and light transmittance in addition to heat loss and supplemented with a simplified structural calculation of frame load capacity and deflection. Based on these calculations, we carried out an analysis of the potential energy savings of the frame. The calculations for a reference office building showed that the heating demand was considerably lower with a window made of GFRP than with the reference frames. It was found that GFRP is suitable for window frames, and windows made of this material are highly competitive in their contribution to the energy savings. A rational product development method was followed, and the process clearly identified the objectives of the investigation and set out the appropriate way to attain them. Using simple rational development methods, a well-defined and effective window was achieved smoothly and quickly, as is illustrated in the case study.

1. Introduction

The basis of this article is the development of window frames made of glass fibre reinforced polyester (GFRP) facilitated by rational product development methods. GFRP is rarely used as a window frame material at the moment and very few window manufactures use it as an alternative to traditional materials [1]. So the article describes an investigation to illustrate the potential benefits of using GFRP for window frames. The investigation focused only on the frame made of GFRP, so the windows all contain the same triple glazing with a warm edge and argon for easy comparison with the reference frames.

Today, a window is considered energy efficient if it has a low thermal transmittance (*U*-value), but this is not sufficient to describe a window's energy performance. Windows are one of the most crucial elements in the building façade, so a more detailed evaluation of the interactions between window performances, energy demands and the indoor environment needs to be carried out. The factors to consider include thermal transmittance, solar energy transmittance, visual transmittance and the durability of the window as well as its influence on a building's energy consumption, artificial light savings by use of daylight, and the visual comfort of occupants.

The energy consumption of buildings is responsible for approximately 40% of energy used in the developed countries. The energy requirements of buildings are defined in the building codes and the Energy Performance of Buildings Directive (EPBD) [2–4] introduces tighter requirements. Windows are typically responsible for a large fraction of the heat loss in buildings, because the *U*-value of the window, including the frame, is much higher than the *U*-value of the other parts of the building envelope. However, windows can also contribute to heating by the solar energy transmitted through the glazing. This contribution is called the solar gain, which depends on the total solar energy transmittance of a window [5]. The window frame generally covers 20–30% of the overall window area and typically has a negative impact on the energy performance with a higher thermal transmittance than the glazing and no solar transmittance. A larger glazed area created by a reduced frame width can improve both the thermal transmittance and the solar gains of the window. These aspects of a window energy performance can be simply evaluated by net energy gains (NEG) [5,6].

Over the last two decades, the energy performance of windows has been greatly improved by introducing low-emissivity coatings, inert gasses with low conductivity in the glazing cavities, and a glazing with a warm edge. In contrast, very few changes have been made in the design of window frames and the selection of suitable materials [7]. Therefore, the greater part of the heat losses can now be assigned to the poor design of the window frame [8]. The most common window frames today are made of either materials with high conductivity, such as aluminium for office buildings and materials with low conductivity, such as wood and polyvinylchloride

* Corresponding author. Tel.: +45 45251856; fax: +45 45883282.
E-mail address: dava@byg.dtu.dk (D. Appelfeld).

0378-7788/$ – see front matter © 2010 Elsevier B.V. All rights reserved.
doi:10.1016/j.enbuild.2010.05.028

Nomenclature

A_f	projected frame area [m^2]
A_g	projected visible glazing area [m^2]
A_w	projected window area [m^2]
U_f	thermal transmittance of a window frame [W/m^2 K]
U_g	thermal transmittance of a glazing [W/m^2 K]
U_w	thermal transmittance of a single window [W/m^2 K]
l_ψ	visible perimeter of glazing [m]
Ψ	linear thermal transmittance due to combination of thermal effect of glazing, spacer and frame [W/m K]
τ_S	total solar energy transmittance of a single window
τ_g	solar energy transmittance of a glazing
τ_f	solar energy transmittance of a frame
NEG	net energy gain [kWh/m^2 year]
I	coefficient for solar gains [kWh/m^2]
D	coefficient for heat loss [kKh]

(PVC). Frames made of materials with low conductivity usually also have low strength, which requires wide frame profiles that reduce the total solar transmittance of the window.

The program iDbuild [9] was used to compare the annual energy consumption for an office building for different windows, and the program Be06 [10] was used to do the same for a domestic building. The thermal transmittance of the GFRP window frames was calculated using the finite element modelling (FEM) program THERM [11].

The article shows that it is possible to use rational product development methods to simulate the development of new windows and that window frames made of GFRP have a positive effect on the building energy performance. Besides the energy saving effect of the reduced frame size, the GFRP frame material contributes to the energy efficiency of the window with a low thermal conductivity of 0.32 W/m K [12], yet still has high strength and durability and requires minimal maintenance.

2. Methods

2.1. Rational product development method

One of our aims was to investigate the feasibility of using a product development strategy to develop a more energy efficient window. Nigel Cross's rational method of product development [13] was selected for this investigation, because of method suitability for purpose of the window development. The main and general principle of the rational method is shown in Fig. 1.

The possibilities in the project have to be identified at the beginning. Next comes the objective and problem specification, which defines the overall problem and by establishing its requirements defines its sub-problems. Furthermore, several design alternatives are generated as sub-solutions, and they are evaluated by quantitative performance calculations. We used the thermal performance and mechanical properties of the window as the performance criteria. This evaluation allowed us to select the final and most appropriate solution of a window frame. Throughout, the principle of the rational method was followed and adjusted to the purposes of window frame development.

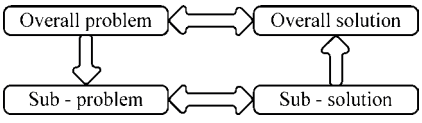

Fig. 1. Skeleton of the rational product development method [13].

2.2. Calculation of thermal performance

Calculation of thermal properties and energy performance was used to evaluate each design alternative. The energy performance evaluation was divided into four steps starting with a calculation of the heat loss coefficient of the frame and ending with a study of a window's effect on the building energy consumption.

As the first step, we calculated the *U*-value of the frames and, from this, the *U*-value of the whole window as a second step. The *U*-values were obtained by fine element method (FEM) in the simulation program Therm [11]. The third step was to use the net energy gains method to make a more complex calculation of the effect of the windows [5], taking into account the contribution of the solar gains minus heat losses of the window. The last step in the energy performance assessment was the comprehensive evaluation of the effect of the window on the energy consumption of the building. Here we took two cases, first an office building evaluated in the program iDbuild [9], and second a domestic building evaluated in the program Be06 [10]. All the proposed window frames were compared with the reference frames which were typical wooden and aluminium frames.

2.2.1. U-value of the frame

The *U*-values of all the frames were calculated based on the prescribed method in ISO 10077-2 [14]. The method is based on using a highly insulated panel which substitutes the glazing and eliminates the effect of thermal bridge by the glazing spacer.

The simulation program Therm [11] uses heat transfer coefficients prescribed by ISO 15099 [15] to solve the conductive heat transfer equations. The geometry of the profiles was drawn using computer-aided design (CAD) files as underlay. When the geometry is redrawn in Therm, the calculated geometry may contain some minor differences from the real shape.

2.2.2. Linear thermal transmittance and spacer

The thermal transmittance of the frame was calculated in the absence of the glazing and the thermal transmittance of the glazing does not include the effect of the spacer and the edge effect. The effect of the assembly edge and spacer is described by the linear thermal transmittance Ψ [14]. For the calculation of Ψ of the edge, the spacer is replaced with a simplified shape with equivalent thermal conductivity [16].

2.2.3. U-value of the window

The standard calculation of *U*-value for a window is prescribed by 10077-2 [14] as mentioned earlier, and it has to include the linear thermal transmittance (Ψ-value) of the assembly of the frame/spacer/glazing and the *U*-value of the frame and glazing [16,17]. The Ψ-value was obtained by simulation of the window frame with glazing in Therm. The *U*-value of the whole window was obtained by the following Eq. (1).

$$U_w = \frac{U_g A_g + U_f A_f + \Psi l_\psi}{A_w} \quad (1)$$

2.2.4. Total solar energy transmittance

The total solar energy transmittance τ_S of a window is defined as the solar energy transmittance value of the glazing area and the frame area together [15]. It has to be emphasized that windows are evaluated by the total solar energy transmittance of a window including the effect of the frame as described in the formula (2).

$$\tau_S = \frac{\sum \tau_g A_g + \sum \tau_f A_f}{A_w} \quad (2)$$

Table 1
Material properties for materials used in the Therm model.

Material	Conductivity ($W m^{-1} k^{-1}$)	Material	Equivalent thermal conductivity ($W m^{-1} k^{-1}$)
Soft wood	0.13	Spacer	0.243
Glass	1	Glazing cavity	0.022
Ethylene propylene diene monomer (EPDM)	0.25		
Silicon (glue)	0.35		
GFRP[a]	0.32		
Polysulphide	0.4		
Aluminium	160		
Insulated panel	0.035		

[a] Ref. [12].

2.2.5. Net energy gains

There are various ways of assessing the energy performance of a window. But it is clearly not sufficient just to evaluate the window *U*-value. The net energy gain (NEG) includes not only the thermal performance of the window, but also the contribution of its solar gains. The NEG method is based on a window's solar gain minus its heat loss in a standard period defined as the heating season depending on the outdoor air temperature. This takes into account the tilt and relative orientation of windows in a reference building [5]. NEG can reveal that a window with a very low *U*-value has a lower NEG than another window with a higher *U*-value.

For example a window with a *U*-value of 1.27 W/m^2 K (frame *U*-value 1.33 W/m^2 K) can have a higher NEG than a window with *U*-value 0.79 W/m^2 K (frame *U*-value 0.75 W/m^2 K) [18]. This would result from the greater area of glazing in the window with a higher *U*-value, which means that the heat loss can be compensated by a higher solar gain. NEG is described by below Eq. (3).

$$E = g\,I - U\,D \tag{3}$$

where *D* is the coefficient for heat loss and *I* is the coefficient for solar gains. Both coefficients are dependent on the location and window orientation. For Denmark, *I* is 196.4 kWh/m^2 and *D* is 90.36 kKh [5]. This approach to energy performance evaluation allows an easy and quick comparison of various windows.

2.2.6. Calculation of energy use of building

The effect on total building energy consumption was evaluated using iDbuild and Be06 [9,10]. iDbuild is a building simulation tool for an evaluation of energy performance and indoor environment based on hourly weather data. The program is able to illustrate how performance parameters and combinations of parameters affect energy performance, thermal indoor environment, air quality, and daylight conditions. As a reference building, we used a low energy class office building with 60 offices and a large glazed staircase space. The office building was simulated to investigate its energy use and the effect on indoor environment with respect to temperature and daylight as Case 1 in thermal evaluation under Step 4. As Case 2 in Step 4, a domestic building was simulated by the program Be06 [10]. Be06 calculations are performed in accordance with the mandatory calculation procedure described in the EU Directive on the energy performance of buildings [2,4,19].

2.3. Mechanical properties

In addition to the energy performance of the window frames, we also made a calculation of structural load capacity and deflections. We investigated three design criteria which affect durability: no air leakage due to frame deformation, no breakage of glass due to frame deformation, and the strength of frame profiles. By ensuring that these three requirements are met, we can ensure that the window will perform well mechanically. The structural calculation establishes maximal dimensions for a window in respect of these requirements.

3. Material properties

Table 1 describes the material properties used in the numerical simulations. Note that the emissivity of all the solid materials was 0.9. It should be mentioned that the equivalent thermal conductivity λ_{eq} for the spacer and glass cavity is based on the individual case. The gas in the cavity was replaced with a solid material which provided the same total thermal transmittance of the glazing, including gas properties and radiation. The equivalent thermal conductivity of a spacer, boundary conditions and surface heat transfer coefficients are in accordance with standard 10077-2 [14] and described in Table 2.

There are several advantages in using GFRP for window frames rather than common window frame materials, such as aluminium, PVC and wood. Table 3 shows that GFRP is eight times stronger than PVC and three and half times stronger than wood, which means that GFRP frames can be slimmer and do not require additional reinforcement. Moreover, the thermal conductivity is several times lower than for aluminium and similar to wood and PVC. According to a correspondence with Fiberline [12], the thermal conductivity of GFRP is 0.32 W/m K. The low thermal conductivity reduces thermal bridges and thus the risk of condensation and the growth of mould on window frames. Furthermore, GFRP does not absorb moisture, corrode or degrade in UV-radiation, so the durability of the material is greater and profiles do not require expensive maintenance. Last but not least, the thermal expansion of GFRP is almost identical to that of glass, which means that gaskets, water striping, glazing and window frame will not be exposed to additional stresses. All the relevant mechanical properties of GFRP and other materials used for windows are listed in Table 3.

4. Product development process

4.1. Problem specification

First of all, the opportunities in developing an energy efficient window using GFRP were identified. This meant that we had to investigate how to use innovative window frame design to reduce the energy demand of buildings, and how to evaluate those effects correctly in comprehensive and detailed calculations taking solar energy into account. The limitations were to use a triple glazing and GFRP material for the frame.

Table 2
Boundary condition of the models.

Name	Temperature (°C)	Heat transfer coefficient ($W m^{-2} K^{-1}$)
Outdoor boundary condition	0	25
Indoor boundary condition	20	7.69
Reduced boundary condition	20	5

Table 3
Mechanical properties of typical materials for window frames.

	E-modulus (GPa)	Tensile strength (MPa)	Thermal conductivity (W/K m)	Thermal expansion (10^{-6}/K)	Density (kg/m^3)
Softwood	7	14	0.13	4.5	500
Aluminium	72	300	160	23	2800
Steel	210	360	50	12	7800
PVC	3	-	0.17	6.1	1390
GFRP[a]	23	240	0.32	9	450
Glass	70	30–90	237	8–9	2700

[a] Ref. [12].

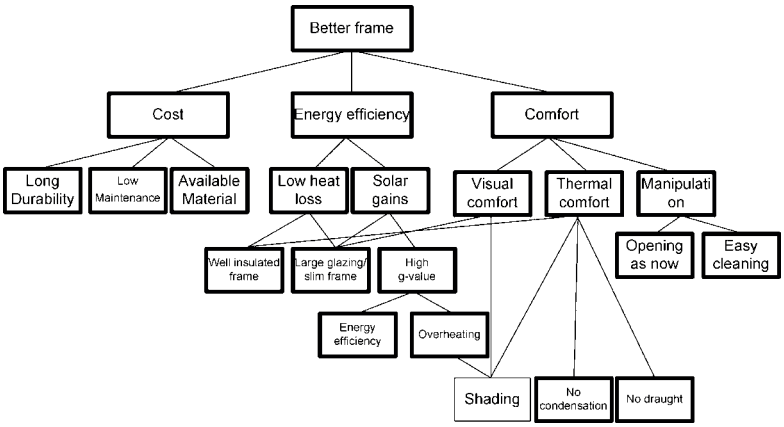

Fig. 2. Hierarchical diagram of relationships between objectives for improved window frame.

4.2. Objective clarification

From the specified opportunities, the problem objectives were explored together with their relationship and connections between levels. The newly developed window frame can serve several purposes and most of them are shown on the objective tree in Fig. 2. This figure shows how the objectives for a frame are clarified from top to low level by asking the question "HOW" and the individual sub-objectives are fulfilled from the lower level to the top by asking the question "WHY".

4.3. Requirements and limitations

All the clarified objectives for such a frame had to fulfill the specifications of a customer, user requirements, and production and technical requirements for producing and usage of the frame as listed in Table 4.

4.4. Designed alternatives

The most important and critical parameters for creating frames are width and thermal resistance of a frame, window solar gains, operability and possibility of cleaning the outside surface of a window from the inside, and the gasket tightness.

Three different alternative frames made of GFRP material were designed and are illustrated in Fig. 3. As the reference, a traditional wooden frame for a family house and a typical aluminium office window frame were used for comparison. To show the effect of the frame, all alternatives, including the reference frames, contain a triple glazing with same properties.

The Reference Frame 1 in Fig. 3(a) is a traditional wooden window used in Danish houses with a single side-hung casement opening outwards. A typical aluminium window, which is mostly used in office buildings but also in domestic buildings, is shown in Fig. 3(b). Alternative 1 of a window frame in GFRP in Fig. 3(c) is a sliding projecting window with top-hung casement and open-

Table 4
List of technical specifications for the frame.

Specification—Window frame from GFRP		
Number	R or W[a]	Requirements
1	R	Using standard double or triple glazing
2	R	Glued glazing into the frame by silicon or epoxy resin
3	W	Frame visible high at the most 50 mm
4	R	Sides of the frame connected by mechanical connections in the corners
5	W	Use same profiles for both triple and double glazed window
6	R	Wooden appearance from inside
7	W	The finishing of the frame has to be available in several colours
8	R	Manipulation by one hand
9	R	Easy operable and easy to clean
10	R	Slim hinges for placement into the frame
11	R	Hinges screwed directly into the wall
12	R	Water and air tight gasket between sash and frame—2 mm
13	R	Maximal deformation 1/300 or max 8 mm of a window side length
14	R	Minimal strength of frame 300 MPa
15	R	Net energy gain minimally of window −20 kWh/m^2 per year for double glazing
16	R	Net energy gain minimally of window 0 kWh/m^2 per year for triple glazing
17	R	Insulation in the wall has to be covered water-tight by the frame
18	R	Minimal thickness of profile wall 1.5 mm

[a] R, requirements; W, wishes.

ing outside. This kind of window is characteristic for the Danish market and allows turning the outer surface to the interior for easy cleaning. Alternatives 2a and 2b in Fig. 3(d) and (e) are tilt and turn windows with openings inward and are the most common window type in Europe. These two alternatives are different in the hinge and the width of the frames. Alternative 2a is equipped with a standard tilt and turn hinge which requires a certain amount of space for mounting and so the frame is larger. The alternative 2b is equipped

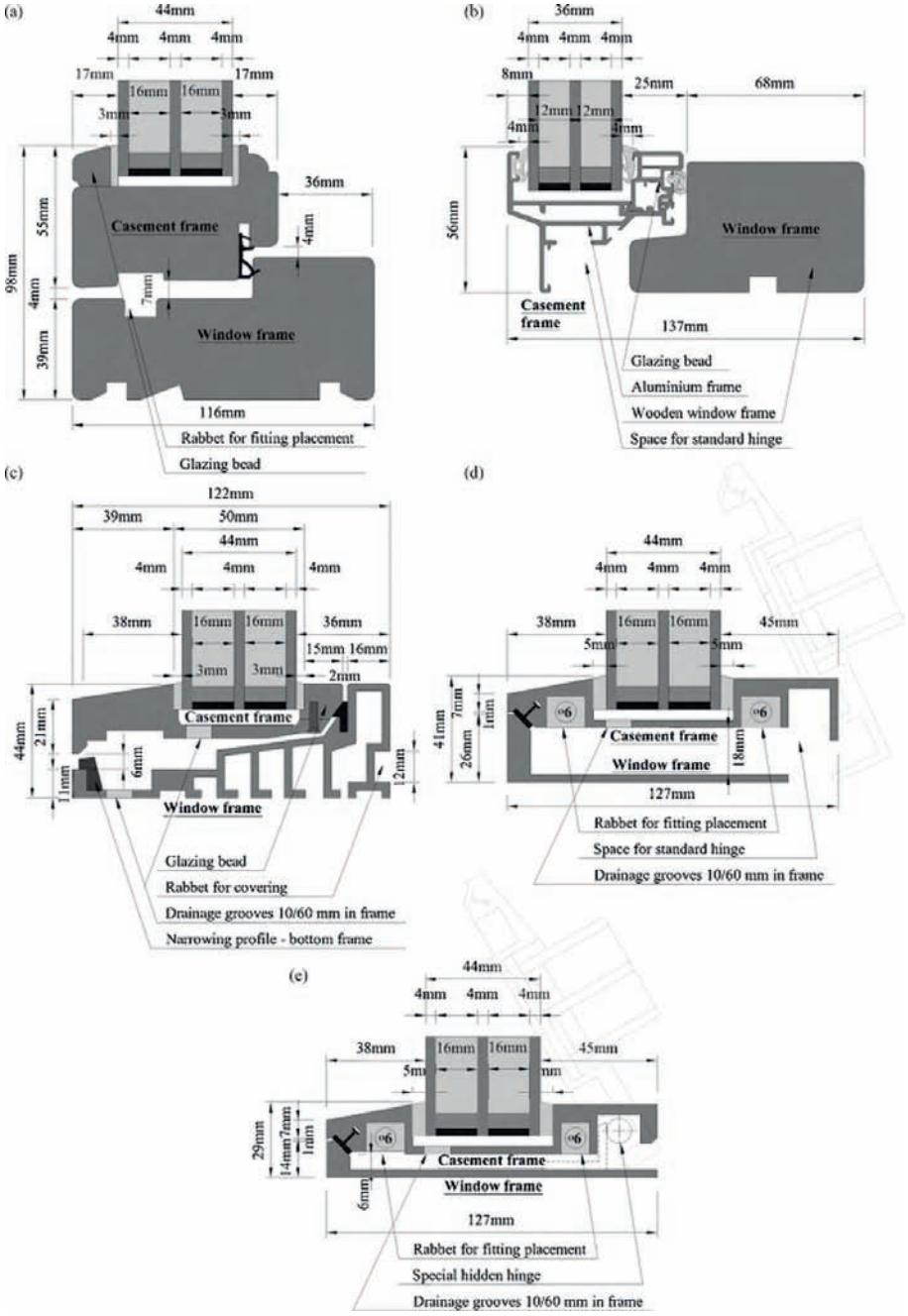

Fig. 3. (a) Reference 1—wooden frame, (b) Reference 2—aluminium frame, (c) Alternative 1, (d) Alternative 2a, (e) Alternative 2b.

Table 5
Window and frame properties of the alternatives evaluated.

Window characteristics	Reference 1	Reference 2	Alternative 1	Alternative 2a	Alternative 2b
Width of frame (mm)	98	56	44	41	29
Linear transmittance—ψ (W/m K)	0.034	0.045	0.032	0.031	0.032
g-Value glazing/window (−)	0.51/0.37	0.51/0.43	0.51/0.45	0.51/0.45	0.51/0.45
Light transmittance of glazing/window (−)	0.7/0.61	0.7/9.59	0.7/0.62	0.7/0.64	0.7/0.51
Frame area of window (%)	27	16.1	12.7	11.8	8.4

Table 6
Thermal and energy properties of evaluated frame alternatives.

	Window characteristics	Reference 1	Reference 2	Alternative 1	Alternative 2a	Alternative 2b
1	Frame U-value (W/m^2 K)	1.22	3.19	1.43	2.00	1.9
2	Window U-value (W/m^2 K)	0.85	1.24	0.79	0.85	0.8
3	NEG (kWh/m^2)	−3.9	−28.4	15.7	11.2	19.3
4	Building energy demand/heating					
	Case 1 (kWh/m^2)	29.5/11	34.5/15	28/9	29/10	28/9
	Case 2 (kWh/m^2)	67.7/61.1	74.9/67.4	66.9/58.1	67.8/58.9	66.9/57.6

with a special hinge that can be hidden in the casement frame and reduces the frame width compared to alternative 2a by 12 mm.

The alternatives were evaluated thermally in four successive steps, which were U-value of frame, U-value of window, net energy gains, and building energy consumption. Furthermore, the load capacity and deformation of the frames were assessed against the wind load.

5. The evaluation of the frames

As one of the last steps in the rational product development method, the proposed alternatives were evaluated. Thermal properties for all the frames were calculated in the program Therm [11]. Table 5 lists the characteristics of the frame alternatives and windows, including visible width of frame, linear transmittance through the glazing/frame/spacer assembly, solar energy and light transmittance of glazing/window and frame area of the window. Table 6 shows frame U-values (Step 1), the U-value of the window (Step 2), NEG (Step 3), and the energy consumption of the reference buildings (Step 4).

5.1. Thermal properties

Considering the U-value of the frames alone shows the best insulated frame to be the Reference Frame 1 with a U-value of 1.22 W/m^2 K. This is due to the fact that the thermal conductivity of wood is lower than that of GFRP. The reference aluminium frame has the highest U-value because of the high thermal conductivity of aluminium. Alternatives 2a and 2b have the highest frame U-values of the proposed frames, which are 2 W/m^2 K and 1.9 W/m^2 K, respectively. The reason is that the air cavity in the frame is large and almost connected to the exterior. Moreover the frame profiles are straight along a heat flux flow, which allows conduction of the heat. One consequence of this could be lower interior frame temperatures with a risk of condensation. However, the frames are sufficiently insulated and the surface temperature is the same or slightly lower than for the reference frames. But the U-value of the frame alone is not a sufficient description of the real energy performance of the frame and does not evaluate the overall window performance, which is required [2].

The second step in the assessment of the frames was to calculate the overall window U-value. The window U-value of the proposed windows was significantly reduced by the slimmer frames because of the larger glazing area. The U-values of all the windows are between 0.85 W/m^2 K and 0.79 W/m^2 K, except for Reference Frame 2, which has a U-value of 1.24 W/m^2 K for a window size of 1230 mm × 1480 mm. The reduction of the window U-value for Alternative 2b compared to 2a is 0.05 W/m^2 K, and this was achieved by hiding the hinge in the casement frame and narrowing the frame. The percentage of the frame area in the total window area was lowered significantly. The frame area compared to the total area of the window with dimensions 1230 mm × 1480 mm was calculated and is presented in Table 5.

The next step in accordance with the methodology was to calculate the NEG [5]. The NEG was negative only for the reference windows; otherwise it was positive for all the proposed frame alternatives. This means that the reference windows have a larger heat loss than their solar energy gain, and the proposed alternatives contributed positively to the heating of the building—firstly, because the heat loss through the window was reduced, and secondly, the energy consumption for heating the space was partially replaced by the solar energy which penetrated the room. Moreover, the partial substitution of the frame area by low U-value glazing also helped reach the lower window U-value. The slimmest frame, alternative 2b, provides the highest positive NEG, 19.3 kWh/m^2 per year, which is 23.2 kWh/m^2 per year better than Reference 1 and 47.9 kWh/m^2 per year better than Reference 2. Alternatives 1 and 2a also provide very high NEG performance: 15.7 kWh/m^2 and 11.2 kWh/m^2, respectively.

The last step of the energy performance evaluation was a simulation of a whole building energy performance in iDbuild and Be06. The results of Step 4 are shown in Table 6 and present two cases: the total energy consumption of a reference office building (Case 1) and of a reference domestic building (Case 2). The total energy consumption of buildings includes heating, cooling, ventilation, hot water and lighting [19].

Case 1 investigates primarily the impact on the energy demand of the office building with the replacement of the aluminium windows. Since the office building has the windows across the whole width of rooms, the big windows were simplified by three identical single window units coupled together. In this arrangement the different window alternatives reduced the building energy consumption from 34.5 kWh/m^2 per year to 28 kWh/m^2 per year for a building with Frame Alternatives 1 and 2b. Alternative 2b provided the biggest total energy saving of approximately 6.5 kWh/m^2 per year over the aluminium window—Reference 2. This comparison reveals the potential of using the slim frame made from GFRP, because of increasing transparent part of the window and reducing heat loss of the frame. The enlarged glazing area of all the alternatives compared to the references increased the total visual

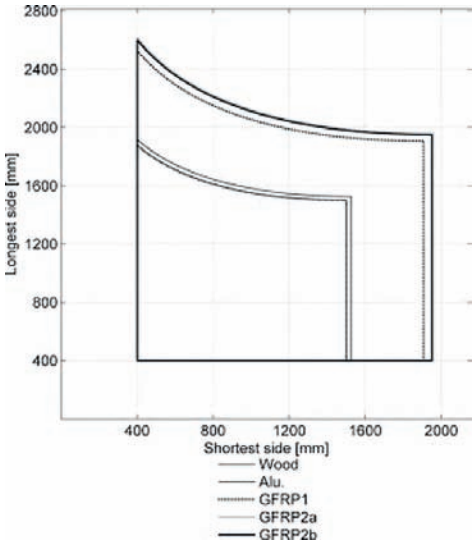

Fig. 4. Envelope of possible window sizes for different frame types.

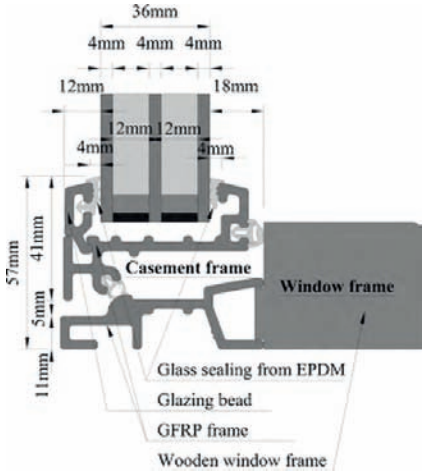

Fig. 5. Example of a real application of a GFRP window frame.

light transmittance of the window so that the daylight factor in the middle of the room increased from 5.4% (Reference 1) and 6.0% (Reference 2) to 6.3%. Moreover, the *g*-value is higher, which increases the solar gains compared to the reference window, see Table 5. Case 1 focuses on comparison with the aluminium window, but Table 6 also presents results for the wooden frame, Reference 1.

In Case 2, the focus is on the replacement of the wooden window frame by a GFRP window frame in a domestic building where wooden window frames are usual—Reference Frame 1. Table 6 shows the energy saving effect achieved when the wooden (or aluminium) window is replaced by the window made of GFRP. Using Frame Alternative 2b reduced the building energy requirement by 3.5 kWh/m^2 per year compared to the wooden frame and by 9.8 kWh/m^2 per year compared to the aluminium frame. It means that the Frame Alternative 2b performs as the best solution between all the frames. The other proposed alternatives have the smaller energy requirement reduction of 2 kWh/m^2 per year compared to Reference 1.

5.2. Structural performance

The structural performance and feasibility of the frames were evaluated and analysed. Three separate requirements were imposed on the structural performance of the windows [20]. The first requirement was a maximum deformation limit with regard to air tightness of the seal, where a serviceability state wind pressure was used. The second requirement was a maximum deformation limit with regard to failure of the glass. For this, an ultimate limit state wind load was applied to the window. The third and last requirement was load capacity. This checked that the bending stresses in the frames due to movement did not exceed the strength of the material. For a given side length it is possible to calculate the largest possible second side length using the above three requirements. The maximal possible size of the window frame is analysed in Fig. 4, which shows an envelope of the results. The lines in Fig. 4 limit the boundaries for a maximal window size. As can be seen, the alternatives proposed provide the possibility of greater window size, which means that the design and the material properties of GFRP allow bigger windows to be built without risk of wind failure.

5.3. Example of commercialized product

Up to this point, the window frames were created using the rational product development method, but one way of showing the feasibility of GRFP is to use a real example. There is a window frame comparable to the suggested frames which is already on the market and is shown in Fig. 5 [21]. This window was primarily developed for the Danish market and that is why it opens outwards. The inside surface of the frame is overlaid with wood. The width of the frame is 57 mm and the frame *U*-value is 1.42 W/m^2 K, which was achieved by optimizing the frame from previous test versions of a window of the size 1230 mm × 1480 mm. The glazing is a triple glazing, which combined with the frame provides an overall *U*-value for the window of 0.76 W/m^2 K, which is low and very similar to the windows we analysed. The NEG is calculated to be 7 kWh/m^2 per year. This is slightly lower compare to the analysed window frames and shows that the suggested frames are realistic.

6. Conclusion

The best solution for the frame is the alternative 2b, which reduced the energy consumption of the office building by 6.5 kWh/m^2 per year compared to the reference frame 2. This building energy consumption reduction and improvement was achieved using windows with slim GFRP frames which also satisfied structural criteria.

Moreover, it can be seen from the Case 1 and the Case 2 in the investigation where the window sizes were the same that this solution is suitable for renovations, requiring the simple replacement of a window [22]. The article has shown that GFRP is the suitable material for window frames and is a serious competitor to other window frame materials. As can be seen from the example of commercialized product and from some window manufactures [1,21], the potential advantages of using GFRP for window frames can be successfully implemented in real-life. The potential benefit of GFRP window frames is in saving energy by lower *U*-value of a window, increasing solar gains by reducing frame width, improving indoor comfort and meeting future energy requirements [2].

The rational product development method illustrated in the development of an energy efficient window was used and showed that it is feasible to use such a method to stimulate innovation in the window industry. The method was based on a successive and

logical chain of rational steps which transform the problem objective into a successful solution. The product development strategy helped to smooth the transition from the problem definition to the solution by a structured process.

Acknowledgements

The research was funded by the Danish Energy Agency program on research and demonstration of energy savings, EFP-2007, under the project name "Development of new types of low energy windows of composite materials", number 033001/33033-0067. The authors would like to acknowledge Fiberline Composites A/S and PRO TEC VINDUER A/S for their co-operation and contribution to this paper. The authors wish to thank Jesper Kragh for his work preceding this research project.

References

[1] S.P. Wake, Pultruded fibreglass: a window frame for the 90s, in: Proceedings of A World Conference on State-of-the-Art Window Technologies for Energy Efficiency in Buildings, Toronto, 1995.
[2] European Directive on the Energy Performance of Buildings (2002). Directive 2002/91/EC of the European Parliament and of the Council of 16 December 2002 on the Energy Performance of Buildings.
[3] Ministry of Climate and Energy, http://www.stm.dk/publikationer/UK_Regeringsgrundlag2007/index.htm.
[4] BR, The Danish Building Code, 2008, http:\\www.BR08.dk.
[5] T.R. Nielsen, K. Duer, S. Svendsen, Energy performance of glazings and windows, Solar Energy 69 (Suppl. 1–6) (2000) 137–143.
[6] A. Gustavsen, et al., Developing low-conductance window frames: capabilities and limitations of current window heat transfer design tools—state-of-the-art review, Journal of Building Physics 32 (2) (2008).
[7] http://www.swisspacer.com, 29.01.2010.
[8] N. Byars, D. Arasteh, Design options for low-conductivity window frames, Solar Energy Materials and Solar Cells 25 (1992) 143–148.
[9] T.R. Nielsen, A.C. Hviid, S. Petersen, iDbuild, BuildingCalc and LightCalc User Guide, Version 3.2.2, 2008, www.iDbuild.dk.
[10] The Calculation Programme Be06 Version 4.9.2.4, Danish Building Research Institute, Aalborg University.
[11] R. Mitchell, C. Kohler, D. Arasteh, THERM 5.2/WINDOW 5.2 NFRC Simulation Manual, Lawrence Berkeley National Laboratory, University of California, Berkeley, CA, 2006.
[12] http://www.fiberline.com, 29.01.2010.
[13] N. Cross, Engineering Design Methods: Strategies for Product Design, 4th ed., John Wiley & Sons, Chichester, 2008, ISBN 9780470519264.
[14] EN ISO 10077-2:2003, Thermal Performance of Windows, Doors and Shutters-Calculation of Thermal Transmittance, Part 2: Numerical Method for Frames, European Committee for Standardization, Brussels, Belgium, 2003.
[15] ISO 2003, ISO 15099:2003(E), Thermal Performance of Windows, Doors and Shading Devices—Detailed Calculations, International Organization for Standardization, Geneva, Switzerland, 2003.
[16] S. Svendsen, B.J. Laustsen, J. Kragh, Linear Thermal Transmittance of the assembly of the Glazing and the Frame in Windows, in: Proceedings of the 7th Symposium on Building Physics in the Nordic Countries, Technical University of Denmark, Department of Civil Engineering, 2005, ISBN 9979-9174-5-8, pp. 995–1002.
[17] Consumer's Guide To Buying Energy-Efficient Windows and Doors, Energy Publications, Office of Energy Efficiency, Natural resources Canada, 2004, ISBN 0-662-37461-4.
[18] B.J. Laustsen, S. Svendsen, Improved Windows for Cold Climates, in: Proceedings of the 7th Symposium on Building Physics in the Nordic Countries, Technical University of Denmark, Department of Civil Engineering, 2005, ISBN 9979-9174-5-8, pp. 987–994.
[19] EN 15603:2008(E), Energy Performance of Buildings—Overall Energy Use and Definition of Energy Ratings, European Committee for Standardization, Brussels, Belgium, 2008.
[20] K. Michael, Performance, durability and sustainability of advanced windows and solar components for building envelopes, in: International Energy Agency, Solar heating & cooling programme, Task 27–Performance of Solar Façade Components, October, 2007.
[21] http://protecwindows.com/da.aspx, 24.02.2010.
[22] H. Tommerup, S. Svendsen, Energy savings in Danish residential building stock, Energy and buildings 38 (2006) 618–826.

Paper II

"Experimental analysis of energy performance of a ventilated window for heat recovery under controlled conditions"

D. Appelfeld & S. Svendsen

Published in: *Energy & Buildings, 2011*

Energy and Buildings 43 (2011) 3200–3207

Contents lists available at SciVerse ScienceDirect

Energy and Buildings

journal homepage: www.elsevier.com/locate/enbuild

Experimental analysis of energy performance f a ventilated window for heat recovery under controlled conditions

David Appelfeld*, Svend Svendsen

Department of Civil Engineering, Technical University of Denmark, Brovej, Building 118 DK-2800 Kgs. Lyngby, Denmark

ARTICLE INFO

Article history:
Received 1 April 2011
Received in revised form 6 April 2011
Accepted 16 August 2011

Keywords:
Ventilated window
Active facade
Heat transfer
Guarded hot box
Thermal measurements

ABSTRACT

A ventilated window in cold climates can be considered as a passive heat recovery system. This study carried out tests to determine the thermal transmittance of ventilated windows by using the Guarded Hot Box. By testing under defined boundary conditions, the investigation described the heat balance of the ventilated window and clarified the methodology for thermal performance evaluation. Comparison between windows with and without ventilation using the window-room-ventilation heat balance revealed that a ventilated window can potentially contribute to energy savings. In addition, it was found that a significant part of preheating occurred through the window frames, which positively influenced the heat recovery of the window but increased the heat loss. Results also showed that increasing air flow decreased the recovery efficiency until the point when the additional thermal transmittance introduced by the ventilation was higher than the effect of heat recovery. Accordingly, the use of the ventilated windows might be most suitable for window unit with low ventilation rates. The results correlated with theoretical calculations in standards and software. However, the concept of a window thermal transmittance (U_w) value is not applicable for energy performance evaluation of ventilated window and requires deeper analysis.

1. Introduction

During recent decades there has been an increased national and international focus on lowering the energy demands in buildings [1,2]. Interest is growing among architects and consultants towards intelligent building components which can achieve building energy effectiveness, complying with strict energy codes and national emissions reduction goals [3,4]. Resulting initiatives with the goal of reducing transmission heat losses through building envelopes have subsequently created almost air tight buildings. However, windows still contribute in a large part to the total building heat loss, in spite of introducing coatings, sealed glazing, and tight gaskets [5]. Building envelopes have continuously improved by reducing thermal transmittance, but by preventing air leakage and air infiltration into buildings, the amount of required background ventilation had to be increased to ensure sufficient fresh air supply. Therefore, ventilation became a large part of the total building heating energy in cases when a heat exchanger cannot be used [6,7]. It is usually not an obstacle to ensure sufficient air exchange by mechanical ventilation in new buildings. However, when existing buildings, especially apartment buildings, are refurbished and air tightened it becomes expensive to build mechanical ventilation with heat recovery. In most cases, an exhaust ventilation system is used, causing an increase in energy demand for heating up the ventilated air to the required room temperature [8].

In a standard situation, a window and ventilation form two separate systems; by combining the two, it is possible to build a ventilated supply window [8]. In the ventilated window, fresh air is passed through a cavity between glass panes and some of the heat transmitted through the window is reclaimed by pre-heating the fresh air. An energy balance of ventilated windows was documented by several investigations, mainly theoretical and numerical [8–11]. The results of the investigations pointed out a potential in reducing heating demand by the air preheating. However, the supply air temperature could not reach the room air temperature [12]. It is thus necessary to further heat the supplied air to room temperature, despite the air pre-heating. Ventilated windows could be beneficial during both heating and cooling seasons; however this investigation focuses on the energy performance during the heating season [6,13].

2. Background

Ventilated windows are already available on the market, but there is little documentation available on their generic thermal energy performances under controlled and defined conditions.

* Corresponding author. Tel.: +45 45251856; fax: +45 45883282.
E-mail address: dava@byg.dtu.dk (D. Appelfeld).

0378-7788/$ – see front matter © 2011 Elsevier B.V. All rights reserved.
doi:10.1016/j.enbuild.2011.08.018

Nomenclature

$U_{w,trans,ext}$	Thermal transmittance of a ventilated window (W/m^2 K)
U_w	Thermal transmittance of a window (W/m^2 K)
$U_{w,vent}$	Ventilation heat loss of window (W/m^2 K)
$U_{w,trans}$	Total thermal transmittance of a window in a ventilated window (W/m^2 K)
T_{ni}	Interior environmental temperature (°C)
T_{ne}	Exterior environmental temperature (°C)
T_{vent}	Ventilation mean air temperature (K)
$Q_{air,vent}$	Energy flux to heat up ventilated air to room temperature (W)
ρ	Density (kg/m^3)
c_p	Specific heat capacity (J/kgK)
$Q_{w,trans}$	Energy flux from indoor environment to window (W)
$Q_{w,trans,ext}$	Energy flux from window to outdoor environment (W)
$Q_{w,vent}$	Advective energy flux (energy transported by ventilated air) (W)
A_w	Window area (m^2)
h_{ci}	Indoor convective heat transfer coefficient (W/m^2 K)
h_{ce}	Outdoor convective heat transfer coefficient (W/m^2 K)
h_{ri}	Indoor radiative heat transfer coefficient (W/m^2 K)
h_{re}	Outdoor radiative heat transfer coefficient (W/m^2 K)
Φ	Volume flow (m^3/s)
T_{si}	Indoor surface temperature of a window (°C)
T_{si}	Outdoor surface temperature of a window (°C)
$T_{gap,in}$	Air temperature in a window inlet valve (°C)
$T_{gap,out}$	Air temperature in a window outlet valve (°C)
W	Width (m)
H	High (m)
Δ	Uncertainty (by associated unit)
q_{sp}	Heat flow rate density of sample (W/m^2)
Φ_{in}	Corrected metering box heat input (W)
Φ_{sur}	Surround panel heat flow rate (W)
Φ_{edge}	Edge zone heat flow rate (W)

Several researches provided models for specific examples and ideas of how to improve the performances; however the experimental results are rarely available [9,14,15]. Impact in a real situation has to be experimentally investigated and validated with well-known boundary conditions to demonstrate the consequences of introducing ventilation through the glazing cavity. It is also important to provide the results independent of a building and HVAC set-up, therefore this investigation suggests a testing procedure which is reproducible. To build a more generic knowledge about ventilated windows, several aspects are excluded from the investigation since they are dependent on parameters such a location and orientation of a building. Therefore a "dark *U*-value", without exposing the testing sample to solar radiation, is considered because it is based only on the temperature difference across the sample which can be interpreted into any building.

This work is motivated by a current lack of available methods for evaluating ventilated window energy performance characteristics such as thermal transmittance. The aim is to determine the preheating of the air under various air flow volumes, since standardized methods of evaluating the ventilated window heat balance by measurements do not currently exist. Another objective of this work was a consolidation of the theory behind the ventilated window heat balance calculation, because presently a consistent theoretical methodology for ventilated window evaluation is missing. ISO 15099 provides notes referring to calculation of the heat balance of the ventilated window, but the ISO 15099 calculation model of thermal transmittance and ventilation heat gain for ventilated cavity windows is for information purposes only [16]. The ISO 15099 method is implemented in the computer program WIS [10]. Correlation between results in WIS and results from our analysis is discussed in this article.

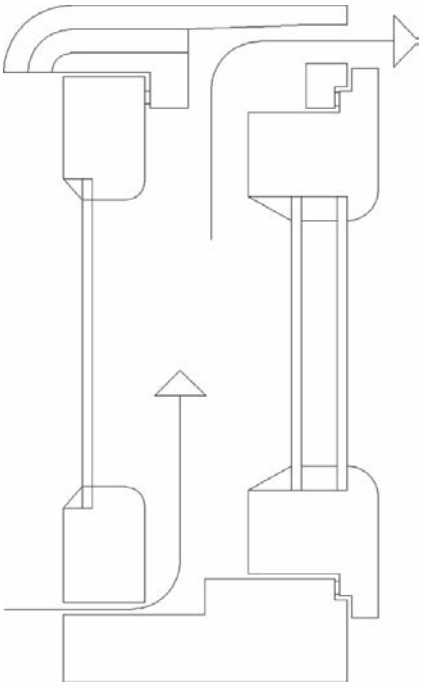

Fig. 1. Schematic picture of the used ventilated window with airflow marked.

3. Experiment

Experimental work focused on quantifying the regained heat loss from the ventilated air cavity and reducing the energy demand for heating during heating season when the temperature gradient between indoor and outdoor is 20 K. All investigations were carried out at the experimental facility at Technical University of Denmark (DTU). Specifically, the experiments utilized a Guarded Hot Box (GHB) with several adjustments compared to the standardised GHB described in ISO 12567-1 [17].

3.1. Ventilated window

The principle of the ventilated window is that the bottom and top window frames have integrated operable vents. The bottom frame connects the outside environment and the glazing air cavity. The top frame connects the air in the cavity to the interior environment. The simplified drawing of the window is shown in Fig. 1.

The tested window was a "1 + 2" coupled window with sealed double glazing on the interior side and a single uncoated glass pane on the exterior. The sealed glazing contains two low-e coatings; a soft coating on position 5 facing the sealed argon filled cavity

and a hard coating, K-glass, on position 3 facing a ventilated air cavity. All glass panes were 4 mm thick, the air gap was 83 mm, and the argon filled cavity in the double sealed glazing was 15 mm. The window frame and sash frames were made of soft wood. The inlet valve-in was positioned in the bottom frame and the air was sucked under the external sash. The valve-out was placed in the wide groove in the top frame and the valve was positioned to lead the air from the ventilated cavity via frame to the interior. The inlet valve was filled with a porous sponge to uniform the air flow.

3.2. Experimental equipment for the thermal transmittance

Thermal transmittance of the ventilated window was investigated by using the Guarded Hot Box (GHB) for measurements of the "dark U_w-value". The GHB was calibrated according to standards EN ISO 12567-1 and EN ISO 8990 [17,18]. The total heat flow through the specimen was measured based on the power input to a metering box. The heat flow through the specimen was generated by exposing the window to a temperature difference of 20 K [17]. The window was placed between a warm and a cold chamber with defined, controlled and measured environmental temperatures, T_{ni} and T_{ne}. The chamber temperatures were collected simultaneously and were based on the air temperatures and radiant temperatures of the baffle and surrounding surfaces. The air temperature in each section was measured by 9 temperature sensors. The radiant temperature was obtained from 9 T-type thermocouples and several thermopiles fixed to the surrounding surfaces, measuring temperatures over all visible surfaces of the sample. The warm chamber was placed within the guarded box to limit the heat flux through the wall of the metering box. The heat input to the metering box kept the temperature difference across the sample in steady-state conditions. The power input together with all temperatures was logged and corrected for lateral heat flow through the surround panel, its edge and the metering box wall heat loss. Both the surround panel and the edge had 8 embedded thermocouples on each side, which accounts for a total of 32 temperature sensors.

According to a method in EN ISO 12567-1 for window thermal transmittance, U_w value, measurements by the GHB, the glazing internal and external surface temperatures are not needed for determining total heat flow over a sample after the calibration. However, temperatures of the accessible window surfaces in the "1 + 2" window were measured to record a temperature gradient over the sample. Measurements were made on surfaces on position 1 (most external), 2, 3, and 6 (most internal). The surfaces in the ventilated cavity were measured in three vertical levels and each level was measured by two temperature sensors. In addition to the surface temperatures, the air in middle of the ventilated air cavity was measured at the same vertical position as on the surfaces in the cavity.

The measurements of the ventilated window were carried out in an adjusted GHB, where the air was sucked by a fan, which had a variable transformer in order to control the ventilated air mass volume. To avoid errors due to insufficient air mixing and to prevent uneven temperature distribution, the ventilated air did not enter the metering box. The air was instead directly returned through a vent to the cold chamber. This solution allowed separating the heat flow belonging to the temperature difference across the window from the amount of recovered heat and the additional energy for heating up the ventilated air to room temperature. The conditions on the cold and warm sides of window remain constant, independent of whether or not the window is ventilated. This allowed comparing the heat loss of the window with and without ventilation. Fig. 1 shows the set-up of the adjusted GHB (Fig. 2).

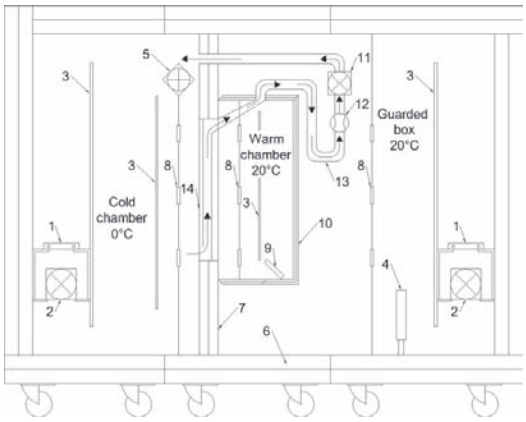

Fig. 2. Set-up of the GHB with air flow, and micro manometer. 1, cooling element; 2, fan; 3, baffle; 4, guarded box electrical heater; 5, cold side wind simulator; 6, sandwich element with polyurethane core; 7, surround panel wall from polystyrene foam (XPS) – 170 mm; 8, air temperature sensors; 9, electrical heater in metering box; 10, metering box wall from polystyrene; 11, fan with variable transformer; 12, micro manometer; 13, flexible sucking duct; 14, measured sample of size 1230 mm × 1480 mm ($w \times h$).

3.3. Experiment – set-up and procedure

During the measurements the temperature in the metering and guarded box were kept same and constant. The tests were influenced by the thermal properties of the window, especially by temperature differences and heat surface coefficients, and hence the temperature on both sides had to be controlled to allow investigation and allocation of different heat flows.

All the data were collected by a data acquisition system and directly processed by controlling software. The controlling software additionally controlled the closed loop to ensure correct electrical heater input into the metering box. Results and unprocessed data were logged for further calculations. The GHB was equipped with temperature sensors made from copper-thermocouples and thermopiles to measure temperatures. Environmental temperatures, air temperatures in the chambers, air temperature in the ventilated air cavity, temperatures in the inlet and outlet ventilated valves, and temperatures of the four window surfaces were measured.

The required air flow rate was defined according to international and national standards [1,19]. The variation of air flow through standard size windows of 1.23 m × 1.48 m was tested for a ventilation flow rate between 1 l/s to 8 l/s per window to ensure the required air change of 0.5 h^{-1}.

Special attention was paid to measuring the temperature of the ventilated air. Unshielded thermocouples made from stripped wire with a thickness of 0.1 mm were used to measure air temperature in the venting valves. Since the valves were relatively small, approximately 30 mm × 15 mm in a cross section, they did not allow the use of sensors with a different shielding technique. A series of these unshielded thermocouples were placed in the ventilation valves in the top and bottom vent of the window to avoid absorbance of radiation into the thermocouples and subsequently to avoid influence of the air temperature on the measurements [20].

3.4. Boundary conditions

The window thermal transmission properties depend on the specimen itself, boundary conditions, specimen dimensions, direction of heat flux, temperature differences, and air velocity on

outdoor and indoor surfaces as well as in the ventilated cavity. The test conditions replicated the standards EN ISO 12567-1, and the values influencing the results were monitored [17]. The actual air flow provided by the fan was read by a micro-manometer. This ensured that the flow was uniform and corresponded to the actual situation. The heat flow from the glazing surface to the ventilated air was conditioned by the laminar flow when the heat surface transfer coefficient can be effectively used. The convectional heat surface transfer coefficient was dependent on the air flow velocity in the cavity and increased with the air flow.

4. Evaluation model

4.1. Principle of the $U_{w,trans}$ value air flow

The principle of a U_w value of window is not applicable in this situation because the heat loss through the window is increased by introducing an air flow and partly reclaimed by the air flow. Therefore during the experiment the heat loss of the ventilated window was separated from heat loss of ventilation. Regained heat was considered as additional heat loss through the window. Instead of U_w, a total $U_{w,trans}$ value was used to describe the performance of the ventilated window. $U_{w,trans}$ consists of the heat loss by the ventilated window $U_{w,trans,ext}$ and heat loss by the ventilation, $U_{w,vent}$, which was needed to preheat the supplied air. Using $U_{w,trans}$, window energy performance could be defined for a window with and without ventilation. The theory behind the experiment and calculation of the heat balances for a ventilated window, was based on the calculations in the program WIS [21,22], standard ISO EN 15099 [16] and work performed by Lau Markussen Raffnsøe [23].

It was possible to derive the total heat loss for a ventilated window based on detailed calculation of the window heat balance. To obtain the $U_{w,trans}$ value as defined above, the heat balances for the window-room and the window itself has to be combined. The value is compounded from three heat transfer parameters: between interior and window, between window and exterior, and ventilation through the window. [16,22,23]. Furthermore, in order to provide comparable values for evaluation of the ventilated window concept, the energy flux to heat up the preheated fresh air to room temperature, $Q_{air,vent}$, has to be added. The thermal energy balance of the window is generally given as an Eq. (1). Energy flux from the indoor environment to the window $Q_{w,trans}$, energy flux from the window to the outdoor environment $Q_{w,trans,ext}$, and energy carried by the ventilated air $Q_{w,vent}$ are depicted in Eqs. (2–4). By a combination of those equations, total energy flux $Q_{w,trans}$ and total heat transmittance of the window could be defined as in Eq. (5) where $Q_{w,trans}$ is defined on the energy fluxes, the area of the sample, and the environmental temperature difference. This concept is applicable for both windows with and without ventilation.

$$Q_{w,trans} = Q_{w,trans,ext} + Q_{w,vent} \quad (1)$$

$$Q_{w,trans} = (h_{ci} + h_{ri}) \times A_w \times (T_{ni} - T_{si}) \quad (2)$$

$$Q_{w,trans,ext} = (h_{ce} + h_{re}) \times A_w \times (T_{se} - T_{ne}) \quad (3)$$

$$Q_{w,vent} = \rho \times c_p \times \varphi \times (T_{gap,out} - T_{gap,in}) \quad (4)$$

$$U_{w,trans} = \frac{Q_{w,trans,ext} + Q_{w,vent}}{A_w} \times (T_{ni} - T_{ne}) \quad (5)$$

Density, ρ, and heat capacity, c_p, are dependent on the actual mean air temperature in the ventilated air cavity. The energy flux to heat up the ventilated air to the room temperature $Q_{air,vent}$, has to be added to the total energy flux through the window in order to quantify the energy consumption of the room-window.

4.2. Pre-heating energy evaluation

Since ventilation changes the heat balance of the window/building and generates heat loss by ventilation, a different evaluation process had to be considered for defining the heat balance. The energy performance of the airflow window is assessed and compared against that of a traditional window, which is exactly the same but without the ventilation applied. Instead, the traditional window is combined with an exhaust ventilation without heat recovery, and the principle of $U_{w,trans}$ is applied. We evaluated the increase of the ventilated air temperature compared to the standard exhaust ventilation without preheating of fresh air. The comparison reflected the decrease in energy for heating the ventilated air.

The ventilation rate was defined for a room of 60 m^3 in a renovated apartment building, which was used for a case study. It was assumed that large apartments have a larger wall-to-window ratio than small flats and thus a low airflow rate was suitable for large apartments and a higher airflow rate for small apartments. The air velocity in the exhaust valve was between 0.08 m/s and 0.5 m/s, which were derived from the size of the valve opening and the airflow volume through the window. The recommended velocity to prevent draught is 0.15 m/s [1,24]. However, lower airflow rates are preferable, because in most of the cases several windows could be used to ventilate the space and therefore they do not operate under the maximum air flow rate. High ventilation rates were used for experimental purposes.

To illustrate the magnitude of decreased energy for heating the ventilated air, a case study was used. In total, nine cases were evaluated by using three different room set-up scenarios. The first scenario depicted the energy for heating a room in the building before the renovation with 1, 2, and 3 windows installed. The second scenario evaluated the room after renovation with 1, 2, and 3 standard windows installed. Scenario three was same as scenario two but with 1, 2, and 3 ventilated windows installed. Depending on the number of windows in the facade, the airflow rates were defined as well as the energy needed to preheat the fresh air to the room temperature. The scenario with one window represented 8l/s of the airflow through the window, with two windows 4l/s and with three windows 2.5l/s.

5. Performance analysis

5.1. Uncertainty analysis

The measured data were subjected to uncertainty analyses in search of measurement errors. The accuracy of measurements in the GHB depended on many factors such as apparatus, operating test conditions, specimen properties, and sensor precision [17]. The uncertainty could be split into two categories. First was the noise and deviation of the individual measurement readings and second was the systematic deviation which was introduced by the measurement equipment precision. The uncertainty was estimated by the law of propagation based on root-sum square (RSS) formulas [17,25]. All thermocouples and power input to the metering box heater were directly adjusted according to the calibration information from manufactures by the control software.

The heat flow rate density of sample q_{sp}, the thermal transmittance of the sample, and the regained energy were functions of several independent variables, u_i, which had known uncertainty Δu_i. For example, the global uncertainty for the density of heat flow rate was defined as a general equation (6).

$$\Delta q_{sp} = \sqrt{\sum_{i=1}^{n} \left[\frac{\partial q_{sp}(u_i)}{\partial u_i} \times \Delta u_i \right]^2} \quad (6)$$

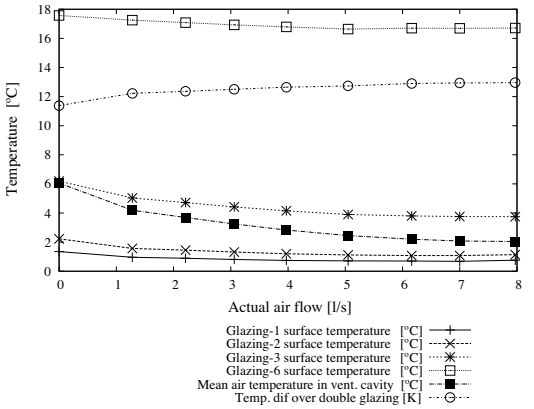

Fig. 3. Surface temperatures of glass on position 1, 2, 3 and 6 and air temperature in the ventilated cavity between the glass panes.

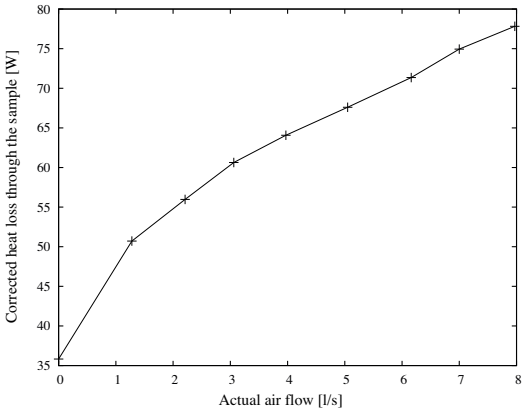

Fig. 4. Total heat loss through the sample, $Q_{w,trans}$.

Δq_{sp} was calculated from the measured total uncertainties of the heat flow rates through the surrounding panel, around the specimen edge, and into the metering box which was corrected for the heat flow through the metering box, and the area of sample by RSS, Eq. (7).

$$\Delta q_{sp} = \sqrt{\Delta \Phi_{in}^2 + \Delta \Phi_{sur}^2 + \Delta \Phi_{edge}^2 + \Delta A_W^2} \quad (7)$$

Uncertainty $\Delta U_{w,trans}$, of the measured $U_{w,trans}$ value was based on same principle. It was found that measurement itself had minimal uncertainty and therefore it could be neglected. The heat flow through the sample uncertainty varied between 0.02% and 0.3%. However the systematic deviation of the temperature measurements was relevant since the thermocouples precision was in the range ±0.5 K.

5.2. Measured temperatures

The environmental temperature in the cold side was 0 °C and steady during all measurement under different airflows. The environmental temperature in the warm side was nearly uniform and varied from 19.5 °C to 19 °C. The average surface temperatures and the average air temperature in the cavity are shown in Fig. 3. The temperatures decreased with the increase of the airflow through the air cavity. The cold air from outside, around 0 °C, entered the air cavity and cooled down the glazing and frames with the ventilation valves. By increasing the air velocity, the surface heat resistance decreased, which raised the surface heat transfer coefficient. The velocity over the surfaces was derived from the actual airflow rate and was between 0.015 m/s (1.3l/s) to 0.091 m/s (8l/s).

The mean air temperature in the cavity decreased steeper than the surface temperatures in the cavity because the volume of the ventilated air increased and the surface heat flux could not compensate for the higher volume of the ventilated cold air. Thus, the mean air temperature was approximating the mean temperature of the cavity surface closer to the exterior. In this situation, the heat transfer through the exterior glass pane was increased by applying an outdoor cold air on the surface. The temperature gradient of all surfaces was similar and indicates that the heat flow through the glass panes was dependent on the volume of the supplied air. By increasing the temperature difference over the glazing as shown in Fig. 3, it was validated that the airflow rate affects the increase of the heat flux through the double glazing. Furthermore, it was observed that the temperature on the surface 3 was relatively low and the ventilated air could not be preheated to the higher temperature. This was caused by using highly insulted double glazing with two low-emissivity coatings which on one side provided good insulating properties but on the other side did not allow air preheating.

5.3. Sample heat loss

The input from the electrical heater into the measuring box was corrected for heat loss through surround panel of the GHB, a linear thermal transmittance of an edge between the sample and the surround panel, and for a heat flow from the warm chamber to the guarded box. During the measurements, the guarded box was warmer than the metering box, which provided an extra input into the metering box. The extra heat input contribution to the metering box was between 0.35 W and 1.71 W in total, depending on the airflow. However, the additional heat input to the metering box was due to the set-up of the GHB and not due to an increase in the airflow. The total heat flux of the measured sample included heat loss of frames, heat loss of the glazing, and energy needed to preheat the air. The total heat flux was between 35.8 W and 77.8 W which corresponded respectively to the window without airflow and the window with maximum airflow. Fig. 4 shows the changes of the heat flux through the sample depending on airflow through the ventilated cavity. The correction for the surround panel and edge between the surround panel and sample was based on the calibration data and the actual temperatures. The temperature gradient at all the sensor positions was the same as for the environmental temperatures in each chamber, which described that the conditions on the both sides of the sample were steady.

5.4. Recovered heat loss and air preheating

As mentioned, the ventilated supply window works as a passive heat recovery system for preheating the ventilated fresh air. During the experiment, the heat loss of the window through a glazing and frames was partly regained by the ventilated air, $Q_{w,vent}$. The regained energy was defined based on the actual airflow volume, the air specific heat capacity, and the temperature difference between the exterior air and the exhaust window air temperature. It was detected that the air was preheated in the bottom frame before entering the glazing cavity, as it is shown by the “Valve In” line in Fig. 5. Based on the fact that air was preheated in the bottom frame, it was also assumed that the ventilated air was further preheated in the top frame. The air temperature after mixing in

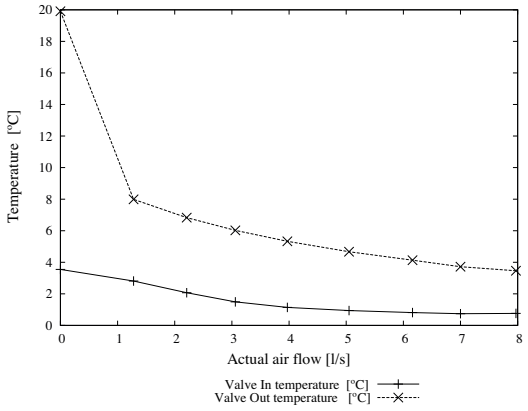

Fig. 5. Air temperatures in the inlet and outlet valves.

the top frame was used to define preheated air temperature, and is shown in Fig. 5 as "Valve Out". The thermal transmittance of the frames without ventilation was calculated based on THERM models [26] and it was estimated that the thermal transmittance of bottom frame was approximately 1.8 W/m^2 K, top frame 2.3 W/m^2 K, while the side frames was 1.7 W/m^2 K. The airflow increased the heat energy transmittance of the frames by introducing a temperature difference. The transmitted energy was partly regained but also transmitted to the exterior. Fig. 5 shows that preheating in the bottom frame varied approximately between 3 °C and 1 °C for airflow between 1.3l/s and 8l/s. From the preheating in frames could be concluded that the frames significantly increase the heat loss of the window under the airflow. The temperatures in valves were monitored by six thermocouples in the window outlet valve and six thermocouples in the window inlet valve. The temperatures in the valves differentiate ±1 °C, most likely due to the off-position from the centre of the valve and incomplete mixing of the air. The average temperatures were also examined by the uncertainty analysis. Assuming that the air was preheated from 0 °C then the air temperature was raised at the outlet by 8 °C for the airflow of 1.3l/s and 3.3 °C for the airflow of 8l/s, respectively. Fig. 6 shows that the regained heat energy varied between 12.9 W (7 W/m^2) and 34.2 W (18.2 W/m^2) for the actual ventilation flow rates between 1.3l/s and 8l/s. The decreasing gradient of the regained energy, dependent on

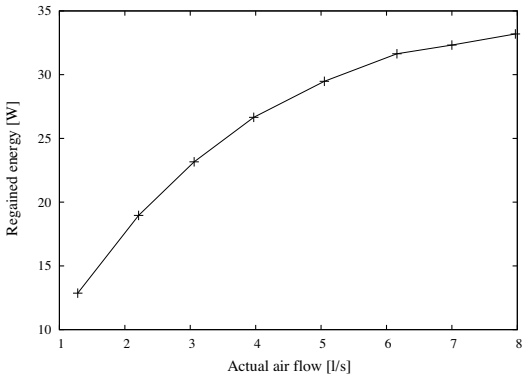

Fig. 6. Amount of recovered heat by ventilated window.

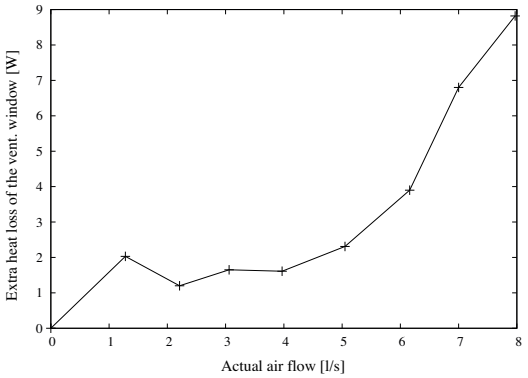

Fig. 7. Extra heat loss of a ventilated window as compared to a traditional window.

the airflow volumes, indicated that lower airflow rates were more efficient.

However, not all transmitted heat was regained by the preheating the ventilated air. Fig. 7 shows that the thermal transmittance, $U_{w,trans,ext}$, of the ventilated window ranged from 1.2 W to 8.8 W greater than the traditional window. The extra heat loss was found from an accumulation of an increased heat loss through the glazing and frames by increasing both the temperature difference and the convection surface heat transfer. Further errors in the measurements were attributed to the uncertainties discussed in paragraph 0. The peak at airflow rate of 1.3l/s was most likely caused by a relative error in the measurement point since the absolute measurements were corrected for all of the extra heat loss. The increase in the extra heat loss indicated that the heat loss through the window correlated with the change in temperature difference across the sample and furthermore with the increase of the convection heat transfer coefficient. This relationship shows that it is not worthwhile to increase the airflow rate because it increases the extra heat loss through the window, which cannot be regained. The surface temperature difference over the sealed double glazing, which corresponds to the temperature difference over the glazing, increased between 7% and 14%, which showed the reasons behind the extra heat loss. The regained energy could be increased by using less insulated double glazing, which provides a larger temperature difference over the glazing. However, double glazing will increase the extra heat loss which will not be regained and will not be beneficial because of the increased ventilated window total heat loss.

Fig. 8 shows a combination of the regained energy and the window extra heat loss, which is not regained. The energy recovery by the ventilated window lost its effect at an airflow around 6l/s. Furthermore, the results were compared to the output of the program WIS and it was found that they are correlating. The experimental results followed the increasing tendencies of the thermal transmittance of the window and higher heating energy demand for heating up the ventilated air. However, WIS did not provide the comparable data between the traditional and ventilated window. Furthermore, it was not clear how the total heat balance was defined in WIS, because the total heating load to warm up the ventilation air was accounted in the standard Uw value, while a window without ventilation misses this part of the heat loss.

5.5. Energy savings

To assess the energy performance of the ventilated window, a comparison case study was calculated. It was based on evaluation

Table 1
Heat energy savings comparison for room with and without the ventilated window.

	Before renovation			After renovation			After renovation + VW		
	1 win	2 win	3 win	1 win	2 win	3 win	1 win	2 win	3 win
Heat loss by ventilation (W)		201.7			201.7		166.4	148.2	136.1
Heat loss by infiltration (W)		201.7			28.2			28.2	
Heat loss by external wall (W)	263.6	227.2	190.8	131.8	113.6	95.4	131.8	113.6	95.4
Heat loss by window (W)	91.0	182.0	273.1	40.0	80.1	120.1	40.0	87.4	142.0
Total heat loss (W)	757.9	812.6	867.2	401.7	423.6	445.4	366.5	377.4	401.7
Ventilation vs. total (%)	26.6	24.8	23.3	50.2	47.6	45.3	45.4	39.3	33.9
Energy decrease by VW (%)		–			0.0		8.8	10.9	9.8

VW, ventilated window.

of energy needed for heating while the required ventilation had to be fulfilled in a room. Calculated energy savings were determined by using a ventilation exchange rate for rooms of 0.5 h^{-1}. It was assumed that air infiltration in the dwelling building was 0.5 h^{-1} before renovation and 0.07 h^{-1} after renovation when the building was air tightened and windows replaced. As representation of the different dwellings in the apartment building, a simplified mid-size room of 4 m × 5 m × 3 m, with floor area of 20 m^2, external walls of 15 m^2 and total volume of 60 m^3 has been selected for assessment of the ventilated window in different scenarios. The room was evaluated with windows with standardized size of 1.48 m × 1.23 m installed. As mentioned previously, three scenarios, each with 1, 2 or 3 windows illustrate preheating of the air under different airflows through the windows. Other parameters were constant over the scenarios to focus only on the evaluation of the effects of the ventilation window on the energy demand for heating. It was assumed that the room did not have any heat loss through the ceiling, floor and interior walls. Scenarios 1 and 2 illustrated how the ventilation heat loss became a more significant part of total energy demand of the heating after the renovation when 10 cm of thermal insulation was added to the 70 cm brick wall. By tightening the building, insulating external walls and changing the windows, the total energy consumption was significantly reduced. The energy needed for heating of the ventilation air changed from 26.6% to 50.2%, from 24.8% to 47.6% and from 23.3% to 45.3% of the total energy demand for the room with one, two and three windows installed. The air temperature difference to preheat was 20 K for scenario 1 and 2, and 16.5 K, 14.7 K and 13.5 K for scenario 3 with 1, 2 and 3 windows. The window's thermal transmittance varied with the ventilation airflow between 1.1 W/m^2 K and 1.3 W/m^2 K compared to the 1 W/m^2 K for the traditional windows and 2.5 W/m^2 K for the windows before the renovation. The increase of ventilation heat loss compared to the situation before renovation is approximately doubled, which shows increasing importance for reducing energy needed to heat the ventilated air. By preheating the air in the ventilated windows, the decrease of the heat load for ventilation reduced the total heating demand for the room by 8.8%, 10.9% and 9.8% for the scenarios with 1, 2 and 3 windows installed. This shows that a higher benefit occurs in the scenario with two windows installed, indicating that high ventilation rates are not feasible for energy savings. Table 1 shows the room set-up parameters for the individual scenario and indicates the potential heating energy saving in each scenario.

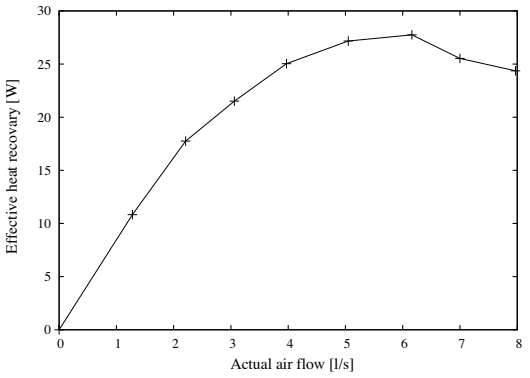

Fig. 8. Effective heat recovery of the window.

6. Conclusion

In this article, the thermal performance of a ventilated window is compared to the thermal performance of a traditional window by experimental testing in a Guarded Hot Box. The window was exposed to eight different airflow rates varying between 1.3l/s and 8 l/s under a constant temperature difference of 20 K across the test sample. Experiments confirmed that fresh air could be preheated by ventilating the fresh air through the window, regaining some of the window heat loss. The recovery efficiency depended on the airflow rate, decreasing with higher ventilation rates. The window investigated in this article was no longer energy-beneficial at airflow rates larger than 6l/s, at which point the increased heat losses due to increased window thermal transmittance became larger than the amount of energy regained by preheating. The investigation revealed that a part of the preheating of the air happened in the frames and was between 3 °C and 1 °C, depending on the airflow rate. However, the preheating of the ventilated air in the frames caused higher heat loss through the window frames with the ventilation valves and consequently caused an increase of the total window thermal transmittance. The case study calculations compared a room in an apartment building with windows with and without ventilation and showed that the total heating demand including the heat loss by ventilation can be reduced by more than 10%. The case with the ventilated window was compared to a room with combination of a traditional window and exhaust ventilation. The ventilated windows can be useful in situations where installation of ventilation with heat recovery is not possible and/or cost effective. However, it is not feasible to use ventilated windows in buildings with high required ventilation rates and a small number of windows because the regaining energy efficiency of ventilated windows decreased with the increasing airflow rates. In addition to the experimental work, the article formed a unified methodology for the assessment of the energy performance of ventilated windows. The heat balance for window-room-ventilation was defined and can be used for comparing a traditional window to a ventilated window.

Acknowledgements

The research performed in this article was funded by the Danish Energy Agency programme on research and development of energy

efficiency, F&U–2008, under the project name “ProVent: Design Knowledge for Ventilation Windows in Low Energy Buildings without Electricity Consuming Mechanical Ventilation with Heat Recovery”, number 340-035. The authors would like to acknowledge project partners Niras A/S and Horn aps for their co-operation and contribution to this paper. The authors also wish to thank colleagues at DTU.BYG for their useful feedback and advice.

References

[1] BR, the Danish Building Code, 2010. http://www.ebst.dk/.
[2] European Directive on the Energy Performance of Buildings, Directive 2002/91/EC of the European Parliament and of the Council of 16 December 2002 on the Energy Performance of Buildings, 2002.
[3] C.E. Ochoa, I.G. Capeluto, Strategic decision-making for intelligent buildings: comparative impact of passive design strategies and active features in a hot climate, Building and Environment 43 (2008) 1829–1839.
[4] E. Lee, et al., High-Performance Commercial Building Facades. Building Technologies Program, Lawrence Berkeley National Laboratory, 2002.
[5] D. Appelfeld, C.S. Hansen, S. Svendsen, Development of a slim window frame made of glass fibre reinforced polyester, Energy and Buildings vol. 42 (2010) 1918–1925.
[6] J. Wei, J. Zhao, Q. Chen, Optimal design for a dual-airflow window for different climate regions in China, Energy and Buildings 42 (2010) 2200–2205.
[7] P.H. Bakert, M.E. McEvey, An investigation into the use of a supply air window as a heat reclaim device, Building Services Engineering Research and Technology 20 (3) (1999) 105–112.
[8] J.R. Gosselin, Q. Chen, A dual airflow window for indoor air quality improvement and energy conservation in buildings, HVAC&R Research 14 (3) (2008) 359–372.
[9] D. Saelens, S. Roels, H. Hens, Strategies to improve the energy performance of multiple-skin facades, Building and Environment 43 (2008) 638–650.
[10] J. Tanimoto, K. Kimura, Simulation study on an air flow window system with an integrated roll screen, Energy and Buildings 26 (1997) 317–325.
[11] (a) D. Saelens, S. Roels, H. Hens, The inlet temperature as a boundary condition for multiple-skin facade modelling, Energy and Buildings vol. 36 (2004) 825–835;
(b) EN 673, Glass in Building – Determination of Thermal Transmittance (*U* value) – Calculation Method, European Committee for Standardization, Brussels, Belgium, 1997.
[12] J.S. Carlos, H. Corvacho, P.D. Silva, J.P. Castro-Gomes, Real climate experimental study of two double window systems with preheating of ventilation air, Energy and Buildings 42 (2010) 928–934.
[13] T.T. Chow, Z. Lin, K.F. Fong, L.S. Chan, M.M. He, Thermal performance of natural airflow window in subtropical and temperate climate zones – A comparative study, Energy Conversion and Management 50 (2009) 1884–1890.
[14] H. Manz, A. Schaelin, H. Simmler, Air of patterns and thermal behaviour of mechanically ventilated glass double facades, Building and Environment 39 (2004) 1023–1033.
[15] M.J. Holmes, Optimisation of the thermal performances of mechanically and naturally ventilated glazed facades, Renewable Energy 5 (1994) 1091–1098, Part II.
[16] ISO 2003, ISO 15099:2003(E), Thermal Performance of Windows, Doors and Shading Devices – Detailed Calculations, International Organization for Standardization, Geneva, Switzerland, 2003.
[17] EN ISO 12567-1, Thermal Performance of Windows and Doors – Determination of Thermal Transmittance by the Hot-Box Method. Part 1. Complete Windows and Doors (ISO/FDIS 12567-1:2010), European Committee for Standardization, Brussels, Belgium, 2010.
[18] EN ISO 8990, Thermal Insulation. Determination of Steady-State Thermal Transmission Properties – Calibrated and Guarded Hot Box, European Committee for Standardization, Brussels, Belgium, 1996.
[19] DS/EN 15242, Ventilation for Buildings – Calculation Methods for the Determination of Air Flow Rates in Buildings Including Infiltration, European Committee for Standardization, Brussels, Belgium, 2007.
[20] K. Duer, Characterisation of advanced windows, in: Determination of Thermal Properties by Measurements, Technical University of Denmark, 2001, ISBN 8778770629.
[21] WinDat, Window Information System software (WIS), WinDatThematic Network, TNO Bouw, Netherlands, 2006. http://www.windat.ucd.ie.
[22] D. van Dijk, R. Versluis, Definitions of *U*- and *g*-value in case of double skin facades or vented windows, WinDat document N3.08 – Public, 2004.
[23] L.M. Raffnsøe, Thermal Performance of Air Flow Windows – Master thesis, Technical University of Denmark, Department of Civil Engineering, 2007.
[24] J. Toftum, R. Nielsen, Draught sensitivity is influenced by general thermal sensation, International Journal of Industrial Ergonomics 18 (1996) 295–305.
[25] S. Yuan, G.A. Russell, W.P. Goss, Uncertainty analysis of a calibrated hot box, insulation materials: testing and applications, in: A.O. Desjarlais, R.R. Zarr (Eds.), ASTM STP 1426, vol. 4, ASTM International, West Conshohocken, PA, 2002, ISBN 978-0803128989.
[26] R. Mitchell, C. Kohler, D. Arasteh, THERM 5.2/WINDOW 5.2 NFRC Simulation Manual, Lawrence Berkeley National Laboratory, University of California, Berkeley, CA, 2006.

Paper III

"An hourly-based performance comparison of an integrated micro-structural perforated shading screen with standard shading systems"

D. Appelfeld, A. McNeil & S. Svendsen

Published in: *Energy & Buildings, 2012*

Energy and Buildings 50 (2012) 166–176

Contents lists available at SciVerse ScienceDirect

Energy and Buildings

journal homepage: www.elsevier.com/locate/enbuild

An hourly based performance comparison of an integrated micro-structural perforated shading screen with standard shading systems

David Appelfeld [a,*], Andrew McNeil [b], Svend Svendsen [a]

[a] Department of Civil Engineering, Technical University of Denmark, Brovej, Building 118 DK-2800 Kgs. Lyngby, Denmark
[b] Building Technologies, Lawrence Berkeley National Laboratory, 1 Cyclotron Road, Berkeley, CA 94720, United States

ARTICLE INFO

Article history:
Received 24 February 2012
Received in revised form 8 March 2012
Accepted 16 March 2012

Keywords:
Shading
Complex fenestration system
Solar gains
Daylight
Building performance modelling

ABSTRACT

This article evaluates the performance of an integrated micro structural perforated shading screen (MSPSS). Such a system maintains a visual connection with the outdoors while imitating the shading functionality of a venetian blind. Building energy consumption is strongly influenced by the solar gains and heat transfer through the transparent parts of the fenestration systems. MSPSS is angular-dependent shading device that provides an effective strategy in the control of daylight, solar gains and overheating through windows. The study focuses on using direct experimental methods to determine bi-directional transmittance properties of shading systems that are not included as standard shading options in readily available building performance simulation tools. The impact on the indoor environment, particularly temperature and daylight were investigated and compared to three other static complex fenestration systems. The bi-directional description of the systems was used throughout the article. The simulations were validated against outdoor measurements of solar and light transmittance.

1. Introduction

Buildings are responsible for usage of significant amount of the energy and account for 40% energy consumption in Europe and the USA. Energy reduction by buildings has become an important part of energy policy and is reflected in building regulations, which require decreased total building energy demand [1,2]. The largest energy usage is attributed to heating, cooling and electrical lighting.

Optimization of window elements can reduce energy consumed for heating, cooling and electric lighting. Optimization strategies consider heating by increasing solar gains, cooling by providing solar protection and lighting by utilizing daylight [3]. All the functions cannot be addressed by a standard window and the traditional windows have to be combined with shading systems, which then can be described as complex fenestration system (CFS). The challenge is to evaluate those parameters in an interconnected context for CFS performance, since some of the functions are contradicting for static systems, e.g. increasing solar gains in winter while providing shading in the summer [4].

In recent decades, new and renovated buildings have become increasingly insulated and air tight. These steps lower building heating loads but they also increase risk of overheating by capturing excess solar gains, especially in office buildings. Removing overheating by mechanically cooling is expensive and can negate the savings from solar gains in the winter, and thus cooling loads are growing in importance. Contemporary commercial and institutional buildings typically have a low heating and high cooling loads as they have high internally generated loads by people/lights/equipment and have well-insulated envelopes. Residential buildings have relatively low internal loads vs. their envelope loads [4]. Solar shading is an effective strategy to reduce overheating and diffuse direct sunlight thus reducing energy consumption [3]. There are many options available for shading systems and it is difficult to precisely describe the energy performance impact of a non-standardized solution [5,6]. Many of the CFSs have angularly dependent solar and light energy properties but use normal-incidence glazing values of the performance indicators, e.g. total solar energy transmittance. The normal-incidence value description is not an accurate indicator for angularly dependant systems, which need to be described with bi-directional data [7]. The limitations of the available simulation tools and testing methods can be overcome by performing state-of-the-art simulation and its validation with measurements [8].

The main motivation for this research is to establish a procedure for generating information, which can be used during product development of CFSs or an initial phase of building design. This paper focuses on the performance modelling of CFSs and comparison between types. The results of the simulations were compared against measurements taken outdoors and in a laboratory. The

* Corresponding author. Tel.: +45 45251856; fax: +45 45883282.
E-mail address: dava@byg.dtu.dk (D. Appelfeld).

0378-7788/$ – see front matter © 2012 Elsevier B.V. All rights reserved.
doi:10.1016/j.enbuild.2012.03.038

aim is to determine the performance criteria of the tested CFSs to indicate impact on the energy and indoor climate in the occupied spaces.

2. Method

Performance is simulated for several shading systems and a comparison is based on the evaluation of various aspects. The bi-directional transmittance simulation results compared to measurements. The performance evaluation is performed with several steps, starting with the shading layer and ending with shading system impact onto a reference room. The design criteria for widows and CFS in modern buildings are:

- Energy use – heating, cooling, electrical lighting
- Thermal comfort – overheating
- Visual comfort – daylight, glare, view to outside

These criteria are interdependent, in this study they are addressed in the context of the following aspects: facade orientation, building location, time of day and year, window size, window position on facade, shading strategy, and human factors (view, comfort and temperature).

The building location determines the climate, including the sun position and sky luminance distribution, which is further dependent on the actual time/date. The central criteria for this article is angular dependant light transmittance (T_{vis}) and solar transmittance (T_{sol}) of the CFS. With these parameters the solar heat gain coefficient (SHGC) could be described, which is also referred as the total solar transmittance (*g*-value) and is central in determining cooling loads of buildings. The thermal transmittance of windows (U_w-value) is one of the major energy performance characteristics controlling heat loss. Transmittance refers to both T_{vis} and T_{sol} further in the paper if not specified otherwise.

In this paper, the interconnections of the above parameters are illustrated in case examples presented throughout the paper. Annual performance simulations are carried out when possible.

2.1. Complex fenestration systems

This study focused on a micro structural perforated shading screen (MSPSS) which is made of an insulated double glazed unit with low-e coating on surface 3 and the MSPSS on surface 2. The MSPSS is made from a stainless steel sheet with elliptical holes smaller than 1 mm. The holes are cut in a downward direction (when viewed from the inside) to reduce transmission from sources above the horizon and increase transmission from below the horizon. MSPSS was selected because the angular dependence is not symmetrical about the normal making it difficult or impossible to evaluate with standard simulation tools. The MSPSS combines solar and glare protection, provides direct view out and is not included in any standard testing software. Fig. 1 shows a side-by-side view through the MSPSS with an unobstructed view. From observations the view appears less obstructed when viewed at a greater distance. The picture is slightly blurry as it was necessary to focus on the shading layer and the background was in the distance.

In order to have a complete understanding of performance, the tested CFS is compared to references systems. MSPSS was compared to clear double glazed windows, without shading, with horizontal venetian blinds, and with a semi-transparent roller shade. The clear glazing reference case was studied to demonstrate the effect of the shading and glazing separately. Venetian blinds were used as a comparison because they are a conventional system that also provides shade and permits view. A roller shade was also used as a reference because it blocks solar gains and glare more efficiently then the semi-opened system, however, unlike MSPS and Venetian blind, it blocks the view to outside.

Fig. 1. View through MSPSS (left), unobstructed view (right).

All the shading systems were simulated with the same glazing. In all cases, the shading was located between the glass panes to limit the variations in the energy performance of the individual systems.

2.2. Determining bi-directional transmission characteristics

T_{sol} and T_{vis} are the fundamental performance indicators for CFS and all the following calculations were based on them. The calculations are carried out in several sequential steps with increasing level of information.

2.2.1. BSDF generation via simulation

Radiance was used to generate a bi-directional scattering distribution function (BSDF). Radiance is an accurate backward ray-tracing Unix-based programme that has been validated for such purposes [9]. The new software development allows generating a BSDF, which describes transmittance dependent on incident angle (IA). A model of the MSPSS was created using detailed geometric drawings from the manufacturer and reflectance measurements of an un-perforated sample also provided by the manufacturer. Radiance's programme genBSDF was used to generate a BSDF matrix [10]. The genBSDF programme generates blocks of values which describe 145 Klem's incidence angles for one of 145 oppositely placed outgoing directions [11]. This data was validated against goniophotometer measurements for a few incident angles [12]. The validated BSDF was used to calculate T_{sol} and T_{vis} of the glazing unit with the shading screen.

2.2.2. Comparing measurement with simulations

Measurements were taken of the MSPSS taken to ensure that daylight simulations using BSDFs would reliably reproduce real-world results. Measurements were taken outdoors in order to include direct light from the sun and diffuse light from the sky reproducing the type of environments experienced by a real building. Both components of daylight are important because together they determine indoor daylight conditions, unlike cooling loads which are highly dependent on the direct sunlight [3]. Measurements were taken on clear days in June and July because clear skies are the most reliably reproduced of the CIE sky types (and clear skies are commonly occur in the summer in Denmark, where the measurements were taken) [9]. The sample was rotated to imitate different incident azimuth and altitude angles so that many

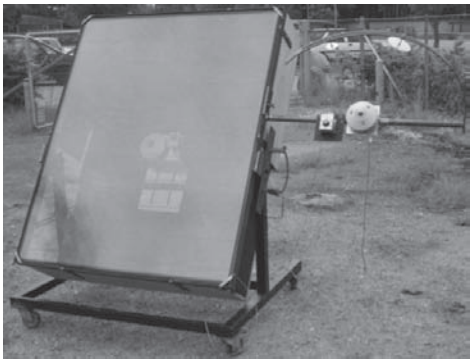

Fig. 2. Movable measurement test rig with sample mounted.

IAs could be tested in a short time. The dynamic sample positioning introduced inconsistent ratios of exposure to sky and ground for the sample. To counteract this, the sample was positioned in the simulation to match the position of the sample during each measurement, and thus the measurements and simulations were analogous.

To quickly rotate samples, a movable rig was used, that safely held the test sample and allowed to adjust the sample with respect to the sun. Due to the size of the sample, only IAs up to 60° could be measured, as accuracy could not be ensured with higher IAs. Transmittances for higher IAs were derived from simulations. The test rig, shown in Fig. 2, consisted of a mounted sample and two sets of illuminance and irradiance meters, which were aligned to the surface of the sample. One illuminance and irradiance sensor was placed behind the sample, close to the glass surface, to measure the light transmitted by the sample. The other illuminance and irradiance sensors were placed on the side of the measurement rig to measure light incident on the sample. Relative transmittance of the sample was calculated by dividing the transmitted measurement by the incident measurement. Using relative measurements accommodates surrounding with obstacles without introducing large error to the results.

A solar pointer, shown in Fig. 3, was used to accurately align the sample for each IA. The pointer, of known length, was positioned perpendicular to the surface of the glazing and a measuring. The measuring grid is marked with shadow points for each incident angle. The sample can be moved until the shadow from the pointer aligns with the shadow point for the desired incident angle. The process allows for accurate sample alignment, reducing errors in IA. Every IA was measured with and without the sensors shaded from the direct light to determine diffuse and direct radiation. Each measurement was repeated at least twice to reduce measurement error.

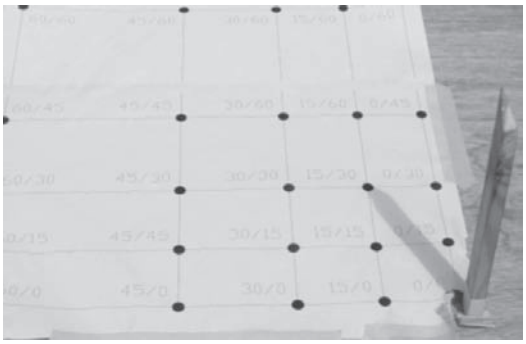

Fig. 3. Solar pointer and measurement grid, the current IA is azimuth of 15° and altitude 30°.

Table 1
Model's surface properties.

	Wall	Ceiling	Floor
Reflectance	0.5	0.8	0.3

By recording the time, sun position, total horizontal hemispherical diffuse illuminance and direct normal illuminance, it was possible to reproduce sky conditions in the simulations. Clear glazing with known properties was tested in the same manner to validate the both the measurement and simulation procedures. The sensors were calibrated before the measurements to minimize the sensor precision error.

The first preliminary test was carried out without a sample to determine how much the test rig shades the sensors. The test verified that this error was smaller than the accuracy of the sensors and therefore could be neglected. The rig was equipped with a shading box behind the sample to shade specular reflections from the sample's back surface and the ambient environment.

2.3. System performance simulations

2.3.1. Model description

The simulated model was a single office for three occupants with dimension of 3.5 m wide, 5.4 m deep, and 2.7 m high. The room model is based on the test office in IEA task 27 in order to have standardized model [13]. The window varies from the test office and is modelled as one large window of 1.2 m × 2.5 m with a 1 m sill. The surface properties of the room are listed in Table 1. The plan view of the room with the furniture is shown in Fig. 4, including view directions. The view height is 1.2 m above the floor, which corresponds to eye-level for a sitting person.

The thermal model of the office was built with an assumption that all adjacent offices have the same temperature, except the exterior wall and window, which were exposed to the outdoors. Thermal transmittance of the external wall was 0.5 W/m^2 K and the infiltration was set to 0.5 AC/h.

2.3.2. Annual daylight simulations

Radiance was also used to simulate of the daylight conditions in the reference office. Work plane illuminance was simulated throughout a year and daylight autonomy was used to evaluate the annual results. The heating and cooling loads of the tested office

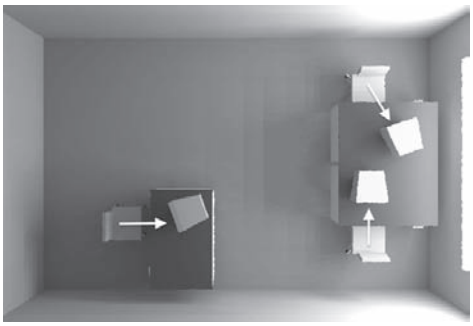

Fig. 4. The plane view of the office with view directions.

were calculated in ESP-r, which allows use bi-directional information about solar energy transmittance of CFS.

The Radiance three phase method (TPM) allows users to calculate the annual daylight performance of CFS using bi-directional information without a significant increase of the computational time. The TPM is based on the multiplication of four matrices describing light through an interior (view matrix), fenestration (transmittance matrix), exterior (daylighting matrix), and sky distribution (sky vector). This process allows for a relatively quick dynamic light and solar radiation simulation over a year. Additionally, by changing only one of the matrixes various aspects could be effectively investigated: different orientations by changing the daylighting matrix, location by changing sky vector, and different CFS by using different BSDF [5].

2.3.3. Electrical light savings and daylight

The electrical light energy was computed for all four scenarios, when no daylight is utilized to fulfil required illuminance criteria. Two work plane illuminance criteria for offices were used: 500 lx according to standard CEN-EN 15251 [14] and 300 lx according to IESNA [15,16]. The office was divided into three 1.8 m deep and 3.5 m wide lighting zones, with zone 1 closest to the window and zone 3 furthest from the window. Each zone was separately controlled. The relatively small zones were used mainly for investigational purposes to show the potential lighting energy savings.

Two control strategies were considered: on/off switching and bi-level switching. For on/off control the electric lighting in a zone was switched off when daylight alone provided the required work plane illuminance. With bi-level switching the electric lighting could be switched to half output (by switching off half of the lamps in the zone) when the daylight illuminance met half of the work plane illuminance criteria and could be switched off entirely when daylight illuminance met the full work plane illuminance criteria.

The lighting power density (LPD) for the working plane illuminance (WPI) of 500 lx of 15 W/m^2 was derived from standard EN 15193 [17]. Electric lighting savings were based on the linear substitution of electrical lighting by daylight and thus are idealized. For the WPI of 300 lx an equivalent LPD of 9 W/m^2 was used.

Daylight was evaluated using daylight autonomy (DA), which is the percentage of hours satisfying the minimal design WPI in the total number of working hours in a year [18].

2.3.4. Glare

Glare was evaluated because visual comfort of the CFS is an important aspect of the CFS performance. Daylight Glare Probability (DGP) was selected as a glare index because it is based on an extensive human evaluation study [19,20]. Glare analysis was performed for all three working positions in the office. Glare was assessed on an annual basis focusing on the working hours between 8:00 and 18:00.

2.3.5. Net energy gains

The glazing unit properties were used to calculate net energy gains (NEG). The NEG calculation method is based on a window's solar gain minus its heat loss based on outdoor temperature during the standard heating season [21,22]. NEG is a simplified method that describes the relationship between a window and a building, in kW h/m^2. The formula for NEG is:

$$E_{\mathrm{ref}} = g \cdot I - U \cdot D$$

where I is the coefficient for solar gains and D is coefficient for heat loss. For Denmark the total coefficient for solar gain is 280.6 kW h/m^2, for north 105 kW h/m^2, for south 431 kW h/m^2 and for east/west 232 kW h/m^2. The solar gain coefficients are further multiplied by an assumed shading factor 0.7 [23]. The assigned contribution from south is 41%, north 26% and east/west 33%. The heat loss coefficient D for the heating season in Denmark is 90.36 kKh [21].

2.3.6. Energy performance

Kuhn et al. found that heating demand in the cold climates calculated using standard evaluation techniques was overestimated up to 23% and that cooling demand was underestimated up to 99% [24,25]. This study aims to determine if bi-directional information, especially angle dependant g-value, provides more accurate results for heating and cooling loads [26]. The evaluated location, Copenhagen, Denmark, is located in a Nordic climate, which could be considered as a moderate climate zone, however the cooling loads have to also be taken into account, as they are a significant part of the energy consumption in modern buildings [27]. Furthermore energy performance was calculated for Prague, Czech Republic, and Rome, Italy, to illustrate the performance based on the location.

The ESP-r model for using bi-directional information about solar energy transmittance is called Black-Box-Model and was validated [6,24,26]. The model 5° resolution for azimuth and altitude incident angles on the surface of the CFS.

3. Results

3.1. Outdoor measurements vs. Radiance simulation

The comparison of Radiance simulation results against outdoor measurements of Tvis and Tsol is shown in Fig. 5. The difference in the corresponding curves is between 0% and 4%, except for visible transmittance at the IA of 60° where the relative error is around 18%. This error was caused by comparing the relatively small values and in absolute numbers would not be significant and/or by slightly off-position of the measuring rig. The Radiance simulation results were generated using the TPM.

3.2. BSDF

BSDF's are generated by programmes genBSDF and Window6 to provide a more comprehensive description of the shading properties dependency on the azimuth and altitude of the sun. These BSDFs were validated by McNeil et al. in a connected study [10]. Fig. 6 contains visualizations of results for the front T_{vis} of the four shading systems, independent of window orientation and location.

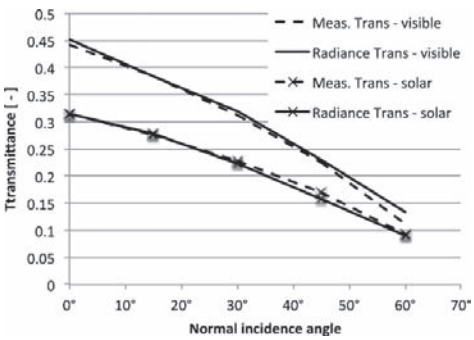

Fig. 5. Comparison of measured and simulated T_{vis} and T_{sol}.

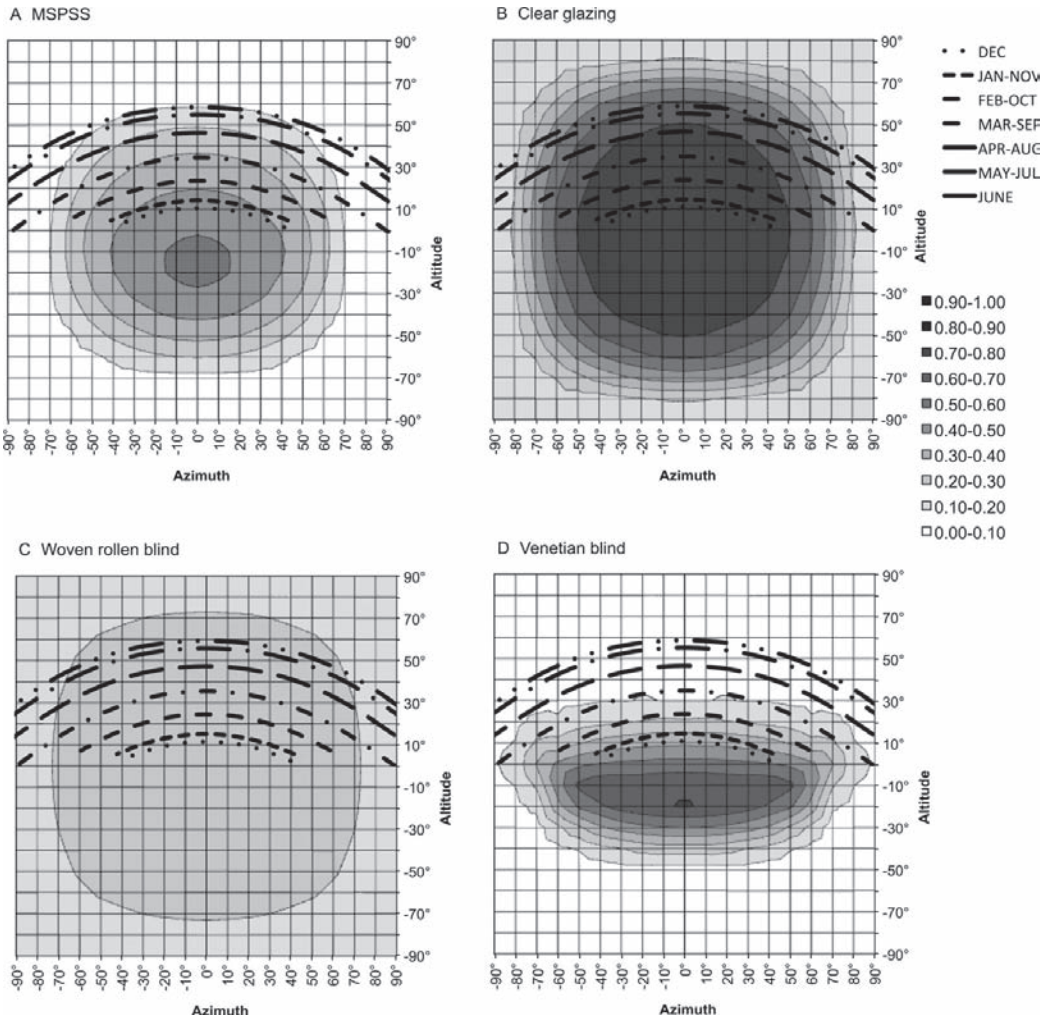

Fig. 6. Visible transmittance of CFSs with solar path of Copenhagen.

For a better understanding of the relation between the transmittance and IA the annual sun path for Copenhagen is added to the charts.

As expected the solar transmittance is the highest for the clear glazing and is symmetrical around the centre. The woven roller shade has the lowest transmittance, as it evenly reduces the transmittance and blocks view to the outside. The MSPSS and venetian blinds are more IA dependent and allow higher transmittance for the negative altitude. In other words, the light is blocked more effectively from sky. Both shadings have their highest transmittance around −15° of altitude.

For the locations of Prague and Rome the shading efficiency will be higher because the sun altitude is also higher. The solar gains can be utilized by angularly dependent systems during the winter months when the sun is low and transmittance is higher. Additionally, effective shading occurs during the summer when the sun altitude is higher. The maximum light transmittance of the MSPSS and venetian blinds was between 0.5 and 0.6, while for clear glazing it was up to 0.8. The glazing with roller shade had high shading effects and the transmittance was as low as 0.2.

3.3. Daylight autonomy

Fig. 7 contains daylight autonomy (DA) results for all four systems on south facing facades. The shaded bands illustrate the percentage when a certain level is reached. For example, for a glazing with MSPSS, 80% of working hours have an exposure of at least to 216 lx at a distance of 0.5 m from facade.

A logarithmic scale was used to provide better visibility of smaller values because the clear glazing provided high illuminance closer to the window and far exceeded other values in the chart, which were still valuable and fulfil the requirements. As expected, DA was higher close to the window and DA was lower in the back of the room. At the back of the room DA did not satisfy the lighting

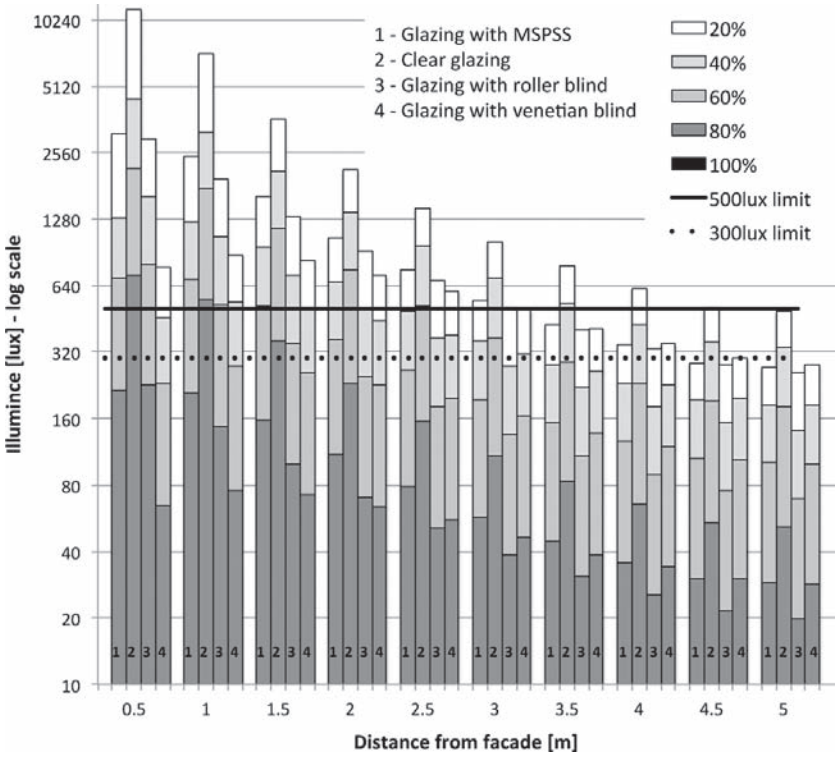

Fig. 7. Daylight autonomy.

requirements. The highest illuminance was provided with the clear glazing with WPI 10 klx close to the facade, which far exceeds WPI criteria thus the energy cannot be fully utilized and may indirectly cause a glare and overheating. The solutions with lower relative WPI can still serve purpose without the risk of a glare and overheating. While there is not a direct correlation between a WPI and glare, values above 4500 lx are generally not desirable [16,19,28]. The illuminance levels for systems with shading systems were similar with slightly better performance for MSPSS.

3.4. Electrical light savings

The analysis assumed that the light in a zone was switched off when the daylight illuminance fulfilled the WPI criteria (on/off control). In addition, bi-level switching was considered, which allows the LPD to reduce by 50% when half the WPI criteria were met by daylight illuminance (i.e. switching off half the lamps in a zone). In Figs. 8 and 9 the savings were split by on/off and bi-level lighting control. The on/off savings mean fulfilment of the criteria 300 lx or 500 lx, and bi-level were the additional savings by introducing bi-level control strategy.

The largest savings generally occurred in zone one, which was commonly saturated by daylight. Zone 3 is less exposed to daylight and thus the savings were smaller.

By illustrating the difference when the light was either fully or 50% switched off it was possible to see that in the front of the room daylight reached higher illuminance and the light was completely off, while in the back off the room the major power savings were because the bi-level lighting control system. Therefore the savings were influenced by the light control strategy. Furthermore, the savings followed illuminance levels in Fig. 7. This indicated that it was possible to shade excessive illuminance, while providing the savings of the lighting energy, as the clear glazing did not produced significantly higher savings. Additionally there was not significant difference between scenario with 500 lx and 300 lx.

The savings in zone 3 were mainly during the winter period when the sun is low and the penetrated light could reach the back of the room.

3.5. Glare assessment

Fig. 10 shows Daylight Glare Probability (DGP) for the four systems and three views. The graphs display the glare rating for every hour during the whole year. All three evaluated views are marked and illustrated in Fig. 4. View 1 was parallel along the window pointing to east and thus the higher DGP values occurred before noon. View 2 faced to southeast and higher DGP values were during afternoon. View 3 was oriented to the window, south, and higher DGP index was at noon.

The most glare occurs with clear glazing, as no direct sunlight was blocked. Conversely, the least glare occurs with the roller shade, particularly for view 1 and view 3 which experience no glare. An expected result would be that the roller shade would also prevent glare for view 2, however the position was close to the source and the roller shade was partially transparent, therefore glare occurred.

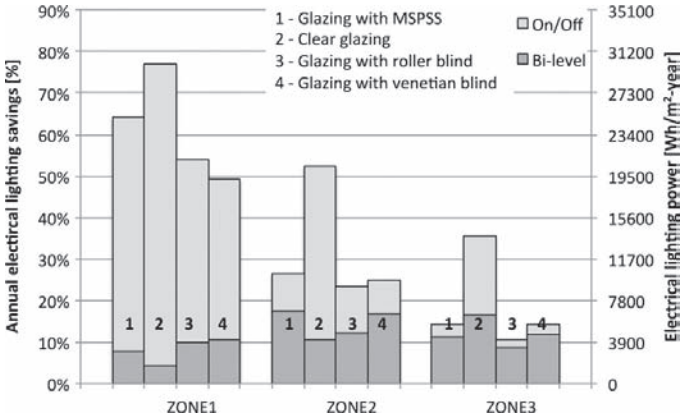

Fig. 8. Electrical light saving for work plane illuminance of 500 lx.

Of the three views studied, view 2 experiences the most glare. Glare occurs year round with clear glazing, while glare occurs only seasonally with the shading systems.

The venetian blinds block slightly more glare than MSPSS in all views, which was caused by more selective transmittance of the venetian blinds, with the lower transmittance under higher IAs. This was also possible to assume from the carpet plots in Fig. 6 and later in Fig. 12, describing angularly dependent transmittance. The observation would not be possible by considering transmission at normal-incidence only.

3.6. Net energy gain

The total solar energy transmittance (*g*-value) is the fraction of the actual solar energy that passes through the window. The CFSs were modelled in Window6 with shading located between the glass panes to avoid favouring internal or external shadings. Table 2 contains the centre pane *U*-values and normal incidence *g*-values. The results in Table 2 for individual sides do not include assigned percentage of the distribution to the individual orientation. The result of NEG for all four shading solution in the respect of the facade orientation is in Fig. 11.

MSPSS had the lowest NEG, which is mainly caused by a negative contribution from a north facade and low solar gains contribution from south. Nevertheless, shading should be used primary for the south facade and considered for the east and west facade. The MSPSS results show that the MSPSS reduces overeating, thus the MSPSS is considered to perform well with regards to shading. The north facade is not typically equipped with shading, so the negative performance of shading solutions on the north can be overlooked. The main focus was on the south orientation values since the simulation model was south facing. Fig. 11 illustrates NEG in a relation to the variable *g*-value. In the case of the large south window the rest of the CFSs generated large solar gains and would cause the space overheating. NEG does not penalize the overheating causing the cooling loads. Therefore the energy performance of the room dependent on the angular properties of the shading including cooling loads which is discussed in the next section.

The clear glazing and the glazing with roller shade had relatively constant NEG up to the normal surface IA of 40°, while the MSPSS' and venetian blinds' NEG decreased sharply from IA of 0°. The sharp drop in *g*-value is a result of the inclined structure of both shades. The solar altitude in northern Europe (Denmark) is mostly below 40° with the maximum below 60°. For shading purposes, a

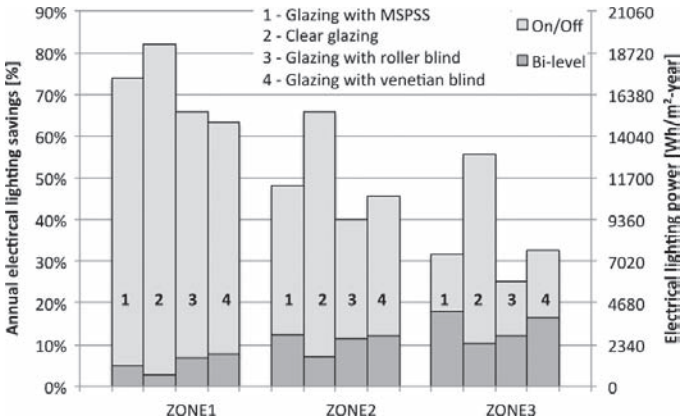

Fig. 9. Electrical light saving for work plane illuminance of 300 lx.

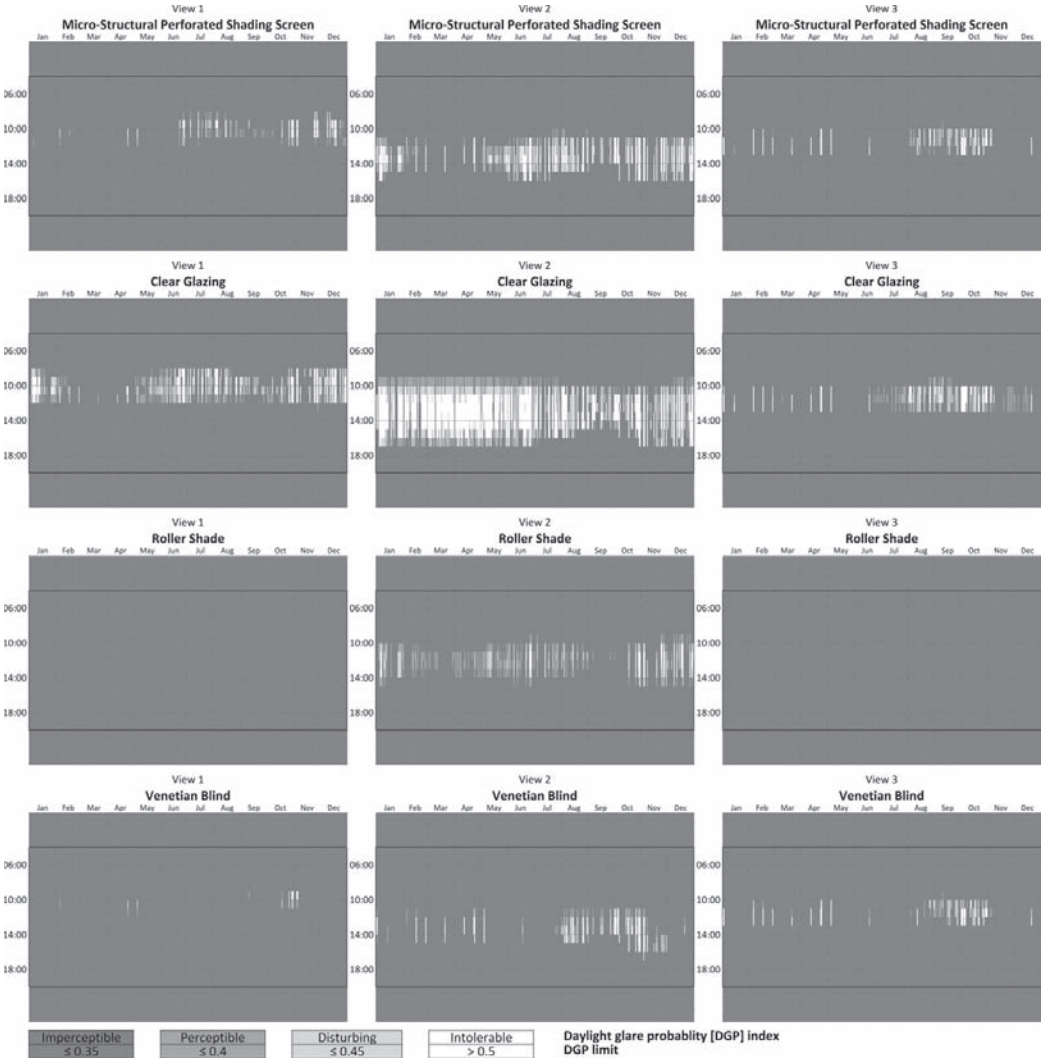

Fig. 10. Annual plots of the DGP for three views and all CFS in the location of Copenhagen.

progressive *g*-value is efficient because it provides the most shading in summer when direct solar radiation is most intense and least desirable. The *g*-value of all tested solutions, shown in Fig. 12, is similar to the front visible transmittance in Fig. 6. The total solar transmittance is less concentrated and the energy is transmitted through wider range of IAs compared to the visible transmittance.

3.7. Energy loads

Heating and cooling loads were evaluated based on the ESP-r simulation model. The model allowed testing different shading systems with the detailed bi-directional transmittance properties. The large sources of energy for heating and cooling were assigned to the

Table 2
Energy performance indicators of selected CFS and NEG.

	Centre *Ug* (W/m²K)	Normal-incidence *g*-value	NEG (W/m² K)			
			All	North	South	East/west
MSPSS	1.23	0.37	−38.8	−84.1	0.1	−51.3
Clear glazing	1.25	0.62	7.8	−67.9	72.6	−13.2
Woven rollen shade	1.16	0.35	−37.4	−79.8	−1.1	−49.2
Venetian blind	1.10	0.49	−3.5	−63.5	47.8	−20.1

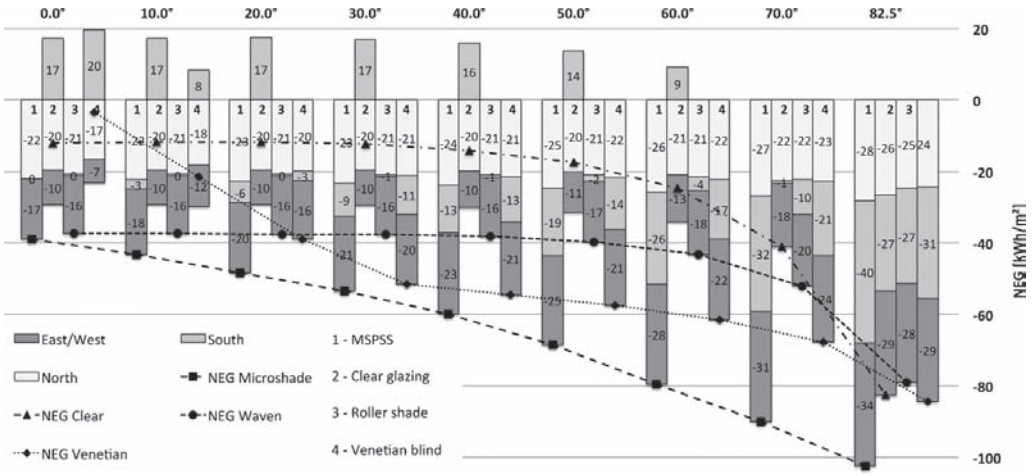

Fig. 11. NEG for four different CFSs, split for different orientation and dependent on IA.

model in the way that they were never exhausted. Table 3 contains the results for the heating and cooling loads. Heating loads excluded solar gains and considered only the energy needed to maintain the set point for heating of 20 °C, during working hours, and 15 °C outside the working hours. Heating loads were relatively low since the building was well insulated. The cooling loads were calculated using the energy needed to cool the space when the air temperature was above 26 °C. The largest cooling loads occurred with clear glazing, which did not provide any shading. All shading solutions provided similar shading protection and reduced cooling loads by 20–30% compared to the window without the shading. The larger heating loads for Prague compare to Copenhagen were caused by a fact that in Prague the temperatures in the winter months are lower as well as there are more extreme temperatures.

4. Discussion

The results describe overall performance of all four CFSs and the complexity is addressed by interconnected evaluation parameters. It was important to validate the simulation results for bi-directional transmittance against measurements since the study is dependent on the bi-directional transmittance data. The measurements and simulations correlate reasonably and thus the results are trustful and the model of the MSPSS is described accordingly to its geometry and properties.

As modern buildings are thermally well-insulated, the importance of shading solar gains for transparent elements becomes more important, especially on the southern and east/west facades, even at higher geographical latitudes. NEG illustrates that even double-glazing provides significant heating gains and has an influence on the overall performance of the building. This conclusion is supported by the results from the energy calculations in ESP-r where the southern climates require more solar protection. When the clear glazing is excluded, all three tested shadings systems provide similar energy performances, however the roller shade reduces visibility and therefore the usage potential is limited because users would likely prefer the other systems. Furthermore, the roller shade system limits daylight penetration and reduces the light energy savings by daylight compared to the more open venetian blind and the MSPSS. On the other hand, shading systems also reduce beneficial heat gains in cold months.

These two aspects are contradictory, as shading would be used during summer and solar heating gains during the winter. The bi-directional description of the performances of the individual systems provides accurate results and is clear description of the properties. By such information, together with knowledge of the local conditions, the building design can be accordingly adjusted to maximise the performance utilization of the particular shading system. From the combination of the results it is possible to see that angularly selective shading systems are the key to energy indicators for cooling and heating. Information about the variable *g*-value is valuable for northern locations where the higher *g*-value is useful during winter when the sun is low.

The transmittance of the system is directly linked to the level of daylight. From the combination of bi-directional transmittance and daylight autonomy it could be justified that more daylight be transmitted in during winter months when the daylight levels are generally lower. Higher solar and light energy protection in summer is desirable, as the light intensity is greater. This is the reason for blocking incoming radiation to protect space from overheating and excessive levels of the WPI. The shading systems provide glare protection in addition to shading extensive solar gains. The glare evaluation was performed with the actual sun position at the time of the evaluation, meaning that the light transmittance varied at each time step. In the case of the visual comfort, blocking direct light is necessary, however even the completely closed roller shade caused visual discomfort and glare. The glare is not dependent only on the shading solution, but mainly on the position of a view to the light source, and therefore optimal view direction is critical. As

Table 3
Energy loads for heating and cooling for all CFSs and investigated locations.

Location	Energy performance (kW h/m²/year)							
	MSPSS		Clear		Roller shade		Venetian blind	
	HL	CL	HL	CL	HL	CL	HL	CL
Copenhagen	8.5	22.5	6.6	30.4	9.0	22.8	9.3	20.3
Prague	12.3	24.4	10.5	30.4	12.7	24.3	13.2	23.2
Rome	0.0	63.5	0.0	78.1	0.0	63.9	0.1	59.4

Note: HL – heating loads; CL – cooling loads; MSPSS – micro structural perforated shading screen.

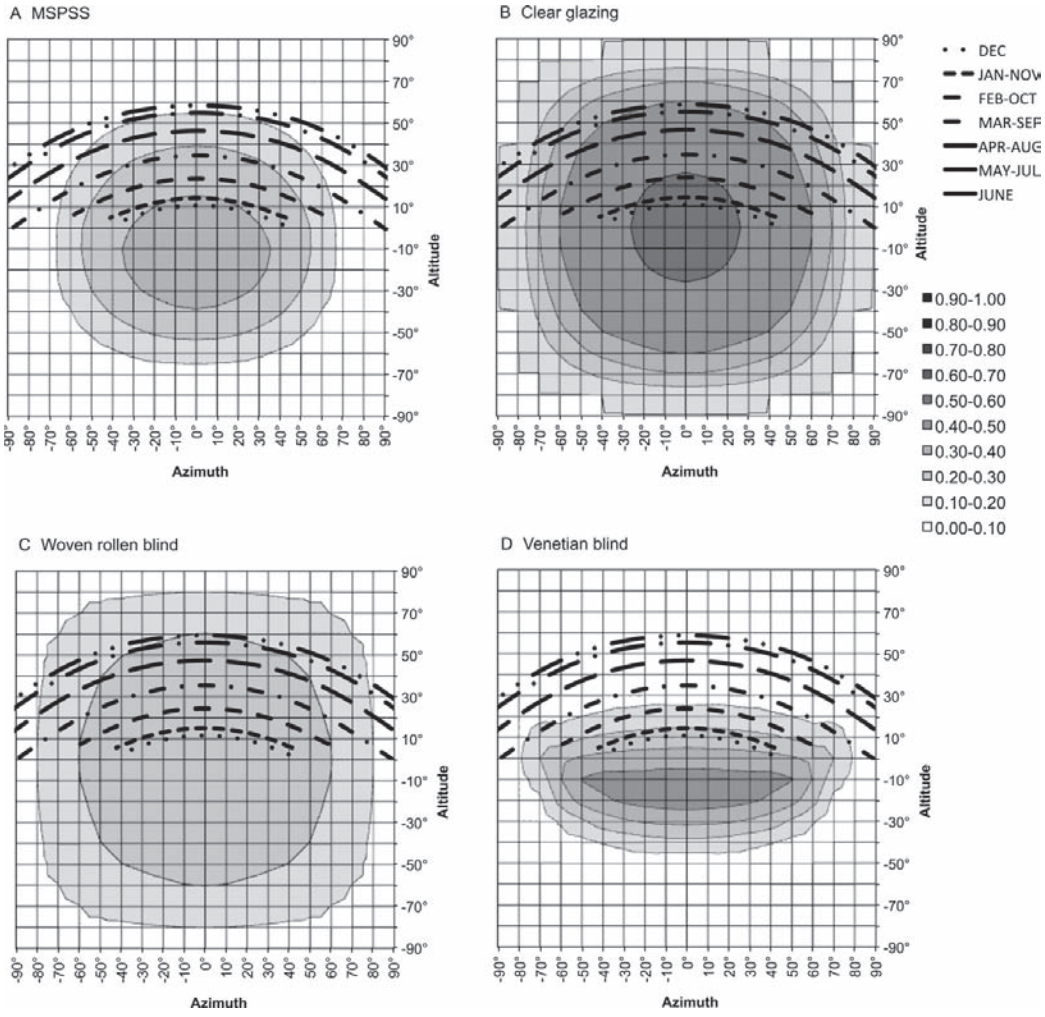

Fig. 12. BSDFs for total solar energy transmittance of the CFSs with sun path of Copenhagen.

such, it is not fully possible to say that the roller shade performs better or worse than the MSPSS or venetian blinds.

When the focus is on the view out, clear glazing would perform the best, however when the glare is included then it can become the worst. The difference between the MSPSS and venetian blind were minimal regarding the visual performance. However the MSPSS is almost invisible and does not disturb the view as venetian blind does.

The optical and thermal performances of the MSPSS could be improved by placing the layer to the external surface, if a durability of the layer allows exposing the MSPSS to the outdoor environment. An indirect shading efficiency would be increased as an absorbed energy in the glass would be reduced with the shading layer on the external surface. Thermally the glazing with the external MSPSS layer would perform better as the emissivity of the coating is lower than the normal emissivity of glass.

Such system would be suitable for renovations by attaching the shading layer onto the glazing surface of an existing window. However, placing the MSPSS layer on either internal or external surface of the glazing would make cleaning and maintenance complicated as dust would deposit in the microstructure.

5. Conclusion

A comparison of several performance indicators was carried out for four different CFSs and benchmarked against each other. The bi-directional transmittance simulations were first validated with outdoor measurements prior to using the data in further. There was a strong correlation between the measurements and simulations. To provide an overview of the CFS performance it was necessary to use several interrelated parameters. By using bi-directional information describing CFS it was possible to accurately depict the shading with a high level of understanding in the context of the IA and location. It was found that the angular dependent shading systems provided improvement all year round in providing daylight,

heating load reduction by controlling solar gains and decreasing risk of overheating during summer days when the sun altitude is high. The visual comfort depended on blocking direct light by optimal positioning of the shading and the direction of the view. This paper demonstrates that it is possible to evaluate unique shading systems, which are not typically included in the building performance simulation tools. However it has to be noted that the process needs to be automated and included in widely used simulation tools in order to shorten the time of the complete performance evaluation with all consequences.

It can be concluded that the MSPSS performed well compare to the rest of the solutions. The layer provided similar shading effect as the venetian blind. Unobstructed view to outdoor through the MSPSS did not generate extensive glare and the utilization of daylight was kept high.

Acknowledgements

The research was co-funded by the Danish Energy Agency program on research and demonstration of energy savings. The authors would like to acknowledge PhotoSolar A/S for providing the test samples and their co-operation and contribution to this paper. This work was also supported by the Assistant Secretary for Energy Efficiency and Renewable Energy, Office of Building Technology, State and Community Programs, Office of Building Research and Standards of the U.S. Department of Energy under Contract No. DE-AC02-05CH11231 and by the California Energy Commission through its Public Interest Energy Research (PIER) Program on behalf of the citizens of California.

References

[1] EU, EPBD recast, Directive 2010/31/EU of the European Parliament and of the Council of 19 May 2010 on the energy performance of buildings (recast), Official Journal of the European Union (July 2010).
[2] US DOE Office of Energy Efficiency and Renewable Energy, Buildings Energy Databook, US Department of Energy, Office of Energy Efficiency and Renewable Energy, 2005.
[3] J. Carmody, S. Selkowitz, E.S. Lee, D. Arasteh, Window Systems for High-Performance Buildings, W.W. Norton & Company, December 2003, ISBN-13:978-0393731217.
[4] M. Sala, The intelligent envelope: the current state of the art, Renewable Energy 5 (1994) 1039–1046.
[5] G. Ward, R. Mistrick, E. Lee, A. McNeil, J. Jonsson, Simulating the daylight performance of complex fenestration systems using bidirectional scattering distribution functions within radiance, Journal of the Illuminating Engineering Society (2011).
[6] F. Frontini, T.E. Kuhn, S. Herkel, P. Strachan, G. Kokogiannakis, Implementation and application of a new bi-directional soar modelling method for complex facades within the ESP-r building simulation program, in: Building Simulation 2011, Sydney, Australia, 2011.
[7] R. Sullivan, L. Beltran, E.S. Lee, M. Rubin, S.E. Selkowitz, Energy and daylight performance of angular selective glazings, in: Proceedings of the ASHRAE/DOE/BTECC Conference, Thermal Performance of the Exterior Envelopes of Buildings VII, Clearwater Beach, FL, December 7–11, 1998, 1998.
[8] A. McNeil, E.S. Lee, Annual Assessment of an Optically-Complex Daylighting System Using Bidirectional Scattering Distribution Functions with Radiance, DOE/LBNL FY10 Technical Report Deliverable.
[9] G. Ward Larson, R. Shakespeare, Rendering with Radiance: The Art and Science of Lighting Visualization, Morgan Kaufmann, San Francisco, 1998.
[10] A. McNeil, C.J. Jonsson, G. Ward, D. Appelfeld, E.S. Lee, Validation of a ray-tracing tool used to generate bi-directional scattering distribution functions for complex fenestration systems, Solar Energy, submitted for publication.
[11] J.H. Klems, A new method for predicting the solar heat gain of complex fenestration systems: I. Overview and derivation of the matrix layer calculation, ASHRAE Transactions 100 (1) (1994) 1065–1072.
[12] M. Andersen, M. Rubin, J.L. Scartezzini, Comparison between ray-tracing simulations and bi-directional transmission measurements on prismatic glazing, Solar Energy 74 (2003) 157–173.
[13] IEA TASK 27, Performance of Solar Facade Components, 2005.
[14] CEN –EN 15251, Indoor Environment Input for Design and Assessment of Energy Performance of Buildings Addressing Indoor Air Quality, Thermal Environment, Lightning and Acoustics, European Committee for Standardization, Brussels, Belgium, 2007.
[15] IESNA Lighting Handbook, Illuminating Engineering, 9th edition, July 2000, ISBN-13:978-0879951504.
[16] J. Mardaljevic, L. Heschong, E. Lee, Daylight metrics and energy savings, Lighting Research and Technology 41 (2009) 261–283.
[17] EN 15193, Energy Performance of Buildings—Energy Requirements for Lighting, European Committee for Standardization, Brussels, Belgium, 2007.
[18] C.F. Reinhart, O. Walkenhorst, Dynamic RADIANCE-based daylight simulations for a full-scale test office with outer venetian blinds, Energy and Buildings 33 (7) (2001) 683–697.
[19] J. Wienold, Dynamic daylight glare evaluation, in: Building Simulation 2009, Glasgow, Scotland, 2009.
[20] J. Wienold, J. Christoffersen, Evaluation methods and development of a new glare prediction method for daylight environments with the use of CCD cameras, Energy and Buildings 38 (7) (2006) 743–757.
[21] T.R. Nielsen, K. Duer, S. Svendsen, Energy performance of glazings and windows, Solar Energy 69 (Suppl. 1–6) (2000) 137–143.
[22] D. Appelfeld, C.S. Hansen, S. Svendsen, Development of a slim window frame made of glass fibre reinforced polyester, Energy and Buildings 42 (2010) 1918–1925.
[23] EN832, Thermal Performance of Buildings — Calculation of Energy Use for Heating — Residential Buildings, CEN, 1998.
[24] T.E. Kuhn, S. Herkel, F. Frontini, P. Strachan, G. Kokogiannakis, Solar control: a general method for modelling of solar gains through complex facades in building simulation programs, Energy and Buildings 43 (2011) 19–27.
[25] T.E. Kuhn, Solar control: a general evaluation method for facades with venetian blinds or other solar control systems to be used 'stand-alone' or within building simulation programs, Energy and Buildings 38 (6) (2006) 648–660.
[26] T.E. Kuhn, C. Buhler, W.J. Platzer, Evaluation of overheating protection with sun-shading systems, Solar Energy 69 (Suppl. 1–6) (2000) 59–74.
[27] S. Lechtenböhmer, A. Schüring, The potential for large-scale savings from insulating residential buildings in the EU, Energy Efficiency 4 (2010) 257–270.
[28] D. Appelfeld, S. Svendsen, S.T. Borup, Performance of a daylight redirecting glass shading system demonstration in an office building, in: Building Simulation 2011, Sydney, Australia, 2011.

Paper IV

"Performance of a daylight-redirecting glass-shading system"

D. Appelfeld, S. Svendsen

Published in: *Energy & Buildings, 2013*

Energy and Buildings 64 (2013) 309–316

Contents lists available at SciVerse ScienceDirect

Energy and Buildings

journal homepage: www.elsevier.com/locate/enbuild

Performance of a daylight-redirecting glass-shading system

David Appelfeld*, Svend Svendsen

Technical University of Denmark, Department of Civil Engineering, Section of Building Physics and Services, Brovej, Building 118, DK-2800 Kgs. Lyngby, Denmark

ARTICLE INFO

Article history:
Received 3 January 2013
Received in revised form 8 May 2013
Accepted 9 May 2013

Keywords:
Shading system
Daylight
Redirecting light
Illuminance measurements
Indoor climate
Visual comfort

ABSTRACT

This paper evaluates the daylighting performance of a prototype external dynamic shading and daylight-redirecting system, and the main focus is on the performance simulation. The demonstration project was carried out on a building with an open-plan office. Part of the original façade was replaced with the prototype façade. This layout allowed the use of the same orientation and surroundings for both façades. The working plane illuminance was measured over several months and the measurements were accompanied with annual daylight simulations. The prototype system improved the daylighting conditions compared to the original system. The visual comfort was evaluated by glare analysis and the redirected daylight did not cause an additional discomfort glare. The higher utilization of daylight can save 20% of the lighting energy. The thermal insulation of the fenestration was maintained, with slightly increased solar gains, but without producing an excessive overheating.

1. Introduction

The energy consumption of buildings in the US and Europe is 40% of the overall energy use (EU, 2010) [1,2]. The electrical lighting energy in commercial buildings accounts for between 20 and 40% of electricity consumption [3]. Moreover, the combination of buildings well insulated against heat losses, high internal loads and large glazed areas in commercial buildings leads to the risk of overheating.

Transparent envelopes of buildings, also known as complex fenestration systems (CFSs), are multifunctional and the functions often conflict with each other [4]. Firstly, they must provide enough light transmittance for daylight. Secondly, they provide a solar energy transmittance during the cold period of a year. Thirdly, the transparent building envelopes provide solar gains, which may result in extensive overheating during the warmer months, so shadings need to be incorporated to prevent excessive solar radiation. Fourthly, they provide a view to the outside, which should be unobstructed and maintained.

The glazed areas in commercial buildings are often large, which increases solar gains during the cold period of a year and increases the working plane illuminance (WPI). Commercial buildings traditionally combine high internal gains generated by people, lighting and equipment, with well-insulated envelopes, resulting in low heating and high cooling loads. The solar gains may contribute to heating but can produce overheating, so they must be included in the total energy balance of buildings [5]. During the warmer season, the glazed façade can cause overheating and glare, so solar shading is necessary.

Cutting energy consumption for electrical lighting by daylight and reducing overheating by shading both have high potential for energy savings in commercial buildings [6]. The motivation of this research was the growing demand for energy savings and the quest for new innovative technology, and its major focus was to investigate the performance of integrated solar shading with the secondary function of increasing daylight utilization by redirecting daylight into a deep office room.

Based on a previous study, the light-redirecting glass-shading system (LRGSS), which combines shading with daylight redirection, was developed and built as a full-scale office building demonstration. The previous study used IESve/Radiance [7] simulations, outdoor measurements of illuminance on a 1:10 mock-up, and measurements of illuminance in a single room test cell. The results indicated that the LRGSS would function both as regular sun protection close to the façade and at the same time improve daylight conditions by reflecting light further into the room where daylight is desirable. Furthermore, the LRGSS overcomes the disadvantages of current shading systems and provides a view out, while still shading against excessive solar gains [8,9].

This investigation was based on a full-scale demonstration in an office building accompanied by annual computer simulations.

The focus is to evaluate the performance of the LRGSS, based on the simulations and measurements. The lighting energy saving potential depends on an evaluation of an offset of artificial lighting by daylight, which is further dependent on a daylight-linked

* Corresponding author. Tel.: +45 45251856.
E-mail address: dava@byg.dtu.dk (D. Appelfeld).

0378-7788/$ – see front matter © 2013 Elsevier B.V. All rights reserved.
http://dx.doi.org/10.1016/j.enbuild.2013.05.017

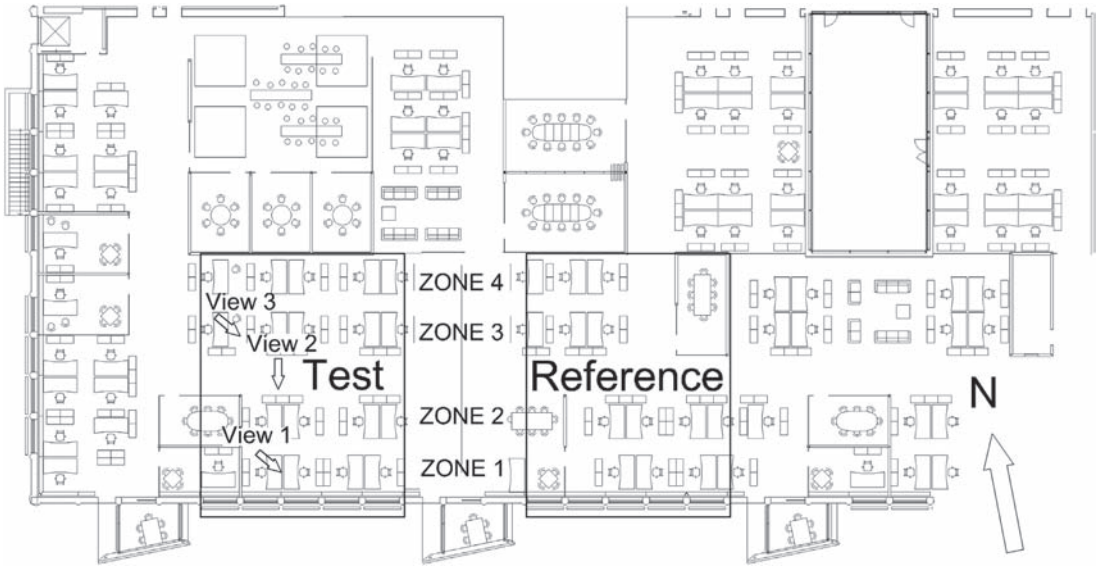

Fig. 1. The layout of the building, view directions and lighting zones. The LRGSS was measured in the test area and the original shading system was measured in the reference area.

lighting control strategy. The redirected sunlight could cause glare discomfort, so both the glare and the visual comfort of the system needed evaluation. It was also necessary to analyze the thermal performance of the system, because it increases the solar energy penetration of the envelope. The visual comfort evaluation combines the illuminance distribution and glare [10].

2. Experiment

2.1. Demonstration building

The demonstration building for testing is located in Humlebaek, 30 km north of Copenhagen in Denmark (55.96° North – 12.49° East). The building is a former production facility refurbished as an open-plan office, in which the working places are far back from the façade. The building is one floor high with 2.26 m high windows. The whole building has dimensions of 66 m × 28 m, with the longer façade oriented 11° west of due south. The surrounding landscape is flat without big trees or high buildings that might shade the façade under investigation. However, an opposite building partly blocks the open horizon, since it is 5 m high, 40 m away and runs parallel to the south façade, so it was included in the simulation model, because it could affect results by up to 10% [11].

The office has a room depth of 14 m. Fig. 1 shows the floor plan of the building. The building and façade made it possible to have two almost identical areas for investigation, 9.5 m wide, 14 m deep and 3.45 m high. One area was used for testing the LRGSS and the other area was used as a reference where the original shading was kept unchanged. Both areas were fitted with illuminance sensors to monitor the WPI and illuminance under the ceiling. The windows are on the south and west façades, 1.98 m wide and 2.26 m high, with 20 cm wide columns between windows and 0.75 m high windowsills. The reflectance of the surfaces in the building was measured with a calibrated universal photometer meter Hagner S4, and the results are shown in Table 1. The roughness and specularity of the surfaces were ignored for the simulation model.

2.2. The shading system

The first area (marked as test in Fig. 1) was equipped with the LRGSS, while the second area (marked as reference in Fig. 1) remained unchanged with the original lamella shading system kept for comparison. There are two major differences between the LRGSS and the original lamella shading system. Firstly, the position of the lamellas and their control strategy is quite different with the LRGSS. Secondly, a different type of glass was used for the LRGSS. All windows in the building included internal shading devices, i.e. Venetian blinds and curtains, which are shown in Fig. 2. These internal shading devices were present during the measurements and could therefore have affected the measured results.

Both shading systems consist of eight horizontal 330 mm wide lamellas on each window. The top four LRGSS lamellas rotate in the opposite direction to those of the original system. In the LRGSS, the outer edge when the lamella is in horizontal position moves upward and its upper surface goes toward the façade when the system is closing.

The rotation directions of the lamellas are illustrated in Fig. 3. The bottom four lamellas in the LRGSS rotate in the opposite direction (i.e. the same direction as the original system). This strategy allows the upper part of the LRGSS to redirect light when in the redirecting position and give shade in the closed position, while the lower part acts as a shading system allowing a view to the outside.

The LRGSS was made of a highly reflective solar-control coated glass to redirect daylight into the back of the office. The lamellas were made of Antelio Silver 10 mm glass produced by Saint Gobain

Table 1
Surface reflectance values.

Surface	Visible reflectance (R_{vis})
Floor	20.5%
White walls	89.3%
Wooden partitions	32.6%
Ceiling	89.9%
Wooden furniture	40.0%

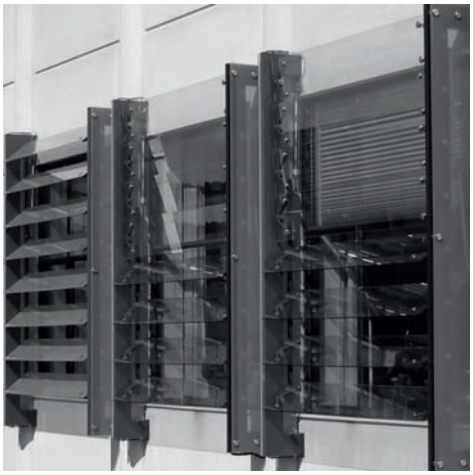

Fig. 2. Façade with the original shading system (far left) and the LRGSS (center and right), including internal shading systems, Venetian blinds and curtains.

Glass (SGG), with a light reflectance of 31%. The lamellas of the original system were made from Parasol Green 8 mm glass with a light reflection of 6%, produced by SGG, with white frit covering 55% of the lamella surface.

The external shading systems were supplemented with internal Venetian blinds and curtains operated manually by the occupants. The internal shading devices were excluded from the simulations, because their position was not monitored and they were outside the scope of the investigation. The position of the interior shading devices was randomly dependent on the occupants' behavior. It is generally difficult to model and monitor occupants' behavior [12], so it is not possible to compare the simulations with the measurements directly. By ignoring the interior shading devices, the simulations investigation focused only on the comparison of the performance of the LRGSS and the original shading system.

2.3. Shading control strategy

The shading strategy of the LRGSS is based on the most effective daylight-redirecting position, which is 30° toward the façade, and on the building's location and sun position [8,9]. The lamellas stay in the redirecting position when the sky is overcast or whenever the total horizontal illuminance is lower than a threshold of 25 klx for longer than 10 min. The time delay of 10 min prevents frequent opening and closing of the shading system, which could disturb the occupants. The threshold for moving lamellas back to the redirecting position was set to 17.5 klx with time offset of at least 20 min. The redirecting position was 30° all year around, except for May and June when the position was set to 25° to avoid direct reflection from the lamellas' surfaces to the occupants' faces. The system was controlled automatically according to a predefined pattern, both in reality and in the simulations. The system had three possible positions:

- Redirecting position 30° (25°) – only for the top four LRGSS lamellas.
- Open position 0° – LRGSS and original system.
- Close position 90° – LRGSS and original system.

Mainly closed and redirecting positions were present during the investigation, as the opened position depended on the occupants' behavior, as they could open it manually.

2.4. Daylight performance matrices

The comparison between the LRGSS and the original shading system was based on working plane illuminance (WPI). The most commonly used daylight performance matrices nowadays are daylight factor (DF), useful daylight illuminance (UDI), and daylight autonomy (DA) [10,13–16]. DF was not used in this investigation because it does not quantify the redistribution of the direct beam of light radiation to provide diffuse illuminance in the indoor space.

Based on the literature and standards review, several thresholds have been observed and evaluated by daylight autonomy (DA) and useful daylight illuminance (UDI) [13–19].

DA is a percentage of hours satisfying the minimum design WPI out of the total number of working hours during a year. The commonly used design WPI is between 300 and 500 lx [18]. 500 lx is described as minimum WPI for office work, so it was used as threshold for DA analysis in this investigation [18]. The UDI matrix quantifies when the daylight is perceived as useful for occupants of an indoor space. This is calculated as the percentage of the occupied working hours when the WPI is between the lower and upper limit. The lower limit for the UDI was set to 100 lx as suggested

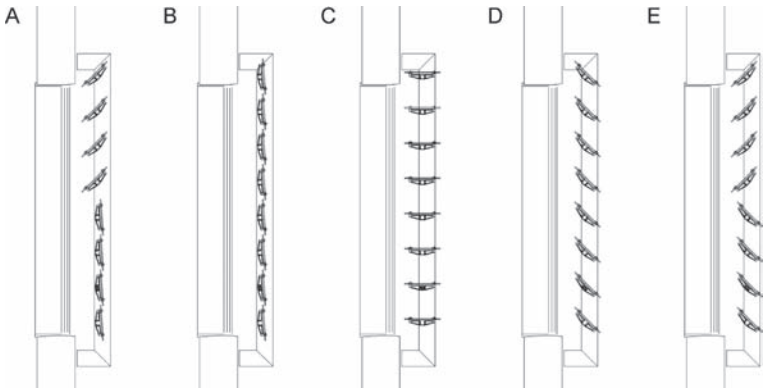

Fig. 3. Illustration of the positions and rotations of the shading systems: (A) LRGSS system in redirecting position with closed lower 4 lamellas; (B) LRGSS and/or original shading system in the closed position (90°); (C) LRGSS and/or original shading system in the open position (0°); (D) original shading system in the rotation of 45°; (E) LRGSS in redirecting position with lower four lamellas in the rotation of 45°.

by Mardaljevic et al. and many other publications [16]. The upper limit is not clearly defined and differs between publications. The upper limit indicates when the occupants may feel uncomfortable and, according to Mardaljevic et al. [16], the upper limit is 2500 lx. However, recent studies and discussion in the daylight design community indicate that higher limits are more realistic. According to Wienold [19], 30% of people find horizontal illuminance above 4500 unsatisfactory, so 4500 lx was used. It can be argued that 4500 lx is too high, but since the investigation was to evaluate the effect on the daylight conditions the more radical limit was desirable. Furthermore, there are several positive non-visual effects of daylight on human beings [20].

Midrange between 100 and 4500 lx can be considered as usable for most of the occupants. Some subjects may consider some of the values in this range as uncomfortable, but such values should not be considered as not useful since every subject perceives illuminance levels differently [16,19].

2.5. Measurements

The WPI and the illuminance under the ceiling were monitored by three illuminance meters. Moreover, the outdoor total horizontal illuminance on the roof was measured and used to monitor outdoor daylight conditions. However, the data collected about the sky distribution were not sufficient to model identical conditions within the simulation model, so the results from the measurements and simulations are not directly comparable. Data from the reference weather file were used to model sky distribution. The assumptions and differences between the measurements and simulations are:

- The boundary conditions were not same for measurements and simulations because the sky model/distribution in the simulations was defined according to the weather information in a test reference year for Copenhagen, Denmark [21].
- In reality, the internal shading devices could be randomly opened/closed. Occupants' behavior was neither modeled in the simulations nor monitored in reality.
- The measurement sensors could occasionally be shaded in the open-plan office.
- The simulations of daylight conditions were carried out without furniture, because the furniture was not fixed and could be moved in reality.

2.6. Annual daylight simulation

It is generally difficult to evaluate the performance of unique complex fenestration systems (CFS), such as LRGSS, using commonly-used daylight simulation programs, since they are mostly designed for specific and simplified solutions. The complexity of the assessment can be seen from many perspectives, such as indoor climate, visual comfort, energy impact, shape, material, cost and operating cost [22]. So more generic and versatile state-of-the-art simulation programs and techniques are needed to evaluate the impact of a unique CFS [23]. However, the simulations of CFS with dynamic boundary conditions, such as variation of the sky conditions, makes it difficult to compare the simulation results with measurements. So the simulations are mainly used for prediction of future performance and conditions.

The program Radiance was used for the simulations of the transparent properties of the shading systems and their effect on the indoor environment [24,25]. To calculate an annual WPI, a three-phase method (TPM) using Radiance was used [26,27]. This method uses the Radiance tool rtcontrib to calculate results in the form of a matrix, generated from the transmission of fenestration system matrix, exterior daylighting matrix and interior view matrix. This approach quickly generates different situations for various fenestration systems, locations and sky conditions by replacing only one-matrix [28]. The last information needed for the multiplication of matrices is a sky vector, which describes the sky distributions. This was derived from the test reference year (TRY) for Copenhagen, Denmark [21]. The sky model uses the Perez sky, which is generated from the direct normal irradiance and horizontal diffuse irradiance [13,29]. The sky was divided into 2305 patches according to a Reinhart's subdivision for detailed results [30]. By multiplying matrices, the total illuminance at the sensors from all sources in the model was calculated. The transmission matrix was generated by the Radiance program genBSDF, which generates a bi-directional scattering distribution function (BSDF) for a given complex fenestration geometry [31]. The program genBSDF uses the Radiance ray-tracing tool to generate a BSDF matrix for any arbitrary CFS and outputs data in the Window 6 XML file format. In addition to daylight simulation, the program Window 6 was used to assess basic thermal and solar energy properties of the system [32]. The solar energy transmittance, the *g*-value, of both systems was calculated and used to supplement the visual light transmittance of the systems.

The illuminance sensors were located in same positions as in the simulation model. They were located in the working plane and under the ceiling facing the floor, to monitor the intensity of light reflected to the ceiling. The spacing of the measuring sensors was 0.5 m, 3.6 m and 8.5 m from the façade in the working plane, and 1.5 m, 3.3 m, 5.1 m and 6.9 m from the façade under the ceiling. A row of virtual illuminance sensors was used for the detailed simulation of the WPI, positioned perpendicular to the façade with spacing of 0.25 m starting 0.5 m from the façade at the height of 0.85 m.

2.7. Glare

Visual comfort was a major criterion in the performance of the daylight-redirecting shading system. Glare analysis was needed because the view out was provided [33], but the perception of glare is often reduced, even under high glare index values, when working under daylighting conditions [34].

Daylight glare probability (DGP) was selected as the glare index, because DGP is based on an extensive human evaluation study [35,36]. The annual DGP analysis was facilitated by an enhanced simplified DGP calculation method that included direct sunlight in the analysis [35]. The glare was assessed for working hours between 8:00 and 18:00 on working days over a year. The three arbitrary views were used for glare assessment because visual comfort depends on both visual zone and view direction [19,37]. The views are shown in Fig. 1. Glare levels were obtained from the rendered images since it was not possible to evaluate the discomfort glare from the horizontal illuminance [16].

2.8. Lighting-energy savings

Energy savings for lighting were calculated for three different lighting control systems. The WPI criteria were based upon a standard CEN EN 15251 [18] for open-plan offices with a WPI of 500 lx. The lighting power density of 15 W/m^2 derives from EN 15193 [38]. The percentage of working hours that satisfied the daylighting conditions annually was calculated. When the minimum light threshold was not reached, the artificial light could be added and the artificial light energy saving was equal to the amount of daylight. The lighting control strategies were linked to daylight and were as follows: on/off control, bi-level control, and continuous control.

For on/off control, the electric lighting in a zone was switched off when the WPI was sufficient by daylight. With bi-level switching, half of the lamps in the zone were switched off when daylight

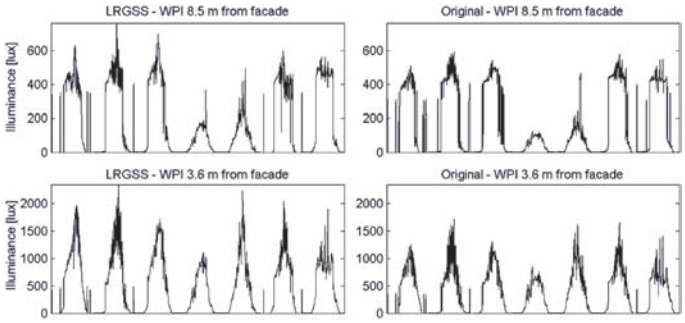

Fig. 4. Measured illuminance in the working plane over 7 days.

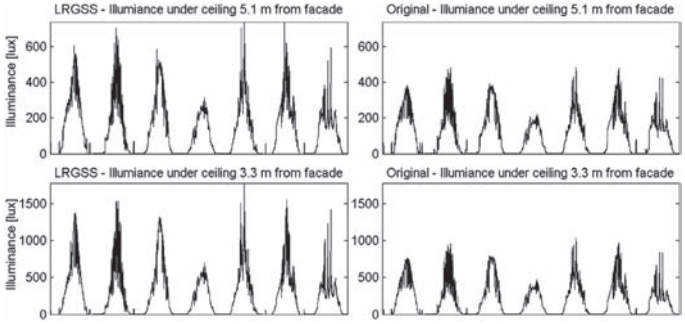

Fig. 5. Measured illuminance under the ceiling over 7 days.

fulfilled half of the required WPI, and they were all switched off when the WPI criteria were fully met. With continuous control, the electrical lighting was linearly dimmed by an amount equal to the available daylight, until a minimum supplied output of 20%, and then switched off when the criteria were met.

The lighting energy savings in the simulations were idealized because they were based on the WPI level. The office space was divided into 4 zones, each consisting of one row of tables parallel to the façade, see Fig. 1. Each zone was approximately 33.25 m^2 of the floor area. The WPI level had to be reached at the back of the each zone, which meant that the whole zone was sufficiently lit.

3. Results and discussion

3.1. Measurements

The measurements were carried out between July and mid-October 2010. Since no month went by without any sensor error, only short periods of measurements, with all sensors working, are presented as example of measurements. The performance evaluation was mainly based on the results from simulations. Figs. 4 and 5 show pairs of graphs comparing measured illuminance with LRGSS and the original shading system. Data were measured at ½ min intervals during the 4th week of July 2010. Table 2 shows the mean value of differences between the illuminance provided by the LRGSS and the original shading system during working hours. From the upper and lower 95% confidential interval, it can be seen that the differences between measurements and simulations were quite constant. In the illustrated period of measurements, there were several sunny and partly sunny days, which meant that the shading systems were closed during the measurements. The closed systems resulted in relatively small differences between the two shading systems investigated. Moreover, higher illuminance levels were measured closer to the façade because the LRGSS has higher light transmittance. The WPI at a distance of 8.5 m from the façade was mainly provided by artificial light, and the sudden increase of WPI in the morning and afternoon is visible in Fig. 4. The WPI at 0.5 m from the façade was excluded from Fig. 4 because this position was too close to the façade and there were differences between illuminance measurements for the LRGSS and the original shading system.

3.2. Simulation results

The illuminance sensor positions simulated were identical to the measuring points. According to Iversen et al. [39], the

Table 2
Difference between the WPI provided with the LRGSS and the original shading systems: one-week measurements.

Position	Floor			Ceiling			
Distance from façade	0.5 m	3.6 m	8.5 m	1.5 m	3.3 m	5.1 m	6.9 m
Mean difference (lx)	1055	47	5	127	31	12	3
Upper confidential interval (lx)	1007	45	4	123	30	11	3
Lower confidential interval (lx)	1103	48	5	130	32	12	3

Table 3
Difference between the WPI provided with the LRGSS and the original shading system: whole-year simulations.

Position	Floor			Ceiling			
Distance from façade	0.5 m	3.6 m	8.5 m	1.5 m	3.3 m	5.1 m	6.9 m
Mean difference (lx)	459	214	23	150	85	41	16
Upper confidential interval (lx)	407	191	18	144	80	37	14
Lower confidential interval (lx)	510	236	29	156	90	44	18

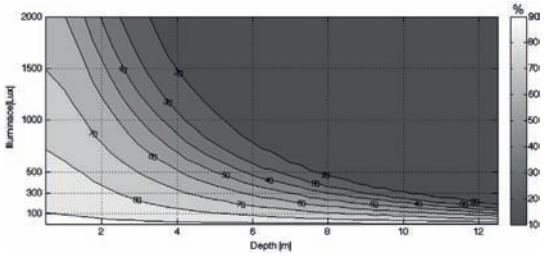

Fig. 6. Daylight autonomy of the LRGSS with dynamically controlled position.

hourly weather data are comparable with weather data at shorter intervals, so hourly intervals were used for the simulations. As described above, the measurements and simulations are not directly comparable due to the high degree of randomness during the measurements as well as using different boundary conditions when using typical year weather data for the simulations. The mean value of averages between the LRGSS and the original system decreases as the level of illuminance decreases with the depth of the space. During the simulations, the only changing parameters were the sky distribution and the position of the shading lamellas; this resulted in a more even re/distribution of daylight in the space. The results from measurements and simulations do not directly correlate, but Tables 2 and 3 show similar trends of WPI increase.

3.3. Daylight autonomy

The simulations of daylight distribution in the space were used to predict daylight conditions. Fig. 6 shows DA for a whole year for the LRGSS under dynamic control, which is a combination of closed and redirecting position. The difference between the LRGSS and the original system was that the LRGSS was designed to be capable of moving to the redirecting position, while the original system could be only in the closed position. For DA results see Fig. 7.

The illuminance threshold for DA was reached more often and at a greater distance from the façade with the LRGSS. The threshold of 500 lx was reached 50% of the time at a distance of 4.5 m from the façade for the LRGSS, compared to 3.2 m for the original system. For the LRGSS, 60% of the occupied hours had a WPI of at least 500 lx at a distance of 4 m from the façade, while the corresponding figure for the original shading system was about 43%. The improvement in daylight conditions is visible all over the space investigated. Furthermore, the part of the room with at least 300 lx 20% of time was increased from 7.8 m to 10.2 m from the façade including most of the working area in the office. The primary purpose of a shading system is to block the light penetrating the indoor space. The LRGSS still blocks the light near the façade, but increases the horizontal illuminance further into the office. Furthermore, DA does not penalize excess illuminance, so the UDI matrix was calculated to illustrate illuminance levels throughout the office.

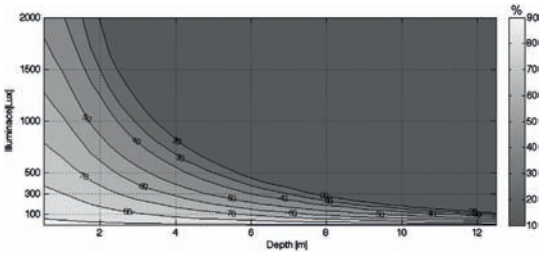

Fig. 7. Daylight autonomy of the original shading system in the closed position.

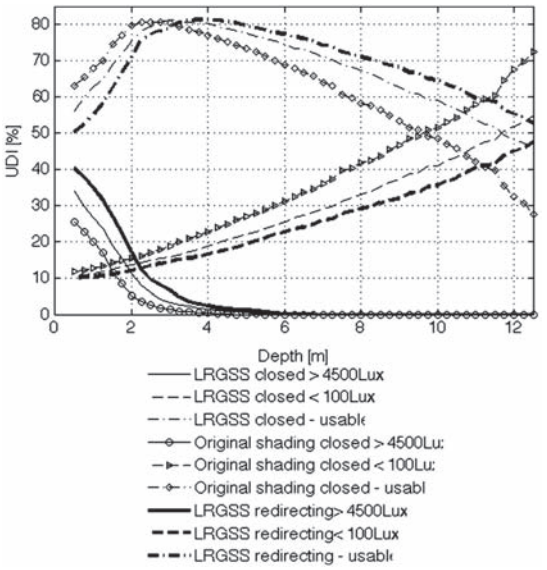

Fig. 8. Annual useful daylight illuminance matrix for various scenarios.

3.4. Useful daylight illuminance

The excess WPI is presented for both shading systems and for all the shading system positions investigated. Fig. 8 shows the horizontal illuminance for the closed and the redirecting position of the LRGSS and the original shading system. The results are split to show the performance of the systems in each position. The depth of the room with an illuminance level higher than 4500 lx increased by approximately 1 m on average, but this is not a significant downgrade, because most of the working places are outside this zone. If the upper limit is exceeded, occupants can close the internal shading system manually in the same way as they would do with the original shading system.

More importantly, the area with insufficient daylighting conditions in the space was limited, and was mostly at the back of the office space. The illuminated zone with horizontal illuminance between 100 and 4500 lx is larger with the LRGSS than with the

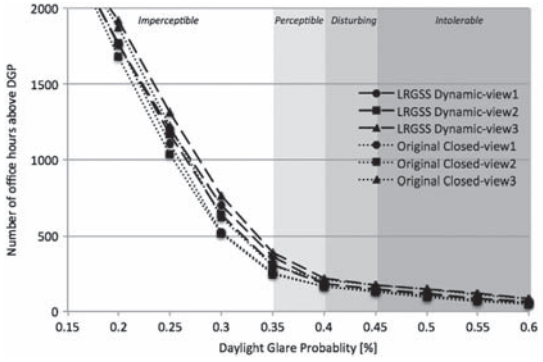

Fig. 9. Annual working hours DGP profile for Views 1, 2 and 3; for the dynamically controlled LRGSS and the original shading system.

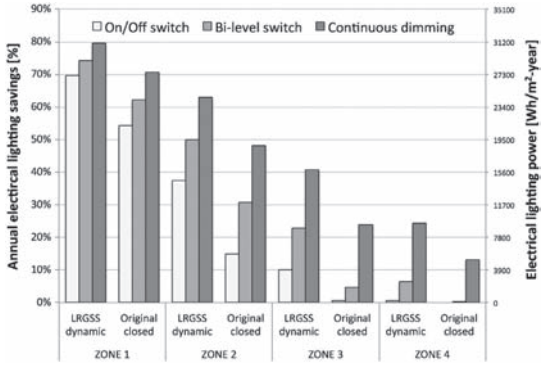

Fig. 10. Electrical light savings for WPI of 500 lx and different daylight-linked lighting control strategies.

original shading. The daylight-redirecting position of the lamellas further increased the zone lit by daylight. The LRGSS provides usable UDI for 20% more of the hours of occupancy at the back of the room than the original system. The percentage of UDI was improved throughout the whole depth of the room beyond 3 m from the façade. The zone with the minimal horizontal illuminance of 100 lx was reduced with the LRGSS, which indicates that the daylight conditions were satisfied in a higher percentage of the working hours.

3.5. Glare analysis

When direct sunlight is redirected to the ceiling, the risk of discomfort glare can increase. By introducing dynamic control of the lamellas reacting to sunlight intensity, the risk of glare from the reflection was reduced by optimizing the position of the lamellas to remove reflections from the glass surface from the occupants' faces. However, discomfort glare could occur in cases when the sun was low in the sky or under conditions of intermediate sky. A horizontal roof illuminance for the simulated weather conditions was calculated and in 17% of the working hours, the threshold was above 25 klx, which defines when the shading systems were in the closed position.

The LRGSS generated more glare, but the difference was minimal. Most of the glare was under View 1, because this position was the closest to the façade. Under View 1, there was a deterioration in visual comfort on the DGP scale 5% of the time; however, most this was in the range of imperceptible glare. This means that the shading capabilities of the LRGSS system are similar to the original shading system and do not generate any significant increase in glare. From these results, it can be concluded that while the LRGSS system increases daylight penetration into the office, the risk of glare was not increased by redirecting and reflecting daylight.

The cumulative DGP curves for dynamically controlled LRGSS in Fig. 9 show that the two systems perform in a similar way and most detected glare was in the range of the imperceptible. This observation shows that it is effective to redirect daylight into the ceiling during days with an outdoor illuminance under 25 klx.

3.6. Artificial light savings

The analysis considered all the savings from utilizing daylight instead of artificial light. Since the lighting control strategy was not predefined during the demonstration project, three lighting controls were investigated. The LRGSS was dynamically controlled while the original shading was in the closed position, and daylight was used when the criteria were met. Fig. 10 shows each zone's savings for each lighting control strategy as well as for both shading systems. In all cases, the LRGSS provided higher savings. Near to the façade (Zone 1), the LRGSS provided between 9 and 15% more savings. The difference between shading systems increased toward the back of the room (Zone 4), due to the LRGSS redirecting daylight into the room. The lighting control strategy's effect on savings increases further from the façade. On/off control provides almost no savings in Zone 4, while the bi-level switching control strategy accounts for approximately 7% of the lighting power and continuous dimming achieves 23% savings compared to the situation when the lights are switched on all the time. The improvement of the LRGSS over the original shading was between 10 and 15% in Zones 1–4 for the continuous dimming and bi-level control.

3.7. Solar gains and energy performance

At different positions, the systems provide different thermal and optical properties. Using generated BSDF matrices for each system, the *g*-value and τ_{vis} were calculated for each position and shading system, and they are shown in Table 4. The thermal transmittance of both systems, the *U*-value, was kept at 0.9 W/m^2 K for all the scenarios. The model included all the surrounding edges of the shadings, such as the windowsills and window frames, as well as the actual size of the window.

From the investigation in Window 6, the LRGSS in the redirecting position provides 17% more visible transmittance but an increase of only 11% in solar energy transmittance. Using this strategy, daylight utilization increases proportionally more than the solar gains. These values are valid for the main properties of the fenestration system.

The LRGSS has a higher *g*-value than the original shading system, so it will admit more solar gains into the building. The building energy simulations lay outside the scope of this investigation, so it is not possible to estimate whether the *g*-value of 0.308 will provide sufficient solar control to avoid air conditioning. From

Table 4
Performance characteristics of the test and reference systems.

Position	Test		Reference	
	g-Value	τ_{vis}	*g*-Value	τ_{vis}
Closed	0.308	0.436	0.257	0.310
Open	0.426	0.645	0.412	0.642
Redirecting	0.391	0.568	0.353	0.486

physical observations at the building, solar gains did not significantly increase the indoor temperature.

4. Conclusion

This paper evaluated a prototype dynamic integrated shading and light-redirecting system designed to optimize daylight conditions in an office building whilst the quality of the indoor environment and view out was preserved and improved. Part of an existing façade with glass lamellas in Humlebaek in Denmark was rebuilt to test and further develop the prototype of the concept. The redirecting glass lamella system and the original façade had the same orientation and layout. The automated external redirecting glass lamella system was synchronized with the actual sun position and sky distribution to expand the zone with the design working plane illuminance lit by daylight and to maximize the view out. In this study, the lighting conditions were simulated and measured during summer and autumn, and accompanied by annual simulations. However, the measured data and the simulation results could not be directly compared, due to the large number of random variables during the measurements.

Daylight improvement was achieved with the redirecting glass lamella shading system compared to the original system. Glare analysis indicated that the daylight-redirecting shading system did not cause additional glare compared to the reference shading system. However, it is recommended that an internal manual shading system should be used to block any excessive glare. Visual comfort was maintained and the daylight conditions in the office were improved. The higher penetration of daylight into the back of the office reduced the need to use electricity for lighting. Depending on the daylight-linked lighting control, the savings were up to 20% greater than the reference system and up to 80% greater in the zone closest to the façade, when compared to using artificial light only.

Acknowledgements

The research for this study was funded by the Danish Energy Agency program for research and development of energy efficiency, PSO – F&U 2008. The authors would like to thank the Danish Building Research Institute (SBi) for assisting and providing measured data.

References

[1] EU, EPBD Recast (2010), Directive 2010/31/EU of the European Parliament and of the Council of 19 May 2010 on the Energy Performance of Buildings (Recast), Official Journal of the European Union, 18/06/2010, EU of the European Parliament, 2010.
[2] US DOE Office of Energy Efficiency and Renewable Energy, Buildings Energy Databook, US Department of Energy, Office of Energy Efficiency and Renewable Energy, 2005.
[3] I. Pyonchan, N. Abderrezek, K. Moncef, Estimation of lighting energy savings from daylighting, Building and Environment 44 (March (3)) (2009) 509–514.
[4] H. Altan, I. Ward, J. Mohelnikova, F. Vajkay, An internal assessment of the thermal comfort and daylighting conditions of a naturally ventilated building with an active glazed facade in a temperate climate, Energy and Buildings 41 (2009) 36–50.
[5] EN 15603:2008, Energy Performance of Buildings – Overall Energy Use and Definition of Energy Ratings, European Committee for Standardization.
[6] E. Lee, Advanced High-Performance Commercial Building Façades Research, Lawrence Berkeley National Laboratory, Berkeley, 2009.
[7] IESve/Radiance, Version 5.5, Integrated Environmental Solutions <Virtual Environment> Ltd., Glasgow, UK, 2003.
[8] J.B. Laustsen, I.D.P. Santos, S. Svendsen, et al., Solar shading system based on daylight directing glass lamellas, in: Building Physics 2008 – 8th Nordic Symposium, 16–18 June 2008, Copenhagen, 2008, pp. 111–118.
[9] A. Iversen, J.B. Laustsen, S. Svendsen, et al., Udvikling af nye typer solafskærmnings-systemer baseret på dagslysdirigerende solafskærmende glaslameller, Technical University of Denmark, Denmark, Lyngby, 2009.
[10] F. Cantin, M.C. Dubois, Daylighting metrics based on illuminance, distribution, glare and directivity, Lighting Research and Technology 43 (3) (2011) 291–307.
[11] S. Nikoofard, V.I.I. Ugursal, I. Beausoleil-Morrison, Effect of external shading on household energy requirement for heating and cooling in Canada, Energy and Buildings 8141 (2011) 1627–1635.
[12] O. Mejri, E.P. Del Barrio, Energy performance assessment of occupied buildings using model identification techniques, Energy and Buildings 43 (2011) 285–299.
[13] A. Nabil, J. Mardaljevic, Useful daylight illuminance: a new paradigm for assessing daylight in buildings, Lighting Research and Technology 37 (1) (2005) 41–59.
[14] C.F. Reinhart, J. Wienold, A simulation-based analysis for daylit spaces, Building and Environment 46 (2011) 386–396.
[15] A. McNeil, E.S. Lee, Annual Assessment of an Optically-Complex Daylighting System Using Bidirectional Scattering Distribution Function with Radiance. DEO/LBNL FY10 Technical Report Deliverable, Lawrence Berkeley National Laboratory, Berkeley, 2010.
[16] J. Mardaljevic, L. Heschong, E. Lee, Daylight metrics and energy savings, Lighting Research and Technology 41 (2009) 261–283.
[17] J. Mardaljevic, Daylight simulation: validation, sky models and daylight coefficients, in: PhD Thesis, De Montfort University, UK, 2000.
[18] CEN – EN 15251:2007, Indoor Environment Input for Design and Assessment of Energy Performance of Buildings Addressing Indoor Air Quality, Thermal Environment, Lightning and Acoustics.
[19] J. Wienold, Daylight glare in offices, in: PhD Thesis, ISE Fraunhofer, Freiburg, Germany, 2010.
[20] A. Webb, Considerations for lighting in the built environment: non-visual effects of light, Energy and Buildings 38 (2006) 721–727.
[21] United States Department of Energy, Weather Data http://apps1.eere.energy.gov/buildings/energyplus/weatherdata/6_europe_wmo_region_6/DNK_Copenhagen.061800_IWEC.zip
[22] D. Appelfeld, A. McNeil, S. Svendsen, An hourly based performance comparison of an integrated micro-structural perforated shading screen with standard shading systems, Energy and Buildings 50 (2012) 166–176.
[23] A. Laouadi, A. Parekh, Optical models of complex fenestration systems, Lighting Research and Technology 39 (2007) 123–145.
[24] G. Ward, R.A. Shakespeare, Rendering with Radiance, Space & Light, Davis, CA, 1998.
[25] C.F. Reinhart, Validation of dynamic RADIANCE-based daylight simulations for a test office with external blinds, Energy and Buildings 33 (2001) 683–697.
[26] G. Ward, R. Mistrick, E. Lee, et al., Simulating the daylight performance of complex fenestration systems using bidirectional scattering distribution functions within Radiance, LEUKOS: Journal of Illuminating Engineering Society of North America 7 (4) (2011) 241–261.
[27] A. Jacobs, Understanding rtcontrib, London, UK, 2010, http://www.jaloxa.eu
[28] G. Ward, Radiance's new rtcontrib program, in: 4th International Radiance Workshop, Montreal, Canada, 2005.
[29] R. Perez, R. Seals, J. Michalsky, All-weather model for sky luminance distribution-preliminary configuration and validation, Solar Energy 50 (3) (1993) 235–245.
[30] G. Ward, Complex fenestration and annual simulation, in: 8th International Radiance Workshop, Boston, USA, 2009.
[31] A. McNeil, C.J. Jonsson, G. Ward, et al., Validation of a ray-tracing tool used to generate bi-directional scattering distribution functions for complex fenestration systems, Energy and Buildings (2012) (submitted for publication), ENB-D-12-00959.
[32] R. Mitchell, C. Kohler, D. Arasteh, THERM 5.2/WINDOW 5 2 NFRC Simulation Manual, Lawrence Berkeley National Laboratory: University of California, Berkeley, 2006.
[33] N. Tuaycharoen, P.R. Tregenza, View and discomfort glare from windows, Lighting Research and Technology 39 (2007) 185–200.
[34] L. Roche, E. Dewey, P. Littlefair, Occupant reactions to daylight in offices, Lighting Research and Technology 32 (2000) 119–126.
[35] J. Wienold, Dynamic daylight glare evaluation, in: Building Simulation 2009, 11th International IBPSA Conference, 27–30 July 2009, Glasgow, Scotland, 2009, pp. 944–951.
[36] J. Wienold, J. Christoffersen, Evaluation methods and development of a new glare prediction method for daylight environments with the use of CCD cameras, Energy and Buildings 38 (7) (2006) 743–757.
[37] J. Jakubiec, C.F. Reinhart, The "adaptive zone" – a concept for assessing discomfort glare throughout daylit spaces, Lighting Research and Technology (2011), http://dx.doi.org/10.1177/1477153511420097 (published online 21.10.11).
[38] EN 15193:2007, Energy Performance of Buildings – Energy Requirements for Lighting, European.
[39] A. Iversen, S. Svendsen, T.R. Nielsen, The effect of different weather data sets and their resolution in climate-based daylight modelling, Lighting Research and Technology (2012), http://dx.doi.org/10.1177/1477153512440545.

Windows are crucial elements of building envelopes and influence indoor comfort and energy efficiency of buildings, so they have a high potential for reducing building energy by using daylight and lowering energy demand for heating and cooling. This Ph.D. work uses comprehensive thermal and optical performance modelling to stimulate the development of advanced window systems with shading, which serve several functions, fulfil new energy regulations and form the basis for the design of low-energy buildings in the future. The evaluation of unique advanced window systems is demonstrated by simulations and measurements of several case examples..

DTU Civil Engineering
Department of Civil Engineering
Technical University of Denmark

Brovej, Building 118
2800 Kgs. Lyngby
Telephone 45 25 17 00

www.byg.dtu.dk

ISBN: 9788778773500
ISSN: 1601-2917